UNIVERSITY OF AMSTERDAM

UvA-DARE (Digital Academic Repository)

Search for a light CP-odd Higgs boson decaying into a pair of τ-leptons in proton-proton collisions at √s = 13 TeV with the ATLAS detector

ATLAS Collaboration

DOI
10.1007/JHEP12(2024)126

Publication date
2024

Document Version
Final published version

Published in
The Journal of High Energy Physics

License
CC BY

Link to publication

Citation for published version (APA):
ATLAS Collaboration (2024). Search for a light CP-odd Higgs boson decaying into a pair of τ-leptons in proton-proton collisions at √s = 13 TeV with the ATLAS detector. *The Journal of High Energy Physics*, *2024*(12), Article 126. https://doi.org/10.1007/JHEP12(2024)126

General rights
It is not permitted to download or to forward/distribute the text or part of it without the consent of the author(s) and/or copyright holder(s), other than for strictly personal, individual use, unless the work is under an open content license (like Creative Commons).

Disclaimer/Complaints regulations
If you believe that digital publication of certain material infringes any of your rights or (privacy) interests, please let the Library know, stating your reasons. In case of a legitimate complaint, the Library will make the material inaccessible and/or remove it from the website. Please Ask the Library: https://uba.uva.nl/en/contact, or a letter to: Library of the University of Amsterdam, Secretariat, P.O. Box 19185, 1000 GD Amsterdam, The Netherlands. You will be contacted as soon as possible.

UvA-DARE is a service provided by the library of the University of Amsterdam (https://dare.uva.nl)

Download date:14 Sept 2026

Published for SISSA by Springer

Received: October 1, 2024
Accepted: November 28, 2024
Published: December 17, 2024

Search for a light CP-odd Higgs boson decaying into a pair of τ-leptons in proton-proton collisions at $\sqrt{s} = 13$ TeV with the ATLAS detector

The ATLAS collaboration

E-mail: atlas.publications@cern.ch

Abstract: This paper reports a search for a light CP-odd scalar resonance with a mass of 20 GeV to 90 GeV in 13 TeV proton-proton collision data with an integrated luminosity of 140 fb^{-1} collected with the ATLAS detector at the Large Hadron Collider. The analysis assumes the resonance is produced via gluon-gluon fusion and decays into a $\tau^+\tau^-$ pair which subsequently decays into a fully leptonic $\mu^+\nu_\mu\bar{\nu}_\tau e^-\bar{\nu}_e\nu_\tau$ or $e^+\nu_e\bar{\nu}_\tau\mu^-\bar{\nu}_\mu\nu_\tau$ final state. No significant excess of events above the predicted Standard Model background is observed. The results are interpreted within a flavour-aligned two-Higgs-doublet model, and a model-independent cross-section interpretation is also given. Upper limits at 95% confidence level between 3.0 pb and 68 pb are set on the cross-section for producing a CP-odd Higgs boson that decays into a $\tau^+\tau^-$ pair.

Keywords: Hadron-Hadron Scattering, Higgs Physics

ArXiv ePrint: 2409.20381

Open Access, Copyright CERN,
for the benefit of the ATLAS Collaboration.
Article funded by SCOAP^3.

https://doi.org/10.1007/JHEP12(2024)126

JHEP12(2024)126

Contents

1 Introduction **1**

2 ATLAS detector **3**

3 Data and simulated event samples **4**
3.1 Selection of data events 4
3.2 Monte Carlo event simulation 4

4 Event reconstruction **6**

5 Signal selection **7**

6 Background estimation **9**
6.1 Background with prompt leptons 9
6.2 Background with non-prompt leptons 10
6.3 Event yields 12

7 Systematic uncertainties **14**
7.1 Experimental uncertainties 15
7.2 Theoretical uncertainties 16

8 Statistical model and results **18**

9 Conclusion **21**

The ATLAS collaboration **32**

JHEP12(2024)126

1 Introduction

The discovery of a Higgs boson [1, 2] at the Large Hadron Collider (LHC) [3] has provided important insight into the mechanism of electroweak symmetry breaking. Experimental studies of the Higgs boson [4, 5] demonstrate consistency with Standard Model (SM) predictions. However, the discovered particle could still be part of an extended scalar sector motivated by several theoretical arguments [6, 7]. One such extension of the SM is the flavour-aligned two-Higgs-doublet model (2HDM), which introduces a second SU(2) doublet [8]. The couplings of the two doublets to fermions are aligned in flavour space such that one doublet obtains Yukawa couplings like those in the SM, while the second has Yukawa couplings proportional to the former ones, which prevents flavour-changing neutral currents. The proportionality constants between the two diagonalised Yukawa matrices are the fermionic coupling parameters ζ_f. Within this model, five physical Higgs bosons arise, of which two are neutral and CP-even (h, H), one is neutral and CP-odd (A), and the remaining two are charged ($H^{\pm}$). The model thus incorporates a Higgs boson h with SM properties, while allowing the presence

of an additional CP-odd A boson with a mass m_A smaller than the mass of the h boson. A search for a light CP-odd A boson hence provides further insights into the scalar sector and may shed light on its particle multiplicity.

Further interest in the search for a light A boson originates from the anomalous magnetic moment of the muon, a_μ, which has been a topic of discussion because of an observed discrepancy of up to $5\,\sigma$ between the experimental measurement and SM predictions [9–11]. While the theoretical situation is unclear due to contradictory calculations of the hadronic contributions [12–15], the apparent discrepancy motivates searches for physics beyond the SM. The flavour-aligned 2HDM predicts additional contributions to a_μ and can therefore significantly impact the level of agreement with experimental measurements [9, 16]. In particular, fermionic two-loop contributions of the Barr-Zee type [17] involving τ-lepton and top-quark loops coupling to Higgs bosons and to the external photon are important [18–22]. However, it was shown that near-maximal contributions may be required to explain the observed value of a_μ [16, 23]. For neutral and charged Higgs bosons with masses $m_H = m_{H^\pm}$ in the range of 150 GeV to 250 GeV, the a_μ contributions are maximised if the CP-odd Higgs boson A is light, with a mass between 5 GeV and 105 GeV. While loop contributions to a_μ involving the A boson are dominated by its large couplings to τ-leptons and top quarks, the A boson coupling to down-type quarks is suppressed [16, 23]. This motivates the search for CP-odd Higgs bosons A produced in proton-proton (pp) collisions at the LHC via gluon-gluon fusion involving a top-quark loop, with subsequent decay into a pair of τ-leptons: $gg \to A \to \tau^+\tau^-$. Within the flavour-aligned 2HDM, subject to the constraints described above, the cross-section for this production process scales with the square of the up-type quark coupling parameter ζ_u. The current upper limit at 95% confidence level (CL) on $|\zeta_\mathrm{u}|$ is 0.5 [16].

In the analysis presented here, A boson masses from 20 GeV to 90 GeV are considered. Previous searches for neutral Higgs bosons produced by gluon-gluon fusion in pp collisions and with decays into τ-lepton pairs were performed by the ATLAS and CMS collaborations and focused on m_A ranges above a starting value of 60 GeV to 100 GeV [24–28]. The mass range from 20 GeV to 60 GeV is thus explored here for the first time for this production and decay mode.

Since the τ-leptons have transverse momentum values of $p_\mathrm{T} \approx m_A/2$, the final-state hadrons, electrons, and muons from the τ-lepton decays are in a transverse momentum range below $p_\mathrm{T} \approx 45$ GeV. Because of the large background from QCD-induced processes in pp collisions, the trigger p_T thresholds for hadronically decaying τ-leptons are typically well above these values. Electron-muon dilepton triggers, however, apply lower p_T thresholds and are better suited for the light A boson search. Therefore, and also to suppress background from $Z \to e^+e^-$ and $Z \to \mu^+\mu^-$ decays, the analysis focuses on the fully leptonic signal process with exactly one electron and one muon in the final state, $gg \to A \to \tau^+\tau^- \to \mu^+\nu_\mu\bar{\nu}_\tau e^-\bar{\nu}_e\nu_\tau$ or $gg \to A \to \tau^+\tau^- \to e^+\nu_e\bar{\nu}_\tau\mu^-\bar{\nu}_\mu\nu_\tau$, as shown in figure 1. These final states correspond to 6.2% of all possible $\tau^+\tau^-$ final states [29]. The CP-odd nature of the A boson and its decay kinematics are exploited to further reduce the background.

JHEP12(2024)126

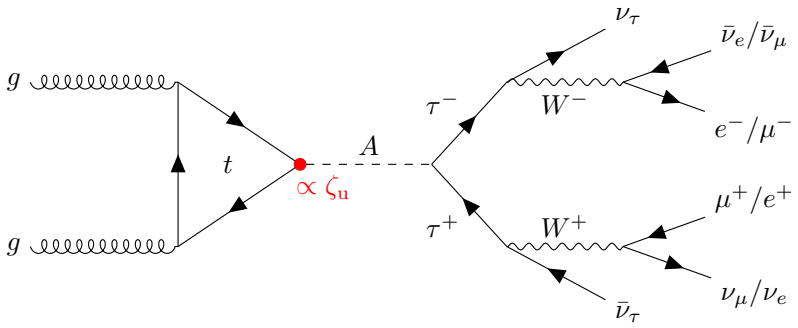

Figure 1. Leading-order Feynman diagrams of the processes $gg \to A \to \tau^+\tau^- \to \mu^+\nu_\mu\bar{\nu}_\tau e^-\bar{\nu}_e\nu_\tau$, $e^+\nu_e\bar{\nu}_\tau\mu^-\bar{\nu}_\mu\nu_\tau$ within the flavour-aligned 2HDM with large A boson couplings to τ-leptons and top quarks, and suppressed couplings to down-type quarks. The vertex in red describes the coupling of the A boson to up-type quarks and scales with ζ_u.

2 ATLAS detector

The ATLAS detector [30] at the LHC covers nearly the entire solid angle around the collision point.[1] It consists of an inner tracking detector surrounded by a thin superconducting solenoid, electromagnetic and hadronic calorimeters, and a muon spectrometer incorporating three large superconducting air-core toroidal magnets.

The inner-detector system (ID) is immersed in a 2 T axial magnetic field and provides charged-particle tracking in the range $|\eta| < 2.5$. The high-granularity silicon pixel detector covers the vertex region and typically provides four measurements per track, the first hit generally being in the insertable B-layer (IBL) installed before Run 2 [31, 32]. It is followed by the SemiConductor Tracker (SCT), which usually provides eight measurements per track. These silicon detectors are complemented by the transition radiation tracker (TRT), which enables radially extended track reconstruction up to $|\eta| = 2.0$. The TRT also provides electron identification information based on the fraction of hits (typically 30 in total) above a higher energy-deposit threshold corresponding to transition radiation.

The calorimeter system covers the pseudorapidity range $|\eta| < 4.9$. Within the region $|\eta| < 3.2$, electromagnetic calorimetry is provided by barrel and endcap high-granularity lead/liquid-argon (LAr) calorimeters, with an additional thin LAr presampler covering $|\eta| < 1.8$ to correct for energy loss in material upstream of the calorimeters. Hadronic calorimetry is provided by the steel/scintillator-tile calorimeter, segmented into three barrel structures within $|\eta| < 1.7$, and two copper/LAr hadronic endcap calorimeters. The solid angle coverage is completed with forward copper/LAr and tungsten/LAr calorimeter modules optimised for electromagnetic and hadronic energy measurements, respectively.

[1] ATLAS uses a right-handed coordinate system with its origin at the nominal interaction point (IP) in the centre of the detector and the z-axis along the beam pipe. The x-axis points from the IP to the centre of the LHC ring, and the y-axis points upwards. Polar coordinates (r, ϕ) are used in the transverse plane, ϕ being the azimuthal angle around the z-axis. The pseudorapidity is defined in terms of the polar angle θ as $\eta = -\ln\tan(\theta/2)$ and is equal to the rapidity $y = \frac{1}{2}\ln\left(\frac{E+p_z}{E-p_z}\right)$ in the relativistic limit. Angular distance is measured in units of $\Delta R \equiv \sqrt{(\Delta y)^2 + (\Delta\phi)^2}$.

JHEP12(2024)126

The muon spectrometer (MS) comprises separate trigger and high-precision tracking chambers measuring the deflection of muons in a magnetic field generated by the superconducting air-core toroidal magnets. The field integral of the toroids ranges between 2.0 and 6.0 T m across most of the detector. Three layers of precision chambers, each consisting of layers of monitored drift tubes, cover the region $|\eta| < 2.7$, complemented by cathode-strip chambers in the forward region, where the background is highest. The muon trigger system covers the range $|\eta| < 2.4$ with resistive-plate chambers in the barrel, and thin-gap chambers in the endcap regions.

The luminosity is measured mainly by the LUCID-2 [33] detector that records Cherenkov light produced in the quartz windows of photomultipliers located close to the beampipe.

Events are selected by the first-level trigger system implemented in custom hardware, followed by selections made by algorithms implemented in software in the high-level trigger [34]. The first-level trigger accepts events from the 40 MHz bunch crossings at a rate below 100 kHz, which the high-level trigger further reduces in order to record complete events to disk at about 1 kHz.

A software suite [35] is used in data simulation, in the reconstruction and analysis of real and simulated data, in detector operations, and in the trigger and data acquisition systems of the experiment.

3 Data and simulated event samples

3.1 Selection of data events

The search presented in this paper uses the full pp collision dataset recorded by the ATLAS detector between 2015 and 2018 (Run 2), with the LHC operating at a centre-of-mass energy of $\sqrt{s} = 13$ TeV and a bunch spacing of 25 ns. In this period, the LHC delivered colliding beams with a peak instantaneous luminosity of $L = 2.1 \times 10^{34}\,\mathrm{cm^{-2}s^{-1}}$, achieved in 2018, and an average number of pp interactions per bunch crossing $\langle\mu\rangle$ of 13, 25, 38, and 36 for 2015, 2016, 2017, and 2018 data, respectively [36]. After applying beam, detector, and data-quality criteria the total integrated luminosity of the data is 140 $\mathrm{fb^{-1}}$. The data were recorded using three partially overlapping electron-muon dilepton triggers [37, 38] that applied identification criteria based on shower shapes in the electromagnetic calorimeter. The first trigger required lepton transverse momenta of $p_{\mathrm{T}}^{e} > 17$ GeV and $p_{\mathrm{T}}^{\mu} > 14$ GeV, while the other two triggers covered the lower p_{T} ranges, with either $p_{\mathrm{T}}^{e} > 7$ GeV and $p_{\mathrm{T}}^{\mu} > 24$ GeV or $p_{\mathrm{T}}^{e} > 24$ GeV and $p_{\mathrm{T}}^{\mu} > 8$ GeV, respectively. These trigger requirements have an efficiency of 72% to 92%, depending on the final state and the dataset, for signal events passing the final signal-region selections.

3.2 Monte Carlo event simulation

All signal and background processes were modelled using Monte Carlo (MC) simulations, with the exception of backgrounds with fake or non-prompt leptons, which were estimated from data (see section 6.2).

Each sample was passed through the full GEANT4 [39, 40] simulation of the ATLAS detector and reconstructed with the same software as used for data. The only exceptions

JHEP12(2024)126

m_A [GeV]	20	25	30	40	50	60	70	75
$\sigma(pp \to A + X)$ [pb]	1854	1394	1090	722	514	385	299	266
$\mathcal{A}_{\text{signal}} \times \varepsilon_{\text{signal}}$ [%]	0.017	0.038	0.060	0.094	0.10	0.091	0.077	0.20

m_A [GeV]	80	85	90
$\sigma(pp \to A + X)$ [pb]	239	215	195
$\mathcal{A}_{\text{signal}} \times \varepsilon_{\text{signal}}$ [%]	0.20	0.19	0.18

Table 1. N^{3}LO prediction of the cross-section for A boson production, $\sigma(pp \to A + X)$, via gluon-gluon fusion in the relevant mass range. Values were calculated with `ggHiggs` [44–55] version 4.0, setting the fermionic coupling strength parameters of the A boson to $\cot\beta = \zeta_u = \zeta_\ell = 1$. The product of the signal acceptance $\mathcal{A}_{\text{signal}}$ and efficiency $\varepsilon_{\text{signal}}$ is the fraction of events generated for gluon-gluon fusion production of the CP-odd Higgs boson A (which is forced to decay into a leptonically decaying $\tau^+\tau^-$ pair) that are reconstructed in the detector and accepted by the analysis event selection described in section 5.

are the signal samples, for which the fast simulation ATLFAST-II [41] was used, where the GEANT4 simulation of calorimeter showers is replaced by a parameterised simulation. The gluon-gluon fusion signal-production process for this analysis, $gg \to A \to \tau^+\tau^-$, was simulated with PYTHIA 8.2 [42], using leading-order (LO) matrix elements (ME) for A bosons with masses of 20 GeV to 90 GeV in steps of 10 GeV, as well as for 25 GeV, 75 GeV and 85 GeV. Both τ-leptons were forced to decay leptonically. The parton shower, hadronisation, and underlying event were modelled with parameter values set according to the A14 tune and with the NNPDF2.3LO set of parton distribution functions (PDF) [43]. The signal's production cross-section was calculated at N^{3}LO with `ggHiggs` [44–55] version 4.0, setting the coupling parameter of the A boson to up-type quarks to $\cot\beta = \zeta_u = 1$, where $\cot\beta$ is the ratio of the vacuum expectation values of the two Higgs doublets and is used by `ggHiggs` to parameterise the fermionic coupling parameter. The cross-section values are shown in table 1 for the relevant mass range.

The MC-simulated background processes considered in this analyses include those with vector bosons (diboson and V+jets, where $V = W, Z$), top quarks ($t\bar{t}$, s- and t-channel single-top, and associated production of a top quark and a W boson (tW)), and SM Higgs bosons, which are all modelled differently.

The V+jets processes were simulated with the SHERPA 2.2.1 [56] generator, with next-to-leading-order (NLO) MEs for up to two partons and LO MEs for up to four partons. The diboson background processes were simulated with NLO MEs for up to one parton and LO MEs for up to three partons, using the SHERPA 2.2.1 [56] or SHERPA 2.2.2 [56] generator, depending on the process. The top-quark-related backgrounds were modelled using the POWHEG BOX v2 [57–60] generator at NLO accuracy in QCD with the NNPDF3.0NLO PDF set [61]. Both the tW and s-channel single-top events were generated using the five-flavour

JHEP12(2024)126

scheme. However, a four-flavour scheme was used for t-channel single-top events. For the $t\bar{t}$ sample, a value of $1.5\,m_t$ was assigned to the resummation damping factor h_{damp}, which controls the matching of the POWHEG ME to the parton shower and thus effectively regulates the high-p_{T} radiation against which the $t\bar{t}$ system recoils.

In order to model the parton shower, hadronisation, and underlying event, the top-quark background events were interfaced to PYTHIA 8.230 with parameter values set according to the A14 tune [62], while the SHERPA parton shower [63], using the MEPS@NLO prescription [64–67] and the set of tuned parameters developed by the SHERPA authors, was applied to W/Z+jets and diboson background events. The NNPDF2.3LO PDF set was used for both types of background.

SM Higgs boson production was simulated using POWHEG BOX v2 [58–60, 68, 69], interfaced with PYTHIA 8 for parton showering and non-perturbative effects. The PDF4LHC15NLO PDF set [70] and the AZNLO tune [71] of PYTHIA 8 were used. SM Higgs boson production via gluon-gluon fusion and via vector-boson fusion was simulated at next-to-next-to-leading-order (NNLO) and NLO accuracy in QCD, respectively. The POWHEG prediction is accurate to NLO for Vh boson plus one-jet production. The loop-induced $gg \to Zh$ process was generated separately at LO. The normalisation of all SM Higgs boson samples accounts for the decay branching ratio calculated with HDECAY [72–74] and PROPHECY4F [75–77]. The MC prediction for SM Higgs boson production via gluon-gluon fusion was normalised to the cross-section calculated to N^{3}LO in QCD with NLO electroweak (EW) corrections [51, 52, 54, 78–85], while that for production via vector-boson fusion was normalised to the cross-section calculated to approximate-NNLO in QCD with NLO EW corrections [86–88]. The MC predictions for $q\bar{q}/qg \to Vh$ and $gg \to Zh$ were normalised to the cross-section calculated to NNLO in QCD with NLO EW corrections or to NLO and next-to-leading-logarithm accuracy in QCD, respectively [89–95].

To model additional pp interactions in the same or neighbouring bunch crossings (pile-up), the hard-scattering events were overlaid with a set of minimum-bias interactions generated using PYTHIA 8.186 [96] and the NNPDF2.3LO PDF set with the A3 set of tuned parameters [97]. Finally, all simulated events are reweighted to match the instantaneous luminosity spectrum in data.

4 Event reconstruction

Charged-particle tracks measured in the ID are used to reconstruct interaction vertices [98], and the one with the highest sum of squared transverse momenta $\sum p_{\text{T}}^2$ of the associated tracks is selected as the primary vertex of the hard interaction.

Electrons are reconstructed from topological clusters of energy deposits in the electromagnetic calorimeter which are matched to a track reconstructed in the ID and are required to satisfy *Loose* identification and *Loose* isolation criteria [99], based on track and shower-shape discriminants.

Muons are reconstructed from signals in the muon spectrometer matched to tracks inside the ID. They are also required to satisfy *Loose* identification and *Loose* isolation criteria based on track information [100].

JHEP12(2024)126

Jets are reconstructed from particle-flow objects [101] using the anti-k_t algorithm [102] with radius parameter $R = 0.4$. This algorithm uses noise-suppressed positive-energy topological clusters in the calorimeter after subtracting energy deposits associated with primary-vertex-matched tracks and including the momenta of those tracks in the clustering instead, thereby improving the jet energy measurement. The jet energy scale is calibrated to the particle level using simulation and further corrected with in-situ methods [103]. Cleaning criteria are used to identify jets arising from non-collision backgrounds or noise in the calorimeters [104]. A dedicated jet-vertex-tagger algorithm [105] is used to remove jets within $|\eta| < 2.5$ that are identified as not being associated with the primary vertex of the hard interaction. Similarly, a dedicated algorithm is used to suppress such "pile-up" jets, arising from additional softer pp interactions, in the forward region [106].

Jets containing b-hadrons are identified using the DL1r [107] b-tagging algorithm. A jet is classified as a b-tagged jet if the DL1r score is above a certain threshold, referred to as an "operating point". In this analysis, the operating point is chosen to obtain an average expected efficiency of 85% for b-jet identification, as determined in simulated $t\bar{t}$ events.

Since the different physical objects are reconstructed independently, multiple objects may be reconstructed from the same detector signal, whereas a signal rarely has contributions from multiple objects. To achieve orthogonality, an overlap removal procedure is performed on objects with small angular separation ΔR to remove the object with lower signal purity. Muons are favoured over electrons if one lies within a $\Delta R = 0.2$ cone around the other, and leptons are favoured over jets if their angular separation is $\Delta R < 0.4$.

The missing transverse momentum $\vec{p}_{\mathrm{T}}^{\,\mathrm{miss}}$ (with magnitude $E_{\mathrm{T}}^{\mathrm{miss}}$) is reconstructed as the negative vector sum of the transverse momenta of leptons, visible hadronic τ-lepton decay products ($\tau_{\text{had-vis}}$) [108], jets, and a "soft term". The "soft term" is calculated as the vector sum of the p_{T} of tracks matched to the primary vertex but not to reconstructed leptons, $\tau_{\text{had-vis}}$ candidates, or jets [109].

An advanced likelihood-based algorithm named the Missing Mass Calculator (MMC) [110, 111] is used to estimate the invariant mass, m_{MMC}, of the τ-lepton pair under the assumption that only neutrinos originating from the τ-lepton decays contribute to $E_{\mathrm{T}}^{\mathrm{miss}}$. In order to resolve the remaining ambiguities in the reconstruction of the neutrino momenta, the method incorporates additional knowledge of the decay kinematics in terms of probability density functions, such as distributions of the expected angular distances between the decay products of the τ-leptons.

5 Signal selection

This analysis focuses on final states with exactly one electron and one muon with opposite charges and p_{T} greater than 10 GeV. Events are required to have been accepted by at least one of the electron-muon triggers that were active during the data-taking periods (see section 3). The leptons firing the trigger must match the two reconstructed leptons with the highest p_{T} in the event. The matching is performed according to the angular distance ΔR between the trigger signature and the reconstructed lepton, requiring $\Delta R < 0.07$ for electrons and $\Delta R < 0.1$ for muons. Furthermore, the selected electron or muon candidates are required to satisfy *Medium* identification and *Tight* or *Tight_VarRad* isolation criteria [99, 100], respectively, in

JHEP12(2024)126

	SR		TCR	ZCR	FVR
	Low-mass	High-mass			
$\lvert\eta_e\rvert$	$[0, 1.37] \cup [1.52, 2.47]$		$[0, 1.37] \cup [1.52, 2.47]$		$[0, 1.37] \cup [1.52, 2.47]$
$\lvert\eta_\mu\rvert$	$[0, 2.7]$		$[0, 2.7]$		$[0, 2.7]$
$\lvert\eta_j\rvert$	$[0, 4.5]$		$[0, 4.5]$		$[0, 4.5]$
p_{T}^{ℓ}	$> 10\,\mathrm{GeV}$		$> 10\,\mathrm{GeV}$		$> 10\,\mathrm{GeV}$
p_{T}^{j}	$> 20\,\mathrm{GeV}$		$> 20\,\mathrm{GeV}$		$> 20\,\mathrm{GeV}$
$E_{\mathrm{T}}^{\mathrm{miss}}$	$> 50\,\mathrm{GeV}$	$> 30\,\mathrm{GeV}$	$> 30\,\mathrm{GeV}$	–	–
$m_{\mathrm{T}}^{\mathrm{tot}}$	$< 45\,\mathrm{GeV}$	$< 65\,\mathrm{GeV}$	$< 65\,\mathrm{GeV}$	$< 65\,\mathrm{GeV}$	$< 65\,\mathrm{GeV}$
$\Delta R_{\ell\ell}$	< 0.7	< 1.0	< 1.0	> 1.4	> 1.4
m_{MMC}	$> 0\,\mathrm{GeV}$	$> 35\,\mathrm{GeV}$ & $< 130\,\mathrm{GeV}$	$> 0\,\mathrm{GeV}$	$> 0\,\mathrm{GeV}$	$> 0\,\mathrm{GeV}$
$q_e \times q_\mu$	-1	-1	-1	-1	1
$n_{b\text{-jets}}$	0	0	≥ 2	0	0

Table 2. Overview of the selection criteria for the most important regions: the low-mass and high-mass signal regions (SR), the top control region (TCR), the $Z \to \tau^+\tau^-$ control region (ZCR) and the fake-lepton validation region (FVR). For the final results of the analysis, *Medium* identification and *Tight* isolation criteria are used [99, 100]. For the fake-lepton background estimation, *Loose* criteria are used additionally.

order to increase the signal region's purity in true reconstructed leptons. Additionally, events with leptons satisfying the *Loose* criteria are used in the fake-lepton estimation.

The signal region (SR) definition depends on the probed A mass value: masses from 20 to 75 GeV are examined in the low-mass SR, and masses from 75 to 90 GeV are examined in the high-mass SR. A common requirement for both SRs is that the number of b-tagged jets, $n_{b\text{-jets}}$, must be zero. This significantly reduces the background from top quarks. In order to optimise the signal sensitivity, the low-mass SR and the high-mass SR have individualised selection criteria for $E_{\mathrm{T}}^{\mathrm{miss}}$, the total transverse mass defined as $m_{\mathrm{T}}^{\mathrm{tot}} = \sqrt{\left(p_{\mathrm{T}}^{e} + p_{\mathrm{T}}^{\mu} + E_{\mathrm{T}}^{\mathrm{miss}}\right)^2 - \left(\vec{p}_{\mathrm{T}}^{\,e} + \vec{p}_{\mathrm{T}}^{\,\mu} + \vec{p}_{\mathrm{T}}^{\,\mathrm{miss}}\right)^2}$, the angular distance between the charged leptons $\Delta R_{\ell\ell}$, and m_{MMC}. The selection criteria are summarised in table 2. The $m_{\mathrm{T}}^{\mathrm{tot}}$ criterion primarily removes diboson events and events with top quarks. The requirement on $\Delta R_{\ell\ell}$ reduces the $Z \to \tau^+\tau^-$ background, motivated by the mass, spin and CP properties of the A boson signal, and requires the emitted leptons to have a small angular separation. This kinematic configuration also enhances the fraction of A bosons produced with sizeable transverse momentum p_{T}^{A}. Thus, the p_{T}^{A} distribution starts at approximately 100 to 200 GeV, depending on the mass hypothesis. Therefore, hadronic jets are emitted in the opposite direction to conserve transverse momentum, meaning the process $pp \to A +$ jets is preferred for this topology (considering only the gluon-gluon fusion production mode as suggested by the flavour-aligned 2HDM).

JHEP12(2024)126

6 Background estimation

There are two primary sources of background events associated with the event selection described in section 5: events with electrons and muons produced in W, Z/γ^*, SM Higgs boson or top-quark decays (prompt leptons) and events that have at least one lepton arising from another source (fake and non-prompt leptons). In the latter case, electrons and muons originate from improper reconstruction of other physics objects such as hadronic jets, heavy-flavour hadron decays or photon conversions. All processes associated with the prompt-lepton background are predominantly well modelled by simulation and therefore estimated from MC event samples, described in section 3.2. Two control regions, enriched in top-quark (TCR) and $Z \to \tau^+\tau^-$ (ZCR) events, are designed to control and validate the major backgrounds modelled by MC simulation. The fake-lepton validation region (FVR) is designed and used to estimate and validate the fake/non-prompt-lepton background using a data-driven method. A summary of the requirements for all regions is given in table 2.

6.1 Background with prompt leptons

The ZCR is used to control the main background in this analysis, which originates from $Z \to \tau^+\tau^-$ decays. The requirements for this region are to have an abundance of $Z \to \tau^+\tau^-$ decays, to be orthogonal to the SR, and to have low contamination from signal events while being kinematically close to the SR. This is achieved by having selection criteria similar to those for the SR, but requiring $\Delta R_{\ell\ell} > 1.4$ because the two leptons originating from the Z boson are well separated. Additionally, the $E_{\mathrm{T}}^{\mathrm{miss}}$ criterion is dropped in order to obtain a large sample of $Z \to \tau^+\tau^-$ decays with low signal contamination.

The distributions of some variables in the ZCR showed mismodelling of $Z \to \tau^+\tau^-$ events. In particular, the event count with the number of jets, n_{jets}, equal to 0 is underestimated in simulation and increasingly overestimated for $n_{\mathrm{jets}} > 1$. Also, for high values of the transverse momentum of the ditau system,[2] $p_{\mathrm{T}}^{\tau\tau} > 50\,\mathrm{GeV}$, and for $E_{\mathrm{T}}^{\mathrm{miss}}$ between 50 and 100 GeV a surplus of background events is observed. This region is especially important for this analysis because the high-mass SR (low-mass SR) requires $E_{\mathrm{T}}^{\mathrm{miss}} > 30\,(50)\,\mathrm{GeV}$, and $Z \to \tau^+\tau^-$ events are the main background in the SR. Therefore, a data-driven reweighting method, similar to the one used in ref. [112], is chosen to obtain better agreement between the prediction and data in the ZCR. The weights are calculated as the ratio of the expected number of $Z \to \tau^+\tau^-$ events to the simulated number in the ZCR and binned in the number of jets. The expected number of events is obtained from data by subtracting the predicted number of other simulated background events, which do not originate from $Z \to \tau^+\tau^-$. The fake-lepton background (see section 6.2) must also be taken into account, so the efficiencies for the "matrix method" described in the next section must be determined prior to the calculation of the $Z \to \tau^+\tau^-$ weights. The weights range from 0.8 to 1.12 with a tendency to be closer to unity for a smaller number of jets. The reweighting not only resolves the mismodeling of n_{jets} but also improves the data-to-background agreement of the $p_{\mathrm{T}}^{\tau\tau}$ and $E_{\mathrm{T}}^{\mathrm{miss}}$ distributions in the ZCR.

The TCR is constructed to control the background resulting from processes involving top quarks, which produce one of the largest backgrounds in this analysis. It has almost

[2]The transverse momentum of the ditau system is defined as the magnitude of the vector sum of the transverse momenta of the electron and the muon and of the missing transverse momentum: $p_{\mathrm{T}}^{\tau\tau} = |\vec{p}_{\mathrm{T}}^{\,e} + \vec{p}_{\mathrm{T}}^{\,\mu} + \vec{p}_{\mathrm{T}}^{\,\mathrm{miss}}|$.

JHEP12(2024)126

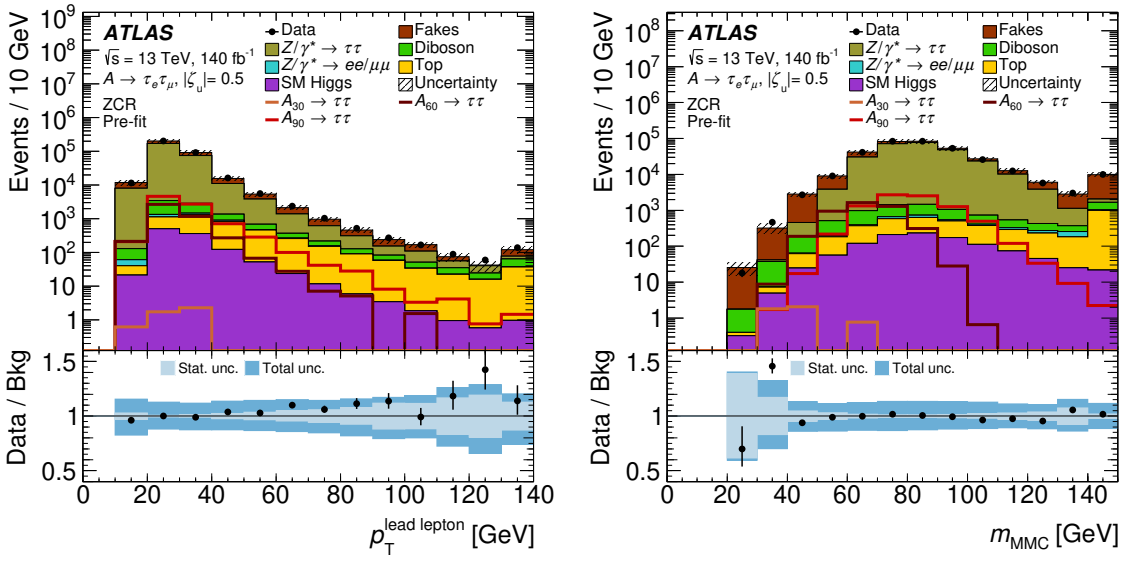

(a) (b)

Figure 2. Pre-fit variable distributions in the ZCR after applying all selection criteria: (a) leading-lepton p_{T} and (b) m_{MMC} mass estimator. The background is estimated by using MC samples and data-driven methods (see text for details). The expected signal contributions for the mass hypotheses $m_A = 30, 60$ and 90 GeV are shown assuming $|\zeta_{\mathrm{u}}| = 0.5$. Events with values exceeding the x-axis range are shown in the last bin of each distribution. The dark blue band in the ratio plot shows the total uncertainty from statistical and systematic sources. The statistical uncertainty band is overlaid in light blue.

the same requirements as the high-mass SR, but at least two b-tagged jets are required. Requiring $n_{b\text{-jets}} \geq 1$ was also tested, but the contamination from signal events was too large. Furthermore, a small improvement to the modelling is incorporated by reweighting each $t\bar{t}$ sample so that its top-quark p_{T} distribution matches that calculated to NNLO in QCD with NLO EW corrections [113]. Figure 2 and figure 3 show the validation of Z+jets and top-quark backgrounds, respectively. In both cases, the observed data agree well with the estimated background within their respective uncertainties.

6.2 Background with non-prompt leptons

The FVR is constructed to perform and validate the fake-lepton estimation in a region enriched in non-prompt leptons. It has the same requirements as the ZCR, except that the two leptons are required to have the same charge. This region can be used for a closure test of the fake-lepton estimation, and systematic uncertainties can be extracted.

To estimate the total contribution of events with fake or non-prompt leptons, as well as leptons with misidentified charge (hereinafter collectively referred to as fake-lepton background), a data-driven matrix method [114] is used, which is especially useful in cases where events with either zero, one, or two fake leptons are expected. Two categories of events are selected, satisfying baseline (*Loose* isolation and *Loose* identification) and tight (*Tight* isolation and *Medium* identification) lepton selection requirements as described in section 5.

JHEP12(2024)126

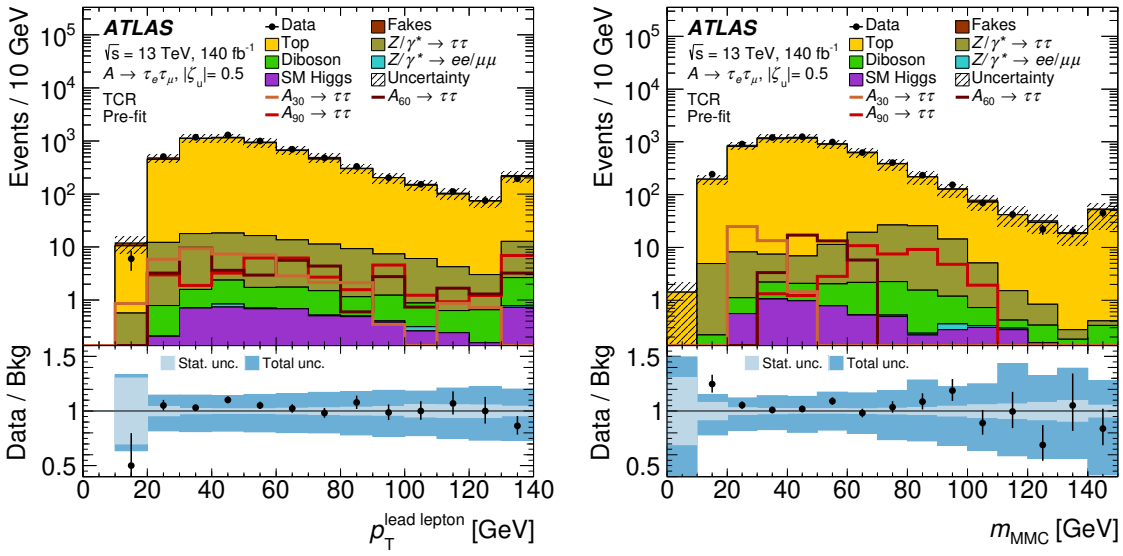

(a) (b)

Figure 3. Pre-fit variable distributions in the TCR after applying all selection criteria: (a) leading-lepton p_{T} and (b) m_{MMC} mass estimator. The background is estimated by using MC samples and data-driven methods (see text for details). The expected signal contributions for the mass hypotheses $m_A = 30, 60$ and $90\,\mathrm{GeV}$ are shown assuming $|\zeta_{\mathrm{u}}| = 0.5$. Events with values exceeding the x-axis range are shown in the last bin of each distribution. The dark blue band in the ratio plot shows the total uncertainty from statistical and systematic sources. The statistical uncertainty band is overlaid in light blue.

The efficiencies for fake leptons, $\varepsilon^{\ell}_{\mathrm{fake}}$, and for real leptons, $\varepsilon^{\ell}_{\mathrm{real}}$, that meet the tight criteria are used to estimate the rate of events with fake leptons from the numbers of tight and non-tight events passing the baseline selection. This is done by inverting the equation

$$\begin{pmatrix} N^{\mathrm{TT}}_{\mathrm{XX}} \\ N^{\mathrm{T\overline{T}}}_{\mathrm{XX}} \\ N^{\mathrm{\overline{T}T}}_{\mathrm{XX}} \\ N^{\mathrm{\overline{T}\overline{T}}}_{\mathrm{XX}} \end{pmatrix} = \begin{pmatrix} \varepsilon^{e}_{\mathrm{real}}\varepsilon^{\mu}_{\mathrm{real}} & \varepsilon^{e}_{\mathrm{real}}\varepsilon^{\mu}_{\mathrm{fake}} & \varepsilon^{e}_{\mathrm{fake}}\varepsilon^{\mu}_{\mathrm{real}} & \varepsilon^{e}_{\mathrm{fake}}\varepsilon^{\mu}_{\mathrm{fake}} \\ \varepsilon^{e}_{\mathrm{real}}\bar{\varepsilon}^{\mu}_{\mathrm{real}} & \varepsilon^{e}_{\mathrm{real}}\bar{\varepsilon}^{\mu}_{\mathrm{fake}} & \varepsilon^{e}_{\mathrm{fake}}\bar{\varepsilon}^{\mu}_{\mathrm{real}} & \varepsilon^{e}_{\mathrm{fake}}\bar{\varepsilon}^{\mu}_{\mathrm{fake}} \\ \bar{\varepsilon}^{e}_{\mathrm{real}}\varepsilon^{\mu}_{\mathrm{real}} & \bar{\varepsilon}^{e}_{\mathrm{real}}\varepsilon^{\mu}_{\mathrm{fake}} & \bar{\varepsilon}^{e}_{\mathrm{fake}}\varepsilon^{\mu}_{\mathrm{real}} & \bar{\varepsilon}^{e}_{\mathrm{fake}}\varepsilon^{\mu}_{\mathrm{fake}} \\ \bar{\varepsilon}^{e}_{\mathrm{real}}\bar{\varepsilon}^{\mu}_{\mathrm{real}} & \bar{\varepsilon}^{e}_{\mathrm{real}}\bar{\varepsilon}^{\mu}_{\mathrm{fake}} & \bar{\varepsilon}^{e}_{\mathrm{fake}}\bar{\varepsilon}^{\mu}_{\mathrm{real}} & \bar{\varepsilon}^{e}_{\mathrm{fake}}\bar{\varepsilon}^{\mu}_{\mathrm{fake}} \end{pmatrix} \cdot \begin{pmatrix} N^{\mathrm{LL}}_{\mathrm{RR}} \\ N^{\mathrm{LL}}_{\mathrm{RF}} \\ N^{\mathrm{LL}}_{\mathrm{FR}} \\ N^{\mathrm{LL}}_{\mathrm{FF}} \end{pmatrix},$$

where $\bar{\varepsilon}^{\ell}_{\mathrm{real/fake}} = 1 - \varepsilon^{\ell}_{\mathrm{real/fake}}$. The indices of the event yields N are to be read as follows. The upper indices describe the tightness of the leptons, where T means that the lepton is required to be tight, $\overline{\mathrm{T}}$ that it has to be non-tight, and L that the lepton is part of the baseline selection without further requirements on the tightness. The lower indices indicate whether an event comes from data or from MC simulation, and in the latter case whether the lepton is real (R), fake (F), or without a requirement on a certain "truth" state (X) in the MC event record. The first index always describes the electron, the second one the muon. For example, $N^{\mathrm{LT}}_{\mathrm{RX}}$ is the number of MC events with a real electron that passes the baseline selection and a tight muon, and $N^{\mathrm{T\overline{T}}}_{\mathrm{Data}}$ is the number of data events with a tight electron and a non-tight muon. The total fake-lepton background is then the sum of the

JHEP12(2024)126

fake-electron, fake-muon, and double-fake-lepton backgrounds

$$N_{\text{fake}}^{\text{TT}} = \varepsilon_{\text{real}}^{e}\varepsilon_{\text{fake}}^{\mu}N_{\text{RF}}^{\text{LL}} + \varepsilon_{\text{fake}}^{e}\varepsilon_{\text{real}}^{\mu}N_{\text{FR}}^{\text{LL}} + \varepsilon_{\text{fake}}^{e}\varepsilon_{\text{fake}}^{\mu}N_{\text{FF}}^{\text{LL}}.$$

The real-lepton (fake-lepton) efficiency is defined as the ratio of the number of real (fake) leptons satisfying the tight selection to the number of real (fake) leptons satisfying the baseline selection. The real-lepton efficiencies are estimated using the "truth particle" classification from the MC event record, while the fake-lepton efficiencies are estimated from data after subtracting the MC-estimated prompt-lepton background. Assuming that the electron efficiencies are independent of the muon produced in the same event and vice versa, the conventional matrix method is valid. In this analysis, however, it was observed that the fake-lepton efficiencies are not entirely independent of the other (fake) lepton in the event. To account for this, a parameterisation of the real- and fake-lepton efficiencies, based on the tightness of the other lepton, is introduced such that the electron efficiencies depend on the muon's tightness and vice versa:

$$\varepsilon_{\text{real}}^{e}(\mu) = \begin{cases} \dfrac{N_{\text{RX}}^{\text{TT}}}{N_{\text{RX}}^{\text{LT}}}, & \mu \text{ tight} \\ \dfrac{N_{\text{RX}}^{\text{T}\overline{\text{T}}}}{N_{\text{RX}}^{\text{L}\overline{\text{T}}}}, & \mu \text{ non-tight} \end{cases}, \qquad \varepsilon_{\text{real}}^{\mu}(e) = \begin{cases} \dfrac{N_{\text{XR}}^{\text{TT}}}{N_{\text{XR}}^{\text{TL}}}, & e \text{ tight} \\ \dfrac{N_{\text{XR}}^{\overline{\text{T}}\text{T}}}{N_{\text{XR}}^{\overline{\text{T}}\text{L}}}, & e \text{ non-tight} \end{cases},$$

$$\varepsilon_{\text{fake}}^{e}(\mu) = \begin{cases} \dfrac{N_{\text{Data}}^{\text{TT}} - N_{\text{RX}}^{\text{TT}}}{N_{\text{Data}}^{\text{LT}} - N_{\text{RX}}^{\text{LT}}}, & \mu \text{ tight} \\ \dfrac{N_{\text{Data}}^{\text{T}\overline{\text{T}}} - N_{\text{RX}}^{\text{T}\overline{\text{T}}}}{N_{\text{Data}}^{\text{L}\overline{\text{T}}} - N_{\text{RX}}^{\text{L}\overline{\text{T}}}}, & \mu \text{ non-tight} \end{cases}, \quad \varepsilon_{\text{fake}}^{\mu}(e) = \begin{cases} \dfrac{N_{\text{Data}}^{\text{TT}} - N_{\text{XR}}^{\text{TT}}}{N_{\text{Data}}^{\text{TL}} - N_{\text{XR}}^{\text{TL}}}, & e \text{ tight} \\ \dfrac{N_{\text{Data}}^{\overline{\text{T}}\text{T}} - N_{\text{XR}}^{\overline{\text{T}}\text{T}}}{N_{\text{Data}}^{\overline{\text{T}}\text{L}} - N_{\text{XR}}^{\overline{\text{T}}\text{L}}}, & e \text{ non-tight} \end{cases}.$$

Additionally, the efficiencies are binned in lepton p_{T} as shown in figure 4, revealing that the fake-lepton efficiencies depend on the tightness of the accompanying lepton for low p_{T}, while the real-lepton efficiencies are statistically compatible.

When considering real-lepton efficiencies in events with a tight accompanying lepton, it is possible to extract them directly from the SR, as it contains a sufficient number of well-modelled real leptons from prompt-lepton MC background events. Also, different real-lepton efficiencies are calculated for the high-mass SR and low-mass SR, with the $E_{\text{T}}^{\text{miss}}$ criterion removed in the latter to increase the event yield. The real efficiencies for events with a non-tight accompanying lepton are calculated in the ZCR because it has more events than the SR. To calculate the fake-lepton efficiencies, one needs a region close to the SR but enriched in fake leptons, conditions best satisfied with enough events by the FVR. Figure 5 shows the validation of the fake-lepton estimate in the FVR, where the fake-lepton efficiencies are measured. In both the $p_{\text{T}}^{\text{lead lepton}}$ and the m_{MMC} distributions, the observed data agrees well with the estimated background within their respective uncertainties.

6.3 Event yields

Table 3 and table 4 summarise the event yields for the signal and background predictions, respectively, in the different regions in comparison with those observed in data. Due to the $Z \to \tau^+\tau^-$ reweighting the data-to-background ratio in the ZCR equals 1 by definition. In the other control regions, the expected yield is in agreement with the observed number of

JHEP12(2024)126

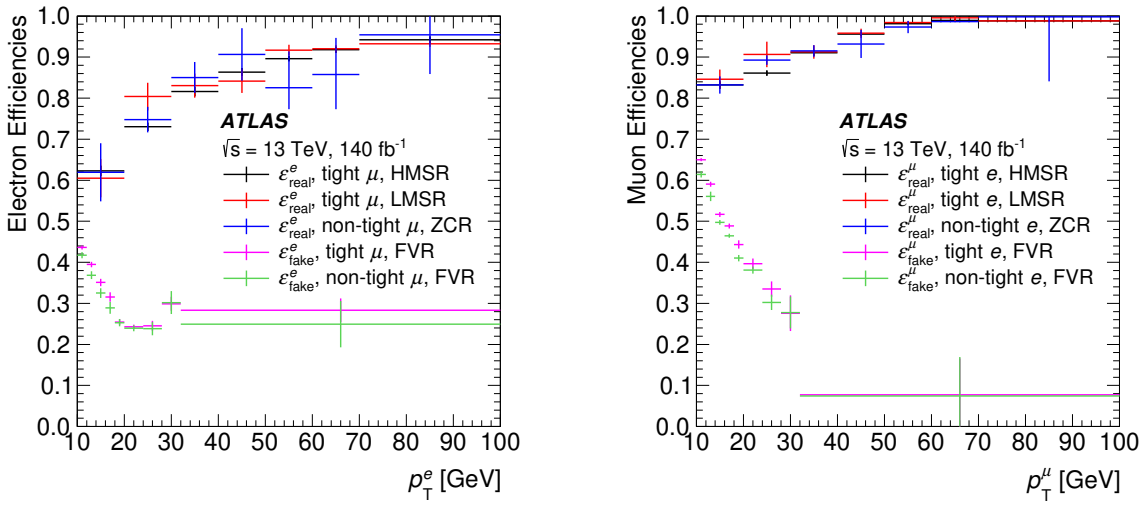

(a) (b)

Figure 4. Fake- and real-lepton efficiencies ($\varepsilon_{\text{fake}}$ and $\varepsilon_{\text{real}}$) for (a) electrons and (b) muons with a tight or non-tight accompanying (a) muon and (b) electron, binned in p_{T}^{e} and p_{T}^{μ}, respectively. Real-lepton efficiencies with a tight accompanying lepton are calculated in the high-mass and low-mass SRs (HMSR and LMSR), real-lepton efficiencies with a non-tight accompanying lepton are calculated in the ZCR, and fake-lepton efficiencies are calculated in the FVR.

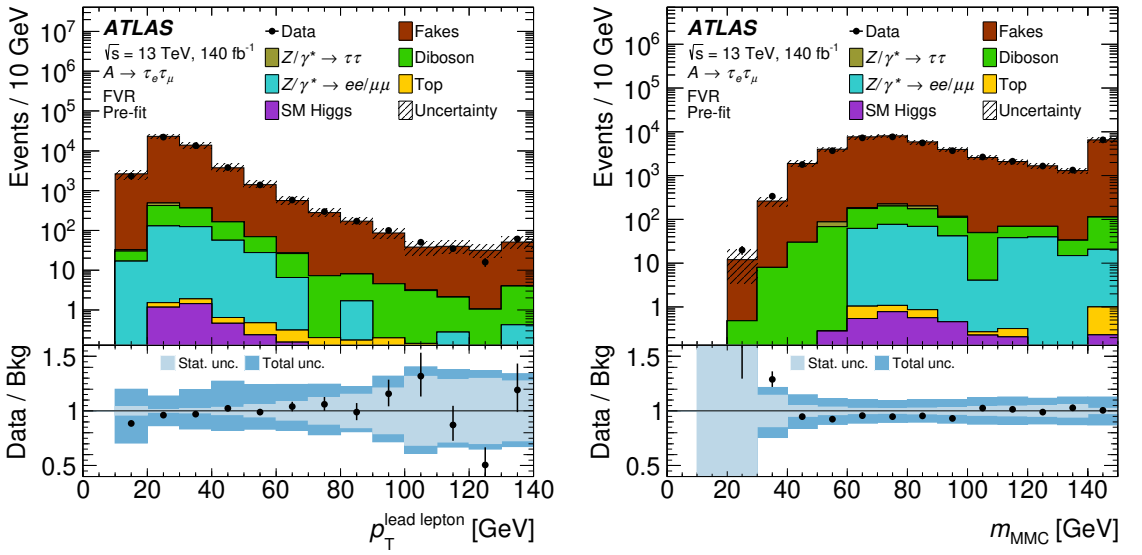

(a) (b)

Figure 5. Pre-fit variable distributions in the FVR after applying all selection criteria: (a) leading-lepton p_{T} and (b) m_{MMC} mass estimator. The background is estimated by using MC samples and data-driven methods (see text for details). Events with values exceeding the x-axis range are shown in the last bin of each distribution. The dark blue band in the ratio plot shows the total uncertainty from statistical and systematic sources. The statistical uncertainty band is overlaid in light blue.

JHEP12(2024)126

m_A [GeV]	ZCR	TCR	Low-mass SR	High-mass SR
20	0.0 ± 0.0	15.4 ± 3.0	1355 ± 27	-
25	0.3 ± 0.3	30.8 ± 3.3	2326 ± 28	-
30	4.7 ± 1.8	39.6 ± 5.3	2865 ± 44	-
40	314 ± 17	59.4 ± 7.6	2940 ± 52	-
50	1706 ± 43	51.2 ± 7.5	2293 ± 51	-
60	4396 ± 71	39.6 ± 7.1	1516 ± 43	-
70	7242 ± 91	53.6 ± 8.1	1002 ± 35	-
75	8083 ± 75	53.9 ± 6.5	774 ± 23	2312 ± 41
80	8520 ± 96	49.9 ± 7.5	-	2011 ± 47
85	8706 ± 76	39.1 ± 5.4	-	1771 ± 35
90	8710 ± 93	39.6 ± 6.3	-	1512 ± 39

Table 3. Pre-fit signal yields in the different analysis regions. The numbers correspond to an integrated luminosity of 140 fb^{-1}. The quoted uncertainties are the statistical uncertainties which arise from the finite number of generated events in the simulated samples. No signal is expected in the FVR. The signal cross-sections are calculated to N^3LO, as summarised in table 1. These cross-section values are multiplied by $0.25 = |\zeta_u|^2 = \cot^2\beta$, which is the highest not-already-excluded value of $|\zeta_u|^2$ [16].

events within the total uncertainty. The systematic uncertainties are described and estimated in the following section. The purity of the $Z \to \tau^+\tau^-$, top-quark and fake-lepton backgrounds reaches 79%, 94% and 97% in the ZCR, TCR and FVR, respectively. No signal is expected in the FVR and it is negligible in both the ZCR and TCR. The purity of the signal in the SR depends on the mass hypothesis, and reaches 60% for masses lower than 60 GeV when scaled according to the cross-sections in table 1 multiplied by 0.25, the highest currently allowed value of $|\zeta_u|^2$ [16].

7 Systematic uncertainties

Systematic uncertainties are categorised into those arising from the measurements (experimental uncertainties) and those due to the modelling of various processes (theoretical uncertainties), where the latter are specific to a single process or a group of processes. In contrast, the experimental uncertainties depend on simulations of the detector and reconstruction of objects, and are therefore independent of the process. A nuisance parameter (NP) with a Gaussian prior is assigned to each systematic uncertainty. Additionally, smoothing and pruning procedures are used to reduce the impact of statistical fluctuations and remove the smallest systematic uncertainties evaluated by performing various "systematic variations". The shape and normalisation components of the systematic uncertainties are dropped if they do not exceed 0.5% for a given process (in the case of the shape uncertainties, if no bin shows an effect greater than 0.5%).

JHEP12(2024)126

	ZCR	FVR	TCR	Low-mass SR	High-mass SR
Fakes	$59\,680 \pm 690$	$44\,850 \pm 430$	213 ± 50	316 ± 45	495 ± 55
	(18%)	(97%)	(3.5%)	(17%)	(9.0%)
$Z/\gamma^* \to \tau^+\tau^-$	$262\,700 \pm 1800$	82 ± 27	116.1 ± 4.0	1210 ± 36	3701 ± 46
	(79%)	(0.18%)	(1.9%)	(63%)	(67%)
Diboson	4552 ± 26	747.3 ± 7.4	10.82 ± 0.50	139.1 ± 2.4	449.2 ± 4.4
	(1.4%)	(1.6%)	(0.18%)	(7.3%)	(8.2%)
$Z/\gamma^* \to \ell^+\ell^-$	468 ± 71	354 ± 68	0.28 ± 0.12	4.0 ± 1.7	9.8 ± 3.3
	(0.14%)	(0.77%)	(< 0.1%)	(0.21%)	(0.18%)
Top	3327 ± 22	2.02 ± 0.51	5653 ± 28	162.9 ± 4.7	611.4 ± 9.3
	(1.0%)	(< 0.1%)	(94%)	(8.5%)	(11%)
SM Higgs	1108.7 ± 2.6	3.63 ± 0.18	5.79 ± 0.23	76.86 ± 0.79	227.4 ± 1.3
	(0.33%)	(< 0.1%)	(0.097%)	(4.0%)	(4.1%)
Total background	$331\,800 \pm 2000$	$46\,040 \pm 440$	5999 ± 57	1908 ± 58	5494 ± 73
Data	331 797	44 587	6227	1987	6119

Table 4. Pre-fit background event yields in the different analysis regions. The numbers correspond to an integrated luminosity of 140 fb^{-1}. The quoted uncertainties are the statistical uncertainties which arise from the finite number of generated events in the simulated samples and from the statistical uncertainties of the measured data as input for the fake-lepton background. The values in parentheses represent the fraction of the corresponding background relative to the total background in each region. For the $Z/\gamma^* \to \ell^+\ell^-$ background, $\ell^+\ell^-$ includes e^+e^- and $\mu^+\mu^-$.

7.1 Experimental uncertainties

The uncertainty in the combined 2015–2018 integrated luminosity[3] is 0.83% [36], obtained using the LUCID-2 detector [33] for the primary luminosity measurements. A systematic uncertainty is assigned to the reweighting procedure, based on the mean number of pp interactions per bunch crossing, used to correct the pile-up profile in MC simulation to match the data. For leptons, systematic uncertainties are assigned to the scale factors applied to correct for all differences between data and simulation that come from the electron and muon identification, reconstruction, isolation and trigger performance [37, 38, 99, 100] or from the lepton momentum scale and resolution. For jets, systematic uncertainties from the mismodelling of jet energy scale and resolution effects [103], jet vertex-tagging efficiencies [105], and jet flavour-tagging efficiencies [115–117] are considered. For the missing transverse momentum, uncertainties from the scale and resolution of the track-based "soft term" are considered [109]. The latter are one-sided variations. For the $E_{\text{T}}^{\text{miss}}$ "hard terms", uncertainties are already covered by electron, muon and jet uncertainties.

[3]The luminosity uncertainty is only included in the limit calculation and not in the variables' distribution plots.

JHEP12(2024)126

Other kinds of uncertainties are considered for the fake- and non-prompt-lepton backgrounds. First, the statistical uncertainties of the real- and fake-lepton efficiencies for electrons and muons are propagated as a single systematic uncertainty for each p_{T} bin. Also, the dependence of the efficiencies on variables other than the lepton p_{T} need to be accounted for. However, due to the limited number of data events, it is not possible to split the efficiencies into more components, so systematic uncertainties for the unaccounted dependencies of the efficiencies are included by parameterising them in η, n_{jets} and $E_{\mathrm{T}}^{\mathrm{miss}}$. For the η dependence, three different bins of absolute η values are introduced: $[0, 0.8)$, $[0.8, 1.7)$ and $[1.7, 2.7]$. The dependence of the efficiencies on the number of jets, n_{jets}, is also modelled, using four n_{jets} values $\{0, 1, 2, \geq 3\}$ for the fake-lepton efficiencies and $\{1, 2, 3, \geq 4\}$ for the real-lepton efficiencies, as there are no events without jets in the signal regions. For the $E_{\mathrm{T}}^{\mathrm{miss}}$ dependence, four different bins of $E_{\mathrm{T}}^{\mathrm{miss}}$ values are used: $[0, 10)$ GeV, $[10, 20)$ GeV, $[20, 30)$ GeV and $[30, \infty)$ GeV. For all those parameterisation uncertainties, the weighted standard deviations of the efficiencies are calculated and used as systematic uncertainties. Furthermore, the region where the efficiencies are measured and the SR could have different compositions. To account for this difference, a composition uncertainty is included by calculating the efficiencies in regions with the same requirements as the signal regions, but with the leptons having the same charge. Also, the m_{MMC} and $E_{\mathrm{T}}^{\mathrm{miss}}$ criteria are omitted to increase the number of events, as the $E_{\mathrm{T}}^{\mathrm{miss}}$ parameterisation is already accounted for by a dedicated uncertainty. Both the parameterisation and composition uncertainties are decorrelated across the regions for the fit because the regions use independent data, and allowing correlations would overly constrain the corresponding NPs. In some cases, a systematic uncertainty may arise from the uncertainty in the MC-event subtraction when calculating the fake-lepton efficiencies. For this analysis, the MC-event contamination in the FVR, where the fake-lepton efficiencies are measured, is only 3%. Thus, the uncertainties coming from the MC-event contamination are not considered in this analysis.

The most significant experimental uncertainties stem from the fake-lepton background estimation, flavour tagging, and muon efficiencies and calibration.

7.2 Theoretical uncertainties

Systematic uncertainties of the signal and background production cross-sections arise from various sources: missing higher-order (MHO) corrections, the PDFs, and the chosen input parameter values. The relative uncertainties in the inclusive cross-sections for backgrounds are 1.9% (5%) [118] for $Z \to \tau^+\tau^-$ with $m_{\ell\ell}$ above (below) 66 GeV, 4.4% [43, 119–122] for top-quark processes (dominated by $t\bar{t}$), and an envelope of 7.1% [123–125] for diboson processes. The relative uncertainties in the signal cross-sections are only taken into account for the model-dependent interpretation, with the estimated values ranging from 6.5% to 11.2%.

Generator systematic uncertainties for $Z \to \tau^+\tau^-$ and diboson processes arise mainly from the renormalisation and factorisation scales (μ_{R} and μ_{F}), as well as α_{s} uncertainties, PDF parameter value choices, and uncertainties in the resummation (QSF) and CKKW matching scales. The related event samples were produced using Sherpa 2.2.1 and 2.2.2, respectively. Systematic uncertainties associated with renormalisation and factorisation scale, PDF and α_{s} variations are assessed using corresponding event weights. All uncertainties

JHEP12(2024)126

are calculated in the high-mass SR and ZCR. The latter are applied in the ZCR and FVR. In all other regions, the ones calculated in the high-mass SR are used. For the QCD scale uncertainties, a 7-point variation is performed by varying μ_{R} and μ_{F} by factors of 2 and 0.5 in different combinations. For each bin, the uncertainty is given by the maximum positive and negative changes due to the variations. The scale uncertainty for the $Z \to \tau^+\tau^-$ process is decorrelated between the regions because of its largely different structure in the high-mass SR and the ZCR and to account for potential problems in the extrapolation of n_{jets} weights from the ZCR described in section 6.1. Using the baseline PDF, NNPDF3.0NLO with a strong coupling value of $\alpha_{\mathrm{s}}(m_Z) = 0.118$, as the nominal one, the standard deviation of 100 PDF variations is determined and taken as a symmetric uncertainty. Also, α_{s} is varied from 0.118 by ± 0.001. The CT14NNLO [126] and MMHT2014NNLO PDF sets with associated 68% confidence-level uncertainty bands [127] are compared with the baseline PDF to cross-check the results. Uncertainties corresponding to CKKW and QSF scale variations are evaluated only for $Z \to \tau^+\tau^-$, via a parameterisation method. For the CKKW matching, the nominal scale used in calculations of the overlap between jets from the ME and parton shower is 20 GeV and is varied between 15 GeV and 30 GeV. The soft-gluon emission resummation scale is varied by factors of 0.5 and 2 from its nominal value. All of the $Z \to \tau^+\tau^-$ and diboson generator uncertainties are calculated in bins of m_{MMC}.

Additional systematic uncertainties are included for the $Z \to \tau^+\tau^-$ reweighting, described in section 6.1, by propagating the statistical uncertainties of MC events and data events, as well as experimental and generator systematic uncertainties of MC events, to the weights. The resulting uncertainties cover a reweighting value of unity in most n_{jets} bins. The NPs are decorrelated across the regions to avoid double-counting the propagation of effects from the ZCR (where the weights were determined) to the SR.

The uncertainty in the modelling of top-quark processes has contributions from different sources. The uncertainties from each source are estimated by comparing the nominal sample (POWHEG BOX v2 at NLO with NNPDF3.0NLO and $h_{\mathrm{damp}} = 1.5\, m_{\mathrm{top}}$; PYTHIA 8.230 with the A14 tune and NNPDF2.3LO; and EVTGEN 1.6.0) with multiple variations. The uncertainties are evaluated in a modified TCR. Compared to the nominal TCR, the requirement on the number of b-tagged jets is loosened to ≥ 1 b-tagged jet in order to accept more events.[4] The impact of using a different parton shower and hadronisation model is evaluated by replacing PYTHIA with HERWIG 7.13 [128, 129] and the MMHT2014LO PDF set; for the impact of using different ME generation and matching to the parton shower, MADGRAPH5_AMC@NLO 2.6.0 [130] is used in place of POWHEG BOX; and to estimate the impact of changing the h_{damp} parameter value, a sample with $h_{\mathrm{damp}} = 3\, m_{\mathrm{top}}$ is used. Separate alternative datasets were simulated for each of the above variations. Initial-state radiation (ISR) uncertainties are estimated by halving and doubling μ_{R} and μ_{F}, and using the A14 tune's Var3cUp and Var3cDown variations corresponding to the variation of α_{s} for ISR. For final-state radiation (FSR), halving and doubling the renormalisation scale for parton shower emissions gives an estimate of the relevant uncertainty. These α_{s} and scale variations use alternative event weights recorded in the nominal simulation datasets. All of the top-quark generator uncertainties are calculated in bins of m_{MMC}.

[4] Systematic variations are performed using simulated top-quark processes only and are thus not affected by a possible signal contamination in an extended TCR.

JHEP12(2024)126

Uncertainties in signal modelling arise from the following sources: MHO corrections, the PDFs, the colour reconnection parameters and α_s. Furthermore, uncertainties from the modelling of ISR and FSR, multi-parton interactions (MPI), parton showers and hadronisation are considered. They are estimated from ratios of nominal-sample event acceptance to variation-sample event acceptance, binned in p_T^A. Uncertainties arising from the modelling of ISR, FSR, MPI and colour reconnection are estimated by adding in quadrature the effects of the Var1, Var2, Var3a, Var3b and Var3c up and down eigenvariations of Pythia 8's A14 tune. The scale uncertainties due to MHO corrections are determined from event weights given for 7-point combinations of different μ_R and μ_F values [78]. Analogously, the PDF and α_s uncertainties are estimated from variations given in the form of event weights, with the NNPDF2.3lo PDF as the baseline, for two α_s values 0.119 and 0.130, and for 100 variations of the PDF set. For every m_A value and each systematic variation, about 5 million events were generated to reduce statistical effects. Finally, a smoothing algorithm is applied, taking into account neighbouring mass hypotheses, to reduce remaining statistical fluctuations.

8 Statistical model and results

The signal strength μ, defined as a multiplicative factor to the cross-section of the hypothetical signal, is obtained from the statistical analysis of the data using a binned likelihood function based on a product of Poisson probability terms. Signal and background predictions depend on systematic uncertainties, which are parameterised as NPs and constrained using Gaussian functions. Normalisation factors for the $Z \to \tau^+\tau^-$ and top-quark backgrounds are also included but are not constrained. The binned likelihood function is constructed in bins of m_{MMC}. The binning was chosen in a way that ensures the statistical uncertainty per bin does not exceed 10% and that there are at least ten background events per bin, while requiring a minimum bin width of 2 GeV. Additionally, at least one fake-lepton event per bin is required. This is technically necessary in order to avoid having bins with negative expected background contributions or background expectations close to zero with large uncertainties in the statistical analysis. The fit model consists of three regions: the low-mass or high-mass SR, depending on the mass hypothesis, and the two control regions, TCR and ZCR. The two control regions allow the extraction of a normalisation factor for the top-quark and $Z \to \tau^+\tau^-$ backgrounds and constrain some of the systematic uncertainties. To account for shape effects in the TCR and ZCR, the regions are split into five and six m_{MMC} bins, respectively. The FVR is not used in the fit. The statistical uncertainties of the simulated background and signal, and those of the fake-lepton background histograms, are modelled by dedicated NPs, which use Poisson constraint terms. They are introduced separately for the signals and the combined backgrounds.

The fit is performed separately for each signal mass hypothesis. The final m_{MMC} distributions after the fit are shown in figure 6 for the 20 GeV mass hypothesis from the low-mass SR and for the 90 GeV mass hypothesis from the high-mass SR, including both the statistical and systematic uncertainties. Although the signal contributions to the control regions are negligible, they are taken into account properly in the fit.

The largest uncertainties in the SR, measured by their grouped impact on the fit result are listed in table 5. The dominant systematic uncertainties originate from the fake-lepton

JHEP12(2024)126

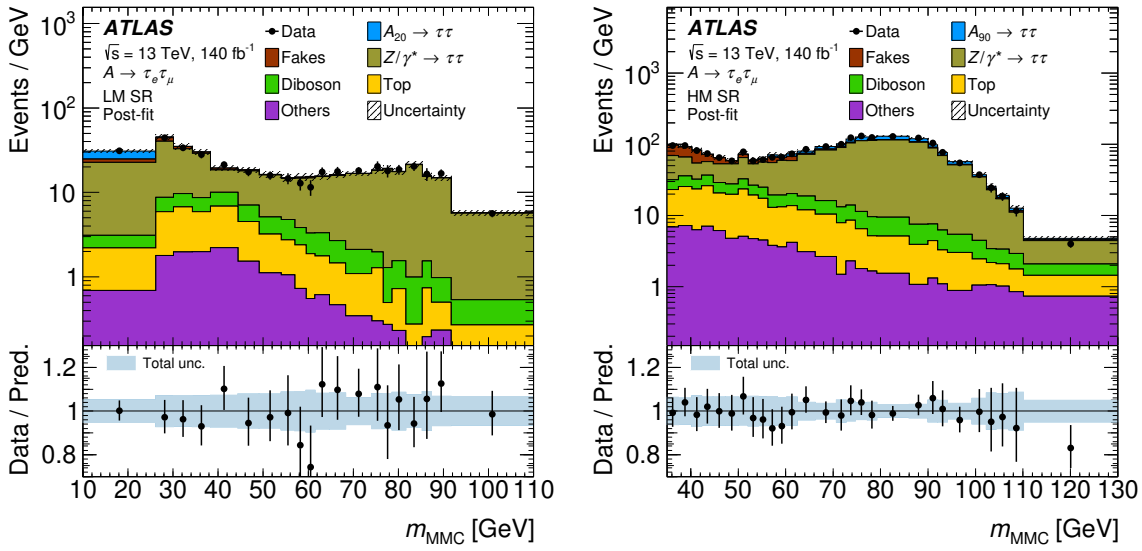

(a) (b)

Figure 6. Post-fit m_{MMC} distributions in (a) the low-mass SR for the $m_A = 20\,\mathrm{GeV}$ signal mass hypothesis and (b) the high-mass SR for the $m_A = 90\,\mathrm{GeV}$ signal mass hypothesis. The fits are performed under the signal-plus-background hypothesis using the signal with the respective m_A. Processes contributing to the "Others" background are $Z/\gamma^* \to \ell^+\ell^-$ and SM Higgs production. In (a), events with values below or above the x-axis range are shown in the first or last bin of the distribution, respectively. The band in the ratio plot shows the total uncertainty of the background estimate.

estimation, the $Z \to \tau^+\tau^-$ modelling, the $Z \to \tau^+\tau^-$ reweighting and the $Z \to \tau^+\tau^-$ MC sample size. Data statistical uncertainties play only a minor direct role; however, they play an important indirect role through the statistical uncertainties of the fake-lepton estimate.

The compatibility of the observed m_{MMC} spectrum with the background-only hypothesis, for a given A boson mass hypothesis, is assessed with a local p_0-value based on the profile-likelihood-ratio test statistic [131]. No significant deviation from the background-only hypothesis is observed. The largest local excess of events is $1.8\,\sigma$, observed for an A boson mass of 20 GeV, followed by a $1.3\,\sigma$ excess for the 85 GeV mass hypothesis.

The observed and expected 95% CL exclusion limits are calculated using a modified frequentist approach, the $\mathrm{CL_s}$ method [132], with the asymptotic approximation to the test-statistic distribution [131]. Limits are set on the signal strength μ and translated into limits on the gluon-gluon fusion production cross-section $\sigma(gg \to A)$ times the branching ratio for A boson decay into two τ-leptons, $\mathcal{B}(A \to \tau\tau)$. The observed and expected upper limits are shown in figure 7 and include all systematic uncertainties detailed in section 7 except for the signal cross-section uncertainties. The observed limits range from 68 pb for $m_A = 20\,\mathrm{GeV}$ to 3.0 pb for $m_A = 60\,\mathrm{GeV}$, increasing to 43 pb at $m_A = 90\,\mathrm{GeV}$ due to the reduced sensitivity near the Z-boson resonance.

In addition, this analysis provides an upper limit on the absolute value of the up-type quark coupling parameter $|\zeta_{\mathrm{u}}|$ within the flavour-aligned 2HDM model. For this, the uncertainties in the cross-sections are added to the fit. Only gluon-gluon fusion production of the A boson via a top-quark loop is considered and an exclusive decay of the A boson into a

JHEP12(2024)126

$m_A = 20\,\text{GeV}$		$m_A = 90\,\text{GeV}$	
Category	Relative contribution to $\Delta\mu$	Category	Relative contribution to $\Delta\mu$
Data statistical	42%	**Data statistical**	10%
Systematic	91%	**Systematic**	99%
Background statistical	81%	Background statistical	67%
$Z \to \tau^+\tau^-$ statistical	75%	$Z \to \tau^+\tau^-$ statistical	48%
Fake-lepton statistical	30%	Fake-lepton statistical	47%
Other background statistical	7%	Other background statistical	8%
Fake-lepton systematic	37%	$Z \to \tau^+\tau^-$ reweighting	55%
Signal modelling	11%	Signal statistical	51%
$Z \to \tau^+\tau^-$ modelling	10%	Fake-lepton systematic	47%
Muon efficiencies	8%	$Z \to \tau^+\tau^-$ modelling	45%
Diboson modelling	8%	$Z \to \tau^+\tau^-$ and $t\bar{t}$ normalisation	34%
Flavour tagging	5%	$t\bar{t}$ modelling	14%
Signal statistical	5%	Flavour tagging	14%
		Muon calibration	13%
		$E_{\text{T}}^{\text{miss}}$	9%
		Diboson modelling	7%
		Electron calibration	6%

Table 5. Breakdown of the relative contributions to the uncertainty of the extracted signal strength μ in the likelihood fit to data. The contributions are obtained by fixing the relevant NPs to their post-fit values in the likelihood fit. The relative impact is determined as the square-root of the difference of the squares of the nominal uncertainty and the obtained uncertainty, divided by the nominal uncertainty. The sum in quadrature of the individual components differs from the total uncertainty because of correlations between uncertainties in the different groups. The uncertainty from data statistical uncertainties is determined from fits with all NPs fixed to their post-fit values. The background statistical uncertainty includes the statistical uncertainty of the fake-lepton background determination and uncertainties due to background MC statistics. Only NP groups with a relative impact larger than 5% are listed.

$\tau^+\tau^-$ pair with $\mathcal{B}(A \to \tau\tau) = 1$ is assumed, according to the model constraints discussed in section 1. Thus, the obtained limits σ_{fit} can be transformed into limits on $|\zeta_{\text{u}}|$ via

$$|\zeta_{\text{u}}| = \sqrt{\frac{\sigma_{\text{fit}}}{\sigma_{\text{ref}}}},$$

where σ_{ref} is the cross-section calculated with `ggHiggs` [44–55] for each of the A boson mass hypotheses. The calculated observed and expected upper limits are displayed in figure 8. As a consequence of the higher production cross-sections for lower A boson masses, the upper limits are more stringent for the lower signal-mass hypotheses around 40 GeV and rise with increasing mass. The quadratic $|\zeta_{\text{u}}|$ dependence attenuates this effect slightly.

JHEP12(2024)126

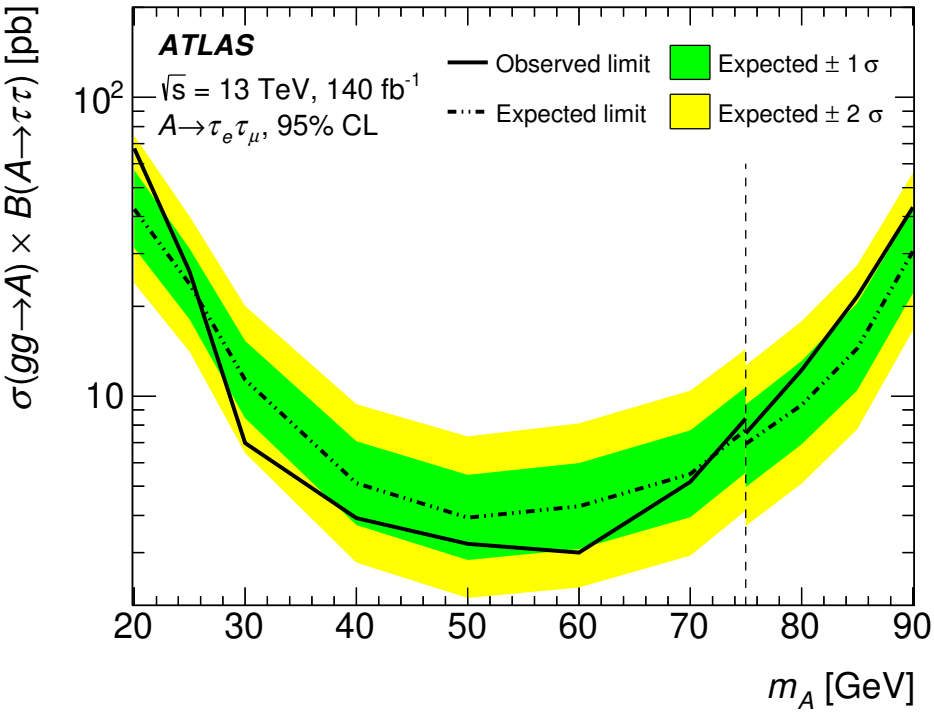

Figure 7. Expected and observed upper limits on the $gg \to A$ production cross-section times the branching ratio for A boson decay into two τ-leptons, for A boson masses from 20 to 90 GeV. The dash-dotted line shows the expected limit with its $1\,\sigma$ and $2\,\sigma$ uncertainty bands in green and yellow. The solid line shows the observed limit. The vertical dashed line indicates the splitting of the SR: the mass hypotheses on the left side are analysed within the low-mass SR and the ones on the right side in the high-mass SR.

9 Conclusion

A search for a light CP-odd Higgs boson, A, produced in proton-proton collisions at a centre-of-mass energy of 13 TeV during Run 2 of the LHC has been carried out, using the 140 fb^{-1} dataset collected with the ATLAS detector. Results are reported for the decay channels $A \to \tau^+\tau^- \to \mu^+\nu_\mu\bar{\nu}_\tau e^-\bar{\nu}_e\nu_\tau$ and $A \to \tau^+\tau^- \to e^+\nu_e\bar{\nu}_\tau\mu^-\bar{\nu}_\mu\nu_\tau$. The search is performed separately in low-mass and high-mass signal regions in order to optimize the signal sensitivity. A data-driven matrix method is applied to estimate the background of fake and non-prompt leptons. Other background expectations are determined by MC simulations. The m_{MMC} variable is used as an estimator of the invariant mass of the τ-lepton pair. Its distributions in the low-mass and high-mass signal regions are utilised in the statistical interpretation of the data. No significant excess of events above the SM background prediction is observed. The 95% CL upper limits placed on the gluon-gluon fusion production cross-section for a CP-odd Higgs boson decaying into the $\tau^+\tau^-$ final state vary between 3.0 pb and 68 pb in the A boson mass range between 20 GeV and 90 GeV. The mass range below 60 GeV had not been probed before. An interpretation of the results in the context of the flavour-aligned two-Higgs-doublet model is also given. Upper limits between 0.074

JHEP12(2024)126

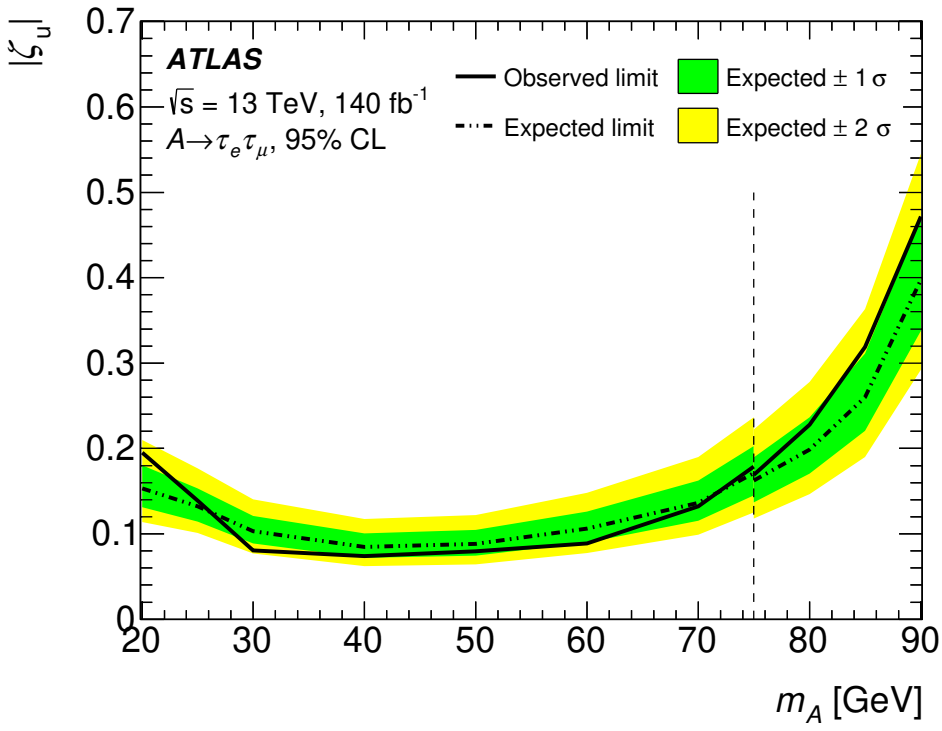

Figure 8. Expected and observed upper limits on the absolute value of the up-type quark coupling parameter $|\zeta_u|$ for masses of the A boson ranging from 20 to 90 GeV, assuming an exclusive decay of the A boson into a $\tau^+\tau^-$ pair. The dash-dotted line shows the expected limit with its $1\,\sigma$ and $2\,\sigma$ uncertainty bands in green and yellow. The solid line shows the observed limit. The vertical dashed line indicates the splitting of the SR: the mass hypotheses on the left side are analysed within the low-mass SR and the ones on the right side in the high-mass SR.

and 0.47 at 95% CL are set on the absolute value of the up-type quark coupling parameter $|\zeta_u|$, improving on previous limits on this parameter [16].

Acknowledgments

We thank CERN for the very successful operation of the LHC and its injectors, as well as the support staff at CERN and at our institutions worldwide without whom ATLAS could not be operated efficiently.

The crucial computing support from all WLCG partners is acknowledged gratefully, in particular from CERN, the ATLAS Tier-1 facilities at TRIUMF/SFU (Canada), NDGF (Denmark, Norway, Sweden), CC-IN2P3 (France), KIT/GridKA (Germany), INFN-CNAF (Italy), NL-T1 (Netherlands), PIC (Spain), RAL (U.K.) and BNL (U.S.A.), the Tier-2 facilities worldwide and large non-WLCG resource providers. Major contributors of computing resources are listed in ref. [133].

We gratefully acknowledge the support of ANPCyT, Argentina; YerPhI, Armenia; ARC, Australia; BMWFW and FWF, Austria; ANAS, Azerbaijan; CNPq and FAPESP, Brazil; NSERC, NRC and CFI, Canada; CERN; ANID, Chile; CAS, MOST and NSFC,

JHEP12(2024)126

China; Minciencias, Colombia; MEYS CR, Czech Republic; DNRF and DNSRC, Denmark; IN2P3-CNRS and CEA-DRF/IRFU, France; SRNSFG, Georgia; BMBF, HGF and MPG, Germany; GSRI, Greece; RGC and Hong Kong SAR, China; ISF and Benoziyo Center, Israel; INFN, Italy; MEXT and JSPS, Japan; CNRST, Morocco; NWO, Netherlands; RCN, Norway; MNiSW, Poland; FCT, Portugal; MNE/IFA, Romania; MSTDI, Serbia; MSSR, Slovakia; ARIS and MVZI, Slovenia; DSI/NRF, South Africa; MICIU/AEI, Spain; SRC and Wallenberg Foundation, Sweden; SERI, SNSF and Cantons of Bern and Geneva, Switzerland; NSTC, Taipei; TENMAK, Türkiye; STFC/UKRI, United Kingdom; DOE and NSF, United States of America.

Individual groups and members have received support from BCKDF, CANARIE, CRC and DRAC, Canada; CERN-CZ, FORTE and PRIMUS, Czech Republic; COST, ERC, ERDF, Horizon 2020, ICSC-NextGenerationEU and Marie Skłodowska-Curie Actions, European Union; Investissements d'Avenir Labex, Investissements d'Avenir Idex and ANR, France; DFG and AvH Foundation, Germany; Herakleitos, Thales and Aristeia programmes co-financed by EU-ESF and the Greek NSRF, Greece; BSF-NSF and MINERVA, Israel; NCN and NAWA, Poland; La Caixa Banking Foundation, CERCA Programme Generalitat de Catalunya and PROMETEO and GenT Programmes Generalitat Valenciana, Spain; Göran Gustafssons Stiftelse, Sweden; The Royal Society and Leverhulme Trust, United Kingdom.

In addition, individual members wish to acknowledge support from Armenia: Yerevan Physics Institute (FAPERJ); CERN: European Organization for Nuclear Research (CERN PJAS); Chile: Agencia Nacional de Investigación y Desarrollo (FONDECYT 1230812, FONDECYT 1230987, FONDECYT 1240864); China: Chinese Ministry of Science and Technology (MOST-2023YFA1605700), National Natural Science Foundation of China (NSFC — 12175119, NSFC 12275265, NSFC-12075060); Czech Republic: Czech Science Foundation (GACR — 24-11373S), Ministry of Education Youth and Sports (FORTE CZ.02.01.01/00/22_008/0004632), PRIMUS Research Programme (PRIMUS/21/SCI/017); EU: H2020 European Research Council (ERC — 101002463); European Union: European Research Council (ERC — 948254, ERC 101089007), European Union, Future Artificial Intelligence Research (FAIR-NextGenerationEU PE00000013), Italian Center for High Performance Computing, Big Data and Quantum Computing (ICSC, NextGenerationEU); France: Agence Nationale de la Recherche (ANR-20-CE31-0013, ANR-21-CE31-0013, ANR-21-CE31-0022, ANR-22-EDIR-0002); Germany: Baden-Württemberg Stiftung (BW Stiftung-Postdoc Eliteprogramme), Deutsche Forschungsgemeinschaft (DFG — 469666862, DFG — CR 312/5-2); Italy: Istituto Nazionale di Fisica Nucleare (ICSC, NextGenerationEU), Ministero dell'Università e della Ricerca (PRIN — 20223N7F8K — PNRR M4.C2.1.1); Japan: Japan Society for the Promotion of Science (JSPS KAKENHI JP22H01227, JSPS KAKENHI JP22H04944, JSPS KAKENHI JP22KK0227, JSPS KAKENHI JP23KK0245); Netherlands: Netherlands Organisation for Scientific Research (NWO Veni 2020 — VI.Veni.202.179); Norway: Research Council of Norway (RCN-314472); Poland: Ministry of Science and Higher Education (IDUB AGH, POB8, D4 no 9722), Polish National Agency for Academic Exchange (PPN/PPO/2020/1/00002/U/00001), Polish National Science Centre (NCN 2021/42/E/ST2/00350, NCN OPUS 2023/51/B/ST2/02507, NCN OPUS nr 2022/47/B/ST2/03059, NCN UMO-2019/34/E/ST2/00393, NCN & H2020 MSCA 945339,

UMO-2020/37/B/ST2/01043, UMO-2021/40/C/ST2/00187, UMO-2022/47/O/ST2/00148, UMO-2023/49/B/ST2/04085, UMO-2023/51/B/ST2/00920); Slovenia: Slovenian Research Agency (ARIS grant J1-3010); Spain: Generalitat Valenciana (Artemisa, FEDER, IDIFEDER/2018/048), Ministry of Science and Innovation (MCIN & NextGenEU PCI2022-135018-2, MICIN & FEDER PID2021-125273NB, RYC2019-028510-I, RYC2020-030254-I, RYC2021-031273-I, RYC2022-038164-I); Sweden: Carl Trygger Foundation (Carl Trygger Foundation CTS 22:2312), Swedish Research Council (Swedish Research Council 2023-04654, VR 2018-00482, VR 2022-03845, VR 2022-04683, VR 2023-03403, VR grant 2021-03651), Knut and Alice Wallenberg Foundation (KAW 2018.0458, KAW 2019.0447, KAW 2022.0358); Switzerland: Swiss National Science Foundation (SNSF — PCEFP2_194658); United Kingdom: Leverhulme Trust (Leverhulme Trust RPG-2020-004), Royal Society (NIF-R1-231091); United States of America: U.S. Department of Energy (ECA DE-AC02-76SF00515), Neubauer Family Foundation.

Data Availability Statement. This article has no associated data or the data will not be deposited.

Code Availability Statement. This article has no associated code or the code will not be deposited.

Open Access. This article is distributed under the terms of the Creative Commons Attribution License (CC-BY4.0), which permits any use, distribution and reproduction in any medium, provided the original author(s) and source are credited.

References

[1] ATLAS collaboration, *Observation of a new particle in the search for the Standard Model Higgs boson with the ATLAS detector at the LHC*, *Phys. Lett. B* **716** (2012) 1 [arXiv:1207.7214] [INSPIRE].

[2] CMS collaboration, *Observation of a new boson at a mass of 125 GeV with the CMS experiment at the LHC*, *Phys. Lett. B* **716** (2012) 30 [arXiv:1207.7235] [INSPIRE].

[3] L. Evans and P. Bryant, *LHC machine*, 2008 *JINST* **3** S08001 [INSPIRE].

[4] ATLAS collaboration, *A detailed map of Higgs boson interactions by the ATLAS experiment ten years after the discovery*, *Nature* **607** (2022) 52 [*Erratum ibid.* **612** (2022) E24] [arXiv:2207.00092] [INSPIRE].

[5] CMS collaboration, *A portrait of the Higgs boson by the CMS experiment ten years after the discovery*, *Nature* **607** (2022) 60 [arXiv:2207.00043] [INSPIRE].

[6] A. Djouadi, *The anatomy of electro-weak symmetry breaking. II. The Higgs bosons in the minimal supersymmetric model*, *Phys. Rept.* **459** (2008) 1 [hep-ph/0503173] [INSPIRE].

[7] G.C. Branco et al., *Theory and phenomenology of two-Higgs-doublet models*, *Phys. Rept.* **516** (2012) 1 [arXiv:1106.0034] [INSPIRE].

[8] A. Pich and P. Tuzon, *Yukawa alignment in the two-Higgs-doublet model*, *Phys. Rev. D* **80** (2009) 091702 [arXiv:0908.1554] [INSPIRE].

JHEP12(2024)126

[9] T. Aoyama et al., *The anomalous magnetic moment of the muon in the Standard Model*, *Phys. Rept.* **887** (2020) 1 [arXiv:2006.04822] [INSPIRE].

[10] MUON G-2 collaboration, *Measurement of the positive muon anomalous magnetic moment to 0.46 ppm*, *Phys. Rev. Lett.* **126** (2021) 141801 [arXiv:2104.03281] [INSPIRE].

[11] MUON G-2 collaboration, *Measurement of the positive muon anomalous magnetic moment to 0.20 ppm*, *Phys. Rev. Lett.* **131** (2023) 161802 [arXiv:2308.06230] [INSPIRE].

[12] G. Colangelo et al., *Prospects for precise predictions of a_μ in the Standard Model*, arXiv:2203.15810 [INSPIRE].

[13] S. Borsanyi et al., *Leading hadronic contribution to the muon magnetic moment from lattice QCD*, *Nature* **593** (2021) 51 [arXiv:2002.12347] [INSPIRE].

[14] A. Boccaletti et al., *High precision calculation of the hadronic vacuum polarisation contribution to the muon anomaly*, arXiv:2407.10913 [INSPIRE].

[15] CMD-3 collaboration, *Measurement of the $e^+e^- \to \pi^+\pi^-$ cross section from threshold to 1.2 GeV with the CMD-3 detector*, *Phys. Rev. D* **109** (2024) 112002 [arXiv:2302.08834] [INSPIRE].

[16] A. Cherchiglia, D. Stöckinger and H. Stöckinger-Kim, *Muon g-2 in the 2HDM: maximum results and detailed phenomenology*, *Phys. Rev. D* **98** (2018) 035001 [arXiv:1711.11567] [INSPIRE].

[17] S.M. Barr and A. Zee, *Electric dipole moment of the electron and of the neutron*, *Phys. Rev. Lett.* **65** (1990) 21 [*Erratum ibid.* **65** (1990) 2920] [INSPIRE].

[18] V. Ilisie, *New Barr-Zee contributions to $(g-2)_\mu$ in two-Higgs-doublet models*, *JHEP* **04** (2015) 077 [arXiv:1502.04199] [INSPIRE].

[19] D. Chang, W.-F. Chang, C.-H. Chou and W.-Y. Keung, *Large two loop contributions to g-2 from a generic pseudoscalar boson*, *Phys. Rev. D* **63** (2001) 091301 [hep-ph/0009292] [INSPIRE].

[20] K.-M. Cheung, C.-H. Chou and O.C.W. Kong, *Muon anomalous magnetic moment, two Higgs doublet model, and supersymmetry*, *Phys. Rev. D* **64** (2001) 111301 [hep-ph/0103183] [INSPIRE].

[21] Y.-L. Wu and Y.-F. Zhou, *Muon anomalous magnetic moment in the standard model with two Higgs doublets*, *Phys. Rev. D* **64** (2001) 115018 [hep-ph/0104056] [INSPIRE].

[22] M. Krawczyk, *Precision muon g-2 results and light Higgs bosons in the 2HDM(II)*, *Acta Phys. Polon. B* **33** (2002) 2621 [hep-ph/0208076] [INSPIRE].

[23] P. Athron et al., *New physics explanations of a_μ in light of the FNAL muon $g-2$ measurement*, *JHEP* **09** (2021) 080 [arXiv:2104.03691] [INSPIRE].

[24] ATLAS collaboration, *Search for neutral MSSM Higgs bosons decaying to $\tau^+\tau^-$ pairs in proton-proton collisions at $\sqrt{s} = 7$ TeV with the ATLAS detector*, *Phys. Lett. B* **705** (2011) 174 [arXiv:1107.5003] [INSPIRE].

[25] ATLAS collaboration, *Search for neutral Higgs bosons of the minimal supersymmetric standard model in pp collisions at $\sqrt{s} = 8$ TeV with the ATLAS detector*, *JHEP* **11** (2014) 056 [arXiv:1409.6064] [INSPIRE].

[26] ATLAS collaboration, *Search for heavy Higgs bosons decaying into two tau leptons with the ATLAS detector using pp collisions at $\sqrt{s} = 13$ TeV*, *Phys. Rev. Lett.* **125** (2020) 051801 [arXiv:2002.12223] [INSPIRE].

JHEP12(2024)126

[27] CMS collaboration, *Search for additional neutral MSSM Higgs bosons in the $\tau\tau$ final state in proton-proton collisions at $\sqrt{s} = 13$ TeV*, *JHEP* **09** (2018) 007 [arXiv:1803.06553] [INSPIRE].

[28] CMS collaboration, *Searches for additional Higgs bosons and for vector leptoquarks in $\tau\tau$ final states in proton-proton collisions at $\sqrt{s} = 13$ TeV*, *JHEP* **07** (2023) 073 [arXiv:2208.02717] [INSPIRE].

[29] Particle Data Group collaboration, *Review of particle physics*, *PTEP* **2022** (2022) 083C01 [INSPIRE].

[30] ATLAS collaboration, *The ATLAS experiment at the CERN Large Hadron Collider*, 2008 *JINST* **3** S08003 [INSPIRE].

[31] ATLAS collaboration, *ATLAS Insertable B-Layer technical design report*, CERN-LHCC-2010-013, CERN, Geneva, Switzerland (2010).

[32] ATLAS IBL collaboration, *Production and integration of the ATLAS Insertable B-Layer*, 2018 *JINST* **13** T05008 [arXiv:1803.00844] [INSPIRE].

[33] G. Avoni et al., *The new LUCID-2 detector for luminosity measurement and monitoring in ATLAS*, 2018 *JINST* **13** P07017 [INSPIRE].

[34] ATLAS collaboration, *Performance of the ATLAS trigger system in 2015*, *Eur. Phys. J. C* **77** (2017) 317 [arXiv:1611.09661] [INSPIRE].

[35] ATLAS collaboration, *Software and computing for run 3 of the ATLAS experiment at the LHC*, arXiv:2404.06335 [INSPIRE].

[36] ATLAS collaboration, *Luminosity determination in pp collisions at $\sqrt{s} = 13$ TeV using the ATLAS detector at the LHC*, *Eur. Phys. J. C* **83** (2023) 982 [arXiv:2212.09379] [INSPIRE].

[37] ATLAS collaboration, *Performance of electron and photon triggers in ATLAS during LHC run 2*, *Eur. Phys. J. C* **80** (2020) 47 [arXiv:1909.00761] [INSPIRE].

[38] ATLAS collaboration, *Performance of the ATLAS muon triggers in run 2*, 2020 *JINST* **15** P09015 [arXiv:2004.13447] [INSPIRE].

[39] GEANT4 collaboration, *GEANT4 — a simulation toolkit*, *Nucl. Instrum. Meth. A* **506** (2003) 250 [INSPIRE].

[40] ATLAS collaboration, *The ATLAS simulation infrastructure*, *Eur. Phys. J. C* **70** (2010) 823 [arXiv:1005.4568] [INSPIRE].

[41] ATLAS collaboration, *The simulation principle and performance of the ATLAS fast calorimeter simulation FastCaloSim*, ATL-PHYS-PUB-2010-013, CERN, Geneva, Switzerland (2010).

[42] T. Sjöstrand et al., *An introduction to PYTHIA 8.2*, *Comput. Phys. Commun.* **191** (2015) 159 [arXiv:1410.3012] [INSPIRE].

[43] R.D. Ball et al., *Parton distributions with LHC data*, *Nucl. Phys. B* **867** (2013) 244 [arXiv:1207.1303] [INSPIRE].

[44] R.D. Ball et al., *Higgs production in gluon fusion beyond NNLO*, *Nucl. Phys. B* **874** (2013) 746 [arXiv:1303.3590] [INSPIRE].

[45] M. Bonvini et al., *Updated Higgs cross section at approximate N^3LO*, *J. Phys. G* **41** (2014) 095002 [arXiv:1404.3204] [INSPIRE].

[46] M. Bonvini, S. Marzani, C. Muselli and L. Rottoli, *On the Higgs cross section at N^3LO+N^3LL and its uncertainty*, *JHEP* **08** (2016) 105 [arXiv:1603.08000] [INSPIRE].

JHEP12(2024)126

[47] T. Ahmed et al., *Pseudo-scalar Higgs boson production at N^3LO_A $+N^3LL'$*, *Eur. Phys. J. C* **76** (2016) 663 [arXiv:1606.00837] [INSPIRE].

[48] M. Bonvini and S. Marzani, *Double resummation for Higgs production*, *Phys. Rev. Lett.* **120** (2018) 202003 [arXiv:1802.07758] [INSPIRE].

[49] M. Bonvini, *An approximate N^3LO cross section for Higgs production in gluon fusion*, *EPJ Web Conf.* **60** (2013) 12008 [arXiv:1306.6633] [INSPIRE].

[50] R.V. Harlander and W.B. Kilgore, *Next-to-next-to-leading order Higgs production at hadron colliders*, *Phys. Rev. Lett.* **88** (2002) 201801 [hep-ph/0201206] [INSPIRE].

[51] R.V. Harlander and K.J. Ozeren, *Finite top mass effects for hadronic Higgs production at next-to-next-to-leading order*, *JHEP* **11** (2009) 088 [arXiv:0909.3420] [INSPIRE].

[52] R.V. Harlander, H. Mantler, S. Marzani and K.J. Ozeren, *Higgs production in gluon fusion at next-to-next-to-leading order QCD for finite top mass*, *Eur. Phys. J. C* **66** (2010) 359 [arXiv:0912.2104] [INSPIRE].

[53] C. Anastasiou et al., *Higgs boson gluon-fusion production beyond threshold in N^3LO QCD*, *JHEP* **03** (2015) 091 [arXiv:1411.3584] [INSPIRE].

[54] C. Anastasiou et al., *High precision determination of the gluon fusion Higgs boson cross-section at the LHC*, *JHEP* **05** (2016) 058 [arXiv:1602.00695] [INSPIRE].

[55] B. Mistlberger, *Higgs boson production at hadron colliders at N^3LO in QCD*, *JHEP* **05** (2018) 028 [arXiv:1802.00833] [INSPIRE].

[56] SHERPA collaboration, *Event generation with Sherpa 2.2*, *SciPost Phys.* **7** (2019) 034 [arXiv:1905.09127] [INSPIRE].

[57] S. Frixione, P. Nason and G. Ridolfi, *A positive-weight next-to-leading-order Monte Carlo for heavy flavour hadroproduction*, *JHEP* **09** (2007) 126 [arXiv:0707.3088] [INSPIRE].

[58] P. Nason, *A new method for combining NLO QCD with shower Monte Carlo algorithms*, *JHEP* **11** (2004) 040 [hep-ph/0409146] [INSPIRE].

[59] S. Frixione, P. Nason and C. Oleari, *Matching NLO QCD computations with parton shower simulations: the POWHEG method*, *JHEP* **11** (2007) 070 [arXiv:0709.2092] [INSPIRE].

[60] S. Alioli, P. Nason, C. Oleari and E. Re, *A general framework for implementing NLO calculations in shower Monte Carlo programs: the POWHEG BOX*, *JHEP* **06** (2010) 043 [arXiv:1002.2581] [INSPIRE].

[61] NNPDF collaboration, *Parton distributions for the LHC run II*, *JHEP* **04** (2015) 040 [arXiv:1410.8849] [INSPIRE].

[62] ATLAS collaboration, *ATLAS Pythia 8 tunes to 7 TeV data*, ATL-PHYS-PUB-2014-021, CERN, Geneva, Switzerland (2014).

[63] S. Schumann and F. Krauss, *A parton shower algorithm based on Catani-Seymour dipole factorisation*, *JHEP* **03** (2008) 038 [arXiv:0709.1027] [INSPIRE].

[64] S. Höche, F. Krauss, M. Schönherr and F. Siegert, *A critical appraisal of NLO+PS matching methods*, *JHEP* **09** (2012) 049 [arXiv:1111.1220] [INSPIRE].

[65] S. Höche, F. Krauss, M. Schönherr and F. Siegert, *QCD matrix elements + parton showers: the NLO case*, *JHEP* **04** (2013) 027 [arXiv:1207.5030] [INSPIRE].

[66] S. Catani, F. Krauss, R. Kuhn and B.R. Webber, *QCD matrix elements + parton showers*, *JHEP* **11** (2001) 063 [hep-ph/0109231] [INSPIRE].

JHEP12(2024)126

[67] S. Höche, F. Krauss, S. Schumann and F. Siegert, *QCD matrix elements and truncated showers*, *JHEP* **05** (2009) 053 [arXiv:0903.1219] [INSPIRE].

[68] K. Hamilton, P. Nason, E. Re and G. Zanderighi, *NNLOPS simulation of Higgs boson production*, *JHEP* **10** (2013) 222 [arXiv:1309.0017] [INSPIRE].

[69] K. Hamilton, P. Nason and G. Zanderighi, *Finite quark-mass effects in the NNLOPS POWHEG+MiNLO Higgs generator*, *JHEP* **05** (2015) 140 [arXiv:1501.04637] [INSPIRE].

[70] J. Butterworth et al., *PDF4LHC recommendations for LHC run II*, *J. Phys. G* **43** (2016) 023001 [arXiv:1510.03865] [INSPIRE].

[71] ATLAS collaboration, *Measurement of the Z/γ^* boson transverse momentum distribution in pp collisions at $\sqrt{s} = 7$ TeV with the ATLAS detector*, *JHEP* **09** (2014) 145 [arXiv:1406.3660] [INSPIRE].

[72] A. Djouadi, J. Kalinowski and M. Spira, *HDECAY: a program for Higgs boson decays in the standard model and its supersymmetric extension*, *Comput. Phys. Commun.* **108** (1998) 56 [hep-ph/9704448] [INSPIRE].

[73] M. Spira, *QCD effects in Higgs physics*, *Fortsch. Phys.* **46** (1998) 203 [hep-ph/9705337] [INSPIRE].

[74] A. Djouadi, M.M. Mühlleitner and M. Spira, *Decays of supersymmetric particles: the program SUSY-HIT (SUspect-SdecaY-Hdecay-InTerface)*, *Acta Phys. Polon. B* **38** (2007) 635 [hep-ph/0609292] [INSPIRE].

[75] A. Bredenstein, A. Denner, S. Dittmaier and M.M. Weber, *Radiative corrections to the semileptonic and hadronic Higgs-boson decays $H \to WW/ZZ \to 4$ fermions*, *JHEP* **02** (2007) 080 [hep-ph/0611234] [INSPIRE].

[76] A. Bredenstein, A. Denner, S. Dittmaier and M.M. Weber, *Precise predictions for the Higgs-boson decay $H \to WW/ZZ \to 4$ leptons*, *Phys. Rev. D* **74** (2006) 013004 [hep-ph/0604011] [INSPIRE].

[77] A. Bredenstein, A. Denner, S. Dittmaier and M.M. Weber, *Precision calculations for the Higgs decays $H \to ZZ/WW \to 4$ leptons*, *Nucl. Phys. B Proc. Suppl.* **160** (2006) 131 [hep-ph/0607060] [INSPIRE].

[78] LHC Higgs Cross Section Working Group collaboration, *Handbook of LHC Higgs cross sections: 4. Deciphering the nature of the Higgs sector*, arXiv:1610.07922 [DOI:10.23731/CYRM-2017-002] [INSPIRE].

[79] C. Anastasiou et al., *Higgs boson gluon-fusion production in QCD at three loops*, *Phys. Rev. Lett.* **114** (2015) 212001 [arXiv:1503.06056] [INSPIRE].

[80] F. Dulat, A. Lazopoulos and B. Mistlberger, *iHixs 2 — inclusive Higgs cross sections*, *Comput. Phys. Commun.* **233** (2018) 243 [arXiv:1802.00827] [INSPIRE].

[81] R.V. Harlander and K.J. Ozeren, *Top mass effects in Higgs production at next-to-next-to-leading order QCD: virtual corrections*, *Phys. Lett. B* **679** (2009) 467 [arXiv:0907.2997] [INSPIRE].

[82] A. Pak, M. Rogal and M. Steinhauser, *Finite top quark mass effects in NNLO Higgs boson production at LHC*, *JHEP* **02** (2010) 025 [arXiv:0911.4662] [INSPIRE].

[83] S. Actis, G. Passarino, C. Sturm and S. Uccirati, *NLO electroweak corrections to Higgs boson production at hadron colliders*, *Phys. Lett. B* **670** (2008) 12 [arXiv:0809.1301] [INSPIRE].

[84] S. Actis, G. Passarino, C. Sturm and S. Uccirati, *NNLO computational techniques: the cases $H \to \gamma\gamma$ and $H \to gg$*, *Nucl. Phys. B* **811** (2009) 182 [arXiv:0809.3667] [INSPIRE].

JHEP12(2024)126

[85] M. Bonetti, K. Melnikov and L. Tancredi, *Higher order corrections to mixed QCD-EW contributions to Higgs boson production in gluon fusion*, *Phys. Rev. D* **97** (2018) 056017 [*Erratum ibid.* **97** (2018) 099906] [arXiv:1801.10403] [INSPIRE].

[86] M. Ciccolini, A. Denner and S. Dittmaier, *Strong and electroweak corrections to the production of Higgs + 2 jets via weak interactions at the LHC*, *Phys. Rev. Lett.* **99** (2007) 161803 [arXiv:0707.0381] [INSPIRE].

[87] M. Ciccolini, A. Denner and S. Dittmaier, *Electroweak and QCD corrections to Higgs production via vector-boson fusion at the LHC*, *Phys. Rev. D* **77** (2008) 013002 [arXiv:0710.4749] [INSPIRE].

[88] P. Bolzoni, F. Maltoni, S.-O. Moch and M. Zaro, *Higgs production via vector-boson fusion at NNLO in QCD*, *Phys. Rev. Lett.* **105** (2010) 011801 [arXiv:1003.4451] [INSPIRE].

[89] M.L. Ciccolini, S. Dittmaier and M. Krämer, *Electroweak radiative corrections to associated WH and ZH production at hadron colliders*, *Phys. Rev. D* **68** (2003) 073003 [hep-ph/0306234] [INSPIRE].

[90] O. Brein, A. Djouadi and R. Harlander, *NNLO QCD corrections to the Higgs-strahlung processes at hadron colliders*, *Phys. Lett. B* **579** (2004) 149 [hep-ph/0307206] [INSPIRE].

[91] O. Brein, R. Harlander, M. Wiesemann and T. Zirke, *Top-quark mediated effects in hadronic Higgs-strahlung*, *Eur. Phys. J. C* **72** (2012) 1868 [arXiv:1111.0761] [INSPIRE].

[92] L. Altenkamp et al., *Gluon-induced Higgs-strahlung at next-to-leading order QCD*, *JHEP* **02** (2013) 078 [arXiv:1211.5015] [INSPIRE].

[93] A. Denner, S. Dittmaier, S. Kallweit and A. Mück, *HAWK 2.0: a Monte Carlo program for Higgs production in vector-boson fusion and Higgs strahlung at hadron colliders*, *Comput. Phys. Commun.* **195** (2015) 161 [arXiv:1412.5390] [INSPIRE].

[94] O. Brein, R.V. Harlander and T.J.E. Zirke, *vh@nnlo — Higgs Strahlung at hadron colliders*, *Comput. Phys. Commun.* **184** (2013) 998 [arXiv:1210.5347] [INSPIRE].

[95] R.V. Harlander, A. Kulesza, V. Theeuwes and T. Zirke, *Soft gluon resummation for gluon-induced Higgs Strahlung*, *JHEP* **11** (2014) 082 [arXiv:1410.0217] [INSPIRE].

[96] T. Sjöstrand, S. Mrenna and P.Z. Skands, *A brief introduction to PYTHIA 8.1*, *Comput. Phys. Commun.* **178** (2008) 852 [arXiv:0710.3820] [INSPIRE].

[97] ATLAS collaboration, *The Pythia 8 A3 tune description of ATLAS minimum bias and inelastic measurements incorporating the Donnachie-Landshoff diffractive model*, ATL-PHYS-PUB-2016-017, CERN, Geneva, Switzerland (2016).

[98] ATLAS collaboration, *Vertex reconstruction performance of the ATLAS detector at* $\sqrt{s} = 13$ *TeV*, ATL-PHYS-PUB-2015-026, CERN, Geneva, Switzerland (2015).

[99] ATLAS collaboration, *Electron and photon performance measurements with the ATLAS detector using the 2015–2017 LHC proton-proton collision data*, 2019 *JINST* **14** P12006 [arXiv:1908.00005] [INSPIRE].

[100] ATLAS collaboration, *Muon reconstruction and identification efficiency in ATLAS using the full run 2 pp collision data set at* $\sqrt{s} = 13$ *TeV*, *Eur. Phys. J. C* **81** (2021) 578 [arXiv:2012.00578] [INSPIRE].

[101] ATLAS collaboration, *Jet reconstruction and performance using particle flow with the ATLAS detector*, *Eur. Phys. J. C* **77** (2017) 466 [arXiv:1703.10485] [INSPIRE].

JHEP12(2024)126

[102] M. Cacciari, G.P. Salam and G. Soyez, *The anti-k_t jet clustering algorithm*, *JHEP* **04** (2008) 063 [arXiv:0802.1189] [INSPIRE].

[103] ATLAS collaboration, *Jet energy scale and resolution measured in proton-proton collisions at $\sqrt{s} = 13$ TeV with the ATLAS detector*, *Eur. Phys. J. C* **81** (2021) 689 [arXiv:2007.02645] [INSPIRE].

[104] ATLAS collaboration, *Selection of jets produced in 13 TeV proton-proton collisions with the ATLAS detector*, ATLAS-CONF-2015-029, CERN, Geneva, Switzerland (2015).

[105] ATLAS collaboration, *Performance of pile-up mitigation techniques for jets in pp collisions at $\sqrt{s} = 8$ TeV using the ATLAS detector*, *Eur. Phys. J. C* **76** (2016) 581 [arXiv:1510.03823] [INSPIRE].

[106] ATLAS collaboration, *Identification and rejection of pile-up jets at high pseudorapidity with the ATLAS detector*, *Eur. Phys. J. C* **77** (2017) 580 [*Erratum ibid.* **77** (2017) 712] [arXiv:1705.02211] [INSPIRE].

[107] ATLAS collaboration, *ATLAS flavour-tagging algorithms for the LHC run 2 pp collision dataset*, *Eur. Phys. J. C* **83** (2023) 681 [arXiv:2211.16345] [INSPIRE].

[108] ATLAS collaboration, *Reconstruction, energy calibration, and identification of hadronically decaying tau leptons in the ATLAS experiment for run-2 of the LHC*, ATL-PHYS-PUB-2015-045, CERN, Geneva, Switzerland (2015).

[109] ATLAS collaboration, *The performance of missing transverse momentum reconstruction and its significance with the ATLAS detector using 140 fb^{-1} of $\sqrt{s} = 13$ TeV pp collisions*, arXiv:2402.05858 [INSPIRE].

[110] A. Elagin, P. Murat, A. Pranko and A. Safonov, *A new mass reconstruction technique for resonances decaying to di-tau*, *Nucl. Instrum. Meth. A* **654** (2011) 481 [arXiv:1012.4686] [INSPIRE].

[111] ATLAS collaboration, *Measurements of Higgs boson production cross-sections in the $H \to \tau^+\tau^-$ decay channel in pp collisions at $\sqrt{s} = 13$ TeV with the ATLAS detector*, *JHEP* **08** (2022) 175 [arXiv:2201.08269] [INSPIRE].

[112] ATLAS collaboration, *Study of $Z \to ll\gamma$ decays at $\sqrt{s} = 8$ TeV with the ATLAS detector*, *Eur. Phys. J. C* **84** (2024) 195 [arXiv:2310.11574] [INSPIRE].

[113] M. Czakon et al., *Top-pair production at the LHC through NNLO QCD and NLO EW*, *JHEP* **10** (2017) 186 [arXiv:1705.04105] [INSPIRE].

[114] ATLAS collaboration, *Tools for estimating fake/non-prompt lepton backgrounds with the ATLAS detector at the LHC*, 2023 *JINST* **18** T11004 [arXiv:2211.16178] [INSPIRE].

[115] ATLAS collaboration, *Measurements of b-jet tagging efficiency with the ATLAS detector using $t\bar{t}$ events at $\sqrt{s} = 13$ TeV*, *JHEP* **08** (2018) 089 [arXiv:1805.01845] [INSPIRE].

[116] ATLAS collaboration, *Measurement of the c-jet mistagging efficiency in $t\bar{t}$ events using pp collision data at $\sqrt{s} = 13$ TeV collected with the ATLAS detector*, *Eur. Phys. J. C* **82** (2022) 95 [arXiv:2109.10627] [INSPIRE].

[117] ATLAS collaboration, *Calibration of the light-flavour jet mistagging efficiency of the b-tagging algorithms with Z+jets events using 139 fb^{-1} of ATLAS proton-proton collision data at $\sqrt{s} = 13$ TeV*, *Eur. Phys. J. C* **83** (2023) 728 [arXiv:2301.06319] [INSPIRE].

JHEP12(2024)126

[118] ATLAS collaboration, *Measurement of $W^{\pm}$ and Z-boson production cross sections in pp collisions at $\sqrt{s} = 13$ TeV with the ATLAS detector*, *Phys. Lett. B* **759** (2016) 601 [arXiv:1603.09222] [INSPIRE].

[119] M. Czakon and A. Mitov, *Top++: a program for the calculation of the top-pair cross-section at hadron colliders*, *Comput. Phys. Commun.* **185** (2014) 2930 [arXiv:1112.5675] [INSPIRE].

[120] M. Botje et al., *The PDF4LHC working group interim recommendations*, arXiv:1101.0538 [INSPIRE].

[121] A.D. Martin, W.J. Stirling, R.S. Thorne and G. Watt, *Uncertainties on α_S in global PDF analyses and implications for predicted hadronic cross sections*, *Eur. Phys. J. C* **64** (2009) 653 [arXiv:0905.3531] [INSPIRE].

[122] J. Gao et al., *CT10 next-to-next-to-leading order global analysis of QCD*, *Phys. Rev. D* **89** (2014) 033009 [arXiv:1302.6246] [INSPIRE].

[123] ATLAS collaboration, *Measurement of fiducial and differential W^+W^- production cross-sections at $\sqrt{s} = 13$ TeV with the ATLAS detector*, *Eur. Phys. J. C* **79** (2019) 884 [arXiv:1905.04242] [INSPIRE].

[124] ATLAS collaboration, *Measurement of ZZ production in the $\ell\ell\nu\nu$ final state with the ATLAS detector in pp collisions at $\sqrt{s} = 13$ TeV*, *JHEP* **10** (2019) 127 [arXiv:1905.07163] [INSPIRE].

[125] ATLAS collaboration, *Measurement of $W^{\pm}Z$ production cross sections and gauge boson polarisation in pp collisions at $\sqrt{s} = 13$ TeV with the ATLAS detector*, *Eur. Phys. J. C* **79** (2019) 535 [arXiv:1902.05759] [INSPIRE].

[126] S. Dulat et al., *New parton distribution functions from a global analysis of quantum chromodynamics*, *Phys. Rev. D* **93** (2016) 033006 [arXiv:1506.07443] [INSPIRE].

[127] L.A. Harland-Lang, A.D. Martin, P. Motylinski and R.S. Thorne, *Parton distributions in the LHC era: MMHT 2014 PDFs*, *Eur. Phys. J. C* **75** (2015) 204 [arXiv:1412.3989] [INSPIRE].

[128] M. Bähr et al., *Herwig++ physics and manual*, *Eur. Phys. J. C* **58** (2008) 639 [arXiv:0803.0883] [INSPIRE].

[129] J. Bellm et al., *Herwig 7.0/Herwig++ 3.0 release note*, *Eur. Phys. J. C* **76** (2016) 196 [arXiv:1512.01178] [INSPIRE].

[130] J. Alwall et al., *The automated computation of tree-level and next-to-leading order differential cross sections, and their matching to parton shower simulations*, *JHEP* **07** (2014) 079 [arXiv:1405.0301] [INSPIRE].

[131] G. Cowan, K. Cranmer, E. Gross and O. Vitells, *Asymptotic formulae for likelihood-based tests of new physics*, *Eur. Phys. J. C* **71** (2011) 1554 [*Erratum ibid.* **73** (2013) 2501] [arXiv:1007.1727] [INSPIRE].

[132] A.L. Read, *Presentation of search results: the CL_s technique*, *J. Phys. G* **28** (2002) 2693 [INSPIRE].

[133] ATLAS collaboration, *ATLAS computing acknowledgements*, ATL-SOFT-PUB-2023-001, CERN, Geneva, Switzerland (2023).

JHEP12(2024)126

The ATLAS collaboration

G. Aad[105], E. Aakvaag[17], B. Abbott[124], S. Abdelhameed[120a], K. Abeling[57], N.J. Abicht[51], S.H. Abidi[30], M. Aboelela[46], A. Aboulhorma[36e], H. Abramowicz[156], H. Abreu[155], Y. Abulaiti[121], B.S. Acharya[71a,71b,l], A. Ackermann[65a], C. Adam Bourdarios[4], L. Adamczyk[88a], S.V. Addepalli[148], M.J. Addison[104], J. Adelman[119], A. Adiguzel[22c], T. Adye[138], A.A. Affolder[140], Y. Afik[41], M.N. Agaras[13], A. Aggarwal[103], C. Agheorghiesei[28c], F. Ahmadov[40,aa], S. Ahuja[98], X. Ai[64e], G. Aielli[78a,78b], A. Aikot[168], M. Ait Tamlihat[36e], B. Aitbenchikh[36a], M. Akbiyik[103], T.P.A. Åkesson[101], A.V. Akimov[150], D. Akiyama[173], N.N. Akolkar[25], S. Aktas[22a], K. Al Khoury[43], G.L. Alberghi[24b], J. Albert[170], P. Albicocco[55], G.L. Albouy[62], S. Alderweireldt[54], Z.L. Alegria[125], M. Aleksa[37], I.N. Aleksandrov[40], C. Alexa[28b], T. Alexopoulos[10], F. Alfonsi[24b], M. Algren[58], M. Alhroob[172], B. Ali[136], H.M.J. Ali[94,u], S. Ali[32], S.W. Alibocus[95], M. Aliev[34c], G. Alimonti[73a], W. Alkakhi[57], C. Allaire[68], B.M.M. Allbrooke[151], J.S. Allen[104], J.F. Allen[54], C.A. Allendes Flores[141f], P.P. Allport[21], A. Aloisio[74a,74b], F. Alonso[93], C. Alpigiani[143], Z.M.K. Alsolami[94], M. Alvarez Estevez[102], A. Alvarez Fernandez[103], M. Alves Cardoso[58], M.G. Alviggi[74a,74b], M. Aly[104], Y. Amaral Coutinho[85b], A. Ambler[107], C. Amelung[37], M. Amerl[104], C.G. Ames[112], D. Amidei[109], B. Amini[56], K.J. Amirie[159], S.P. Amor Dos Santos[134a], K.R. Amos[168], D. Amperiadou[157], S. An[86], V. Ananiev[129], C. Anastopoulos[144], T. Andeen[11], J.K. Anders[37], A.C. Anderson[61], A. Andreazza[73a,73b], S. Angelidakis[9], A. Angerami[43], A.V. Anisenkov[39], A. Annovi[76a], C. Antel[58], E. Antipov[150], M. Antonelli[55], F. Anulli[77a], M. Aoki[86], T. Aoki[158], M.A. Aparo[151], L. Aperio Bella[50], C. Appelt[156], A. Apyan[27], S.J. Arbiol Val[89], C. Arcangeletti[55], A.T.H. Arce[53], J-F. Arguin[111], S. Argyropoulos[157], J.-H. Arling[50], O. Arnaez[4], H. Arnold[150], G. Artoni[77a,77b], H. Asada[114], K. Asai[122], S. Asai[158], N.A. Asbah[37], R.A. Ashby Pickering[172], K. Assamagan[30], R. Astalos[29a], K.S.V. Astrand[101], S. Atashi[163], R.J. Atkin[34a], H. Atmani[36f], P.A. Atmasiddha[132], K. Augsten[136], A.D. Auriol[21], V.A. Austrup[104], G. Avolio[37], K. Axiotis[58], G. Azuelos[111,ae], D. Babal[29b], H. Bachacou[139], K. Bachas[157,p], A. Bachiu[35], E. Bachmann[52], A. Badea[41], T.M. Baer[109], P. Bagnaia[77a,77b], M. Bahmani[19], D. Bahner[56], K. Bai[127], J.T. Baines[138], L. Baines[97], O.K. Baker[177], E. Bakos[16], D. Bakshi Gupta[8], L.E. Balabram Filho[85b], V. Balakrishnan[124], R. Balasubramanian[4], E.M. Baldin[39], P. Balek[88a], E. Ballabene[24b,24a], F. Balli[139], L.M. Baltes[65a], W.K. Balunas[33], J. Balz[103], I. Bamwidhi[120b], E. Banas[89], M. Bandieramonte[133], A. Bandyopadhyay[25], S. Bansal[25], L. Barak[156], M. Barakat[50], E.L. Barberio[108], D. Barberis[59b,59a], M. Barbero[105], M.Z. Barel[118], T. Barillari[113], M-S. Barisits[37], T. Barklow[148], P. Baron[126], D.A. Baron Moreno[104], A. Baroncelli[64a], A.J. Barr[130], J.D. Barr[99], F. Barreiro[102], J. Barreiro Guimarães da Costa[14], M.G. Barros Teixeira[134a], S. Barsov[39], F. Bartels[65a], R. Bartoldus[148], A.E. Barton[94], P. Bartos[29a], A. Basan[103], M. Baselga[51], A. Bassalat[68,b], M.J. Basso[160a], S. Bataju[46], R. Bate[169], R.L. Bates[61], S. Batlamous[102], B. Batool[146], M. Battaglia[140], D. Battulga[19], M. Bauce[77a,77b], M. Bauer[81], P. Bauer[25], L.T. Bazzano Hurrell[31], J.B. Beacham[53], T. Beau[131], J.Y. Beaucamp[93], P.H. Beauchemin[162], P. Bechtle[25], H.P. Beck[20,o], K. Becker[172], A.J. Beddall[84], V.A. Bednyakov[40], C.P. Bee[150], L.J. Beemster[16], T.A. Beermann[37],

JHEP12(2024)126

M. Begalli[85d], M. Begel[30], A. Behera[150], J.K. Behr[50], J.F. Beirer[37], F. Beisiegel[25], M. Belfkir[120b], G. Bella[156], L. Bellagamba[24b], A. Bellerive[35], P. Bellos[21], K. Beloborodov[39], D. Benchekroun[36a], F. Bendebba[36a], Y. Benhammou[156], K.C. Benkendorfer[63], L. Beresford[50], M. Beretta[55], E. Bergeaas Kuutmann[166], N. Berger[4], B. Bergmann[136], J. Beringer[18a], G. Bernardi[5], C. Bernius[148], F.U. Bernlochner[25], F. Bernon[37], A. Berrocal Guardia[13], T. Berry[98], P. Berta[137], A. Berthold[52], S. Bethke[113], A. Betti[77a,77b], A.J. Bevan[97], N.K. Bhalla[56], S. Bhatta[150], D.S. Bhattacharya[171], P. Bhattarai[148], Z.M. Bhatti[121], K.D. Bhide[56], V.S. Bhopatkar[125], R.M. Bianchi[133], G. Bianco[24b,24a], O. Biebel[112], M. Biglietti[79a], C.S. Billingsley[46], Y. Bimgdi[36f], M. Bindi[57], A. Bingham[176], A. Bingul[22b], C. Bini[77a,77b], G.A. Bird[33], M. Birman[174], M. Biros[137], S. Biryukov[151], T. Bisanz[51], E. Bisceglie[45b,45a], J.P. Biswal[138], D. Biswas[146], I. Bloch[50], A. Blue[61], U. Blumenschein[97], J. Blumenthal[103], V.S. Bobrovnikov[39], M. Boehler[56], B. Boehm[171], D. Bogavac[37], A.G. Bogdanchikov[39], L.S. Boggia[131], C. Bohm[49a], V. Boisvert[98], P. Bokan[37], T. Bold[88a], M. Bomben[5], M. Bona[97], M. Boonekamp[139], A.G. Borbély[61], I.S. Bordulev[39], G. Borissov[94], D. Bortoletto[130], D. Boscherini[24b], M. Bosman[13], K. Bouaouda[36a], N. Bouchhar[168], L. Boudet[4], J. Boudreau[133], E.V. Bouhova-Thacker[94], D. Boumediene[42], R. Bouquet[59b,59a], A. Boveia[123], J. Boyd[37], D. Boye[30], I.R. Boyko[40], L. Bozianu[58], J. Bracinik[21], N. Brahimi[4], G. Brandt[176], O. Brandt[33], B. Brau[106], J.E. Brau[127], R. Brener[174], L. Brenner[118], R. Brenner[166], S. Bressler[174], G. Brianti[80a,80b], D. Britton[61], D. Britzger[113], I. Brock[25], R. Brock[110], G. Brooijmans[43], A.J. Brooks[70], E.M. Brooks[160b], E. Brost[30], L.M. Brown[170], L.E. Bruce[63], T.L. Bruckler[130], P.A. Bruckman de Renstrom[89], B. Brüers[50], A. Bruni[24b], G. Bruni[24b], D. Brunner[49a,49b], M. Bruschi[24b], N. Bruscino[77a,77b], T. Buanes[17], Q. Buat[143], D. Buchin[113], A.G. Buckley[61], O. Bulekov[39], B.A. Bullard[148], S. Burdin[95], C.D. Burgard[51], A.M. Burger[37], B. Burghgrave[8], O. Burlayenko[56], J. Burleson[167], J.T.P. Burr[33], J.C. Burzynski[147], E.L. Busch[43], V. Büscher[103], P.J. Bussey[61], J.M. Butler[26], C.M. Buttar[61], J.M. Butterworth[99], W. Buttinger[138], C.J. Buxo Vazquez[110], A.R. Buzykaev[39], S. Cabrera Urbán[168], L. Cadamuro[68], D. Caforio[60], H. Cai[133], Y. Cai[14,115c], Y. Cai[115a], V.M.M. Cairo[37], O. Cakir[3a], N. Calace[37], P. Calafiura[18a], G. Calderini[131], P. Calfayan[35], G. Callea[61], L.P. Caloba[85b], D. Calvet[42], S. Calvet[42], R. Camacho Toro[131], S. Camarda[37], D. Camarero Munoz[27], P. Camarri[78a,78b], M.T. Camerlingo[74a,74b], D. Cameron[37], C. Camincher[170], M. Campanelli[99], A. Camplani[44], V. Canale[74a,74b], A.C. Canbay[3a], E. Canonero[98], J. Cantero[168], Y. Cao[167], F. Capocasa[27], M. Capua[45b,45a], A. Carbone[73a,73b], R. Cardarelli[78a], J.C.J. Cardenas[8], M.P. Cardiff[27], G. Carducci[45b,45a], T. Carli[37], G. Carlino[74a], J.I. Carlotto[13], B.T. Carlson[133,q], E.M. Carlson[170,160a], J. Carmignani[95], L. Carminati[73a,73b], A. Carnelli[139], M. Carnesale[37], S. Caron[117], E. Carquin[141f], I.B. Carr[108], S. Carrá[73a], G. Carratta[24b,24a], A.M. Carroll[127], M.P. Casado[13,i], M. Caspar[50], F.L. Castillo[4], L. Castillo Garcia[13], V. Castillo Gimenez[168], N.F. Castro[134a,134e], A. Catinaccio[37], J.R. Catmore[129], T. Cavaliere[4], V. Cavaliere[30], L.J. Caviedes Betancourt[23b], Y.C. Cekmecelioglu[50], E. Celebi[84], S. Cella[37], V. Cepaitis[58], K. Cerny[126], A.S. Cerqueira[85a], A. Cerri[151], L. Cerrito[78a,78b], F. Cerutti[18a],

JHEP12(2024)126

B. Cervato[146], A. Cervelli[24b], G. Cesarini[55], S.A. Cetin[84], P.M. Chabrillat[131], D. Chakraborty[119], J. Chan[18a], W.Y. Chan[158], J.D. Chapman[33], E. Chapon[139], B. Chargeishvili[154b], D.G. Charlton[21], M. Chatterjee[20], C. Chauhan[137], Y. Che[115a], S. Chekanov[6], S.V. Chekulaev[160a], G.A. Chelkov[40,a], A. Chen[109], B. Chen[156], B. Chen[170], H. Chen[115a], H. Chen[30], J. Chen[64c], J. Chen[147], M. Chen[130], S. Chen[90], S.J. Chen[115a], X. Chen[64c], X. Chen[15,ad], Y. Chen[64a], C.L. Cheng[175], H.C. Cheng[66a], S. Cheong[148], A. Cheplakov[40], E. Cheremushkina[50], E. Cherepanova[118], R. Cherkaoui El Moursli[36e], E. Cheu[7], K. Cheung[67], L. Chevalier[139], V. Chiarella[55], G. Chiarelli[76a], N. Chiedde[105], G. Chiodini[72a], A.S. Chisholm[21], A. Chitan[28b], M. Chitishvili[168], M.V. Chizhov[40,r], K. Choi[11], Y. Chou[143], E.Y.S. Chow[117], K.L. Chu[174], M.C. Chu[66a], X. Chu[14,115c], Z. Chubinidze[55], J. Chudoba[135], J.J. Chwastowski[89], D. Cieri[113], K.M. Ciesla[88a], V. Cindro[96], A. Ciocio[18a], F. Cirotto[74a,74b], Z.H. Citron[174], M. Citterio[73a], D.A. Ciubotaru[28b], A. Clark[58], P.J. Clark[54], N. Clarke Hall[99], C. Clarry[159], J.M. Clavijo Columbie[50], S.E. Clawson[50], C. Clement[49a,49b], Y. Coadou[105], M. Cobal[71a,71c], A. Coccaro[59b], R.F. Coelho Barrue[134a], R. Coelho Lopes De Sa[106], S. Coelli[73a], L.S. Colangeli[159], B. Cole[43], J. Collot[62], P. Conde Muiño[134a,134g], M.P. Connell[34c], S.H. Connell[34c], E.I. Conroy[130], F. Conventi[74a,af], H.G. Cooke[21], A.M. Cooper-Sarkar[130], F.A. Corchia[24b,24a], A. Cordeiro Oudot Choi[131], L.D. Corpe[42], M. Corradi[77a,77b], F. Corriveau[107,z], A. Cortes-Gonzalez[19], M.J. Costa[168], F. Costanza[4], D. Costanzo[144], B.M. Cote[123], J. Couthures[4], G. Cowan[98], K. Cranmer[175], L. Cremer[51], D. Cremonini[24b,24a], S. Crépé-Renaudin[62], F. Crescioli[131], M. Cristinziani[146], M. Cristoforetti[80a,80b], V. Croft[118], J.E. Crosby[125], G. Crosetti[45b,45a], A. Cueto[102], H. Cui[99], Z. Cui[7], W.R. Cunningham[61], F. Curcio[168], J.R. Curran[54], P. Czodrowski[37], M.J. Da Cunha Sargedas De Sousa[59b,59a], J.V. Da Fonseca Pinto[85b], C. Da Via[104], W. Dabrowski[88a], T. Dado[37], S. Dahbi[153], T. Dai[109], D. Dal Santo[20], C. Dallapiccola[106], M. Dam[44], G. D'amen[30], V. D'Amico[112], J. Damp[103], J.R. Dandoy[35], D. Dannheim[37], M. Danninger[147], V. Dao[150], G. Darbo[59b], S.J. Das[30], F. Dattola[50], S. D'Auria[73a,73b], A. D'Avanzo[74a,74b], C. David[34a], T. Davidek[137], I. Dawson[97], H.A. Day-hall[136], K. De[8], C. De Almeida Rossi[159], R. De Asmundis[74a], N. De Biase[50], S. De Castro[24b,24a], N. De Groot[117], P. de Jong[118], H. De la Torre[119], A. De Maria[115a], A. De Salvo[77a], U. De Sanctis[78a,78b], F. De Santis[72a,72b], A. De Santo[151], J.B. De Vivie De Regie[62], J. Debevc[96], D.V. Dedovich[40], J. Degens[95], A.M. Deiana[46], F. Del Corso[24b,24a], J. Del Peso[102], L. Delagrange[131], F. Deliot[139], C.M. Delitzsch[51], M. Della Pietra[74a,74b], D. Della Volpe[58], A. Dell'Acqua[37], L. Dell'Asta[73a,73b], M. Delmastro[4], C.C. Delogu[103], P.A. Delsart[62], S. Demers[177], M. Demichev[40], S.P. Denisov[39], L. D'Eramo[42], D. Derendarz[89], F. Derue[131], P. Dervan[95], K. Desch[25], C. Deutsch[25], F.A. Di Bello[59b,59a], A. Di Ciaccio[78a,78b], L. Di Ciaccio[4], A. Di Domenico[77a,77b], C. Di Donato[74a,74b], A. Di Girolamo[37], G. Di Gregorio[37], A. Di Luca[80a,80b], B. Di Micco[79a,79b], R. Di Nardo[79a,79b], K.F. Di Petrillo[41], M. Diamantopoulou[35], F.A. Dias[118], T. Dias Do Vale[147], M.A. Diaz[141a,141b], A.R. Didenko[40], M. Didenko[168], E.B. Diehl[109], S. Díez Cornell[50], C. Diez Pardos[146], C. Dimitriadi[166], A. Dimitrievska[21], J. Dingfelder[25], T. Dingley[130], I-M. Dinu[28b], S.J. Dittmeier[65b], F. Dittus[37],

JHEP12(2024)126

M. Divisek[137], B. Dixit[95], F. Djama[105], T. Djobava[154b], C. Doglioni[104,101], A. Dohnalova[29a], Z. Dolezal[137], K. Domijan[88a], K.M. Dona[41], M. Donadelli[85d], B. Dong[110], J. Donini[42], A. D'Onofrio[74a,74b], M. D'Onofrio[95], J. Dopke[138], A. Doria[74a], N. Dos Santos Fernandes[134a], P. Dougan[104], M.T. Dova[93], A.T. Doyle[61], M.A. Draguet[130], M.P. Drescher[57], E. Dreyer[174], I. Drivas-koulouris[10], M. Drnevich[121], M. Drozdova[58], D. Du[64a], T.A. du Pree[118], F. Dubinin[39], M. Dubovsky[29a], E. Duchovni[174], G. Duckeck[112], O.A. Ducu[28b], D. Duda[54], A. Dudarev[37], E.R. Duden[27], M. D'uffizi[104], L. Duflot[68], M. Dührssen[37], I. Duminica[28g], A.E. Dumitriu[28b], M. Dunford[65a], S. Dungs[51], K. Dunne[49a,49b], A. Duperrin[105], H. Duran Yildiz[3a], M. Düren[60], A. Durglishvili[154b], D. Duvnjak[35], B.L. Dwyer[119], G.I. Dyckes[18a], M. Dyndal[88a], B.S. Dziedzic[37], Z.O. Earnshaw[151], G.H. Eberwein[130], B. Eckerova[29a], S. Eggebrecht[57], E. Egidio Purcino De Souza[85e], L.F. Ehrke[58], G. Eigen[17], K. Einsweiler[18a], T. Ekelof[166], P.A. Ekman[101], S. El Farkh[36b], Y. El Ghazali[64a], H. El Jarrari[37], A. El Moussaouy[36a], V. Ellajosyula[166], M. Ellert[166], F. Ellinghaus[176], N. Ellis[37], J. Elmsheuser[30], M. Elsawy[120a], M. Elsing[37], D. Emeliyanov[138], Y. Enari[86], I. Ene[18a], S. Epari[13], P.A. Erland[89], D. Ernani Martins Neto[89], M. Errenst[176], M. Escalier[68], C. Escobar[168], E. Etzion[156], G. Evans[134a,134b], H. Evans[70], L.S. Evans[98], A. Ezhilov[39], S. Ezzarqtouni[36a], F. Fabbri[24b,24a], L. Fabbri[24b,24a], G. Facini[99], V. Fadeyev[140], R.M. Fakhrutdinov[39], D. Fakoudis[103], S. Falciano[77a], L.F. Falda Ulhoa Coelho[134a], F. Fallavollita[113], G. Falsetti[45b,45a], J. Faltova[137], C. Fan[167], K.Y. Fan[66b], Y. Fan[14], Y. Fang[14,115c], M. Fanti[73a,73b], M. Faraj[71a,71b], Z. Farazpay[100], A. Farbin[8], A. Farilla[79a], T. Farooque[110], J.N. Farr[177], S.M. Farrington[138,54], F. Fassi[36e], D. Fassouliotis[9], M. Faucci Giannelli[78a,78b], W.J. Fawcett[33], L. Fayard[68], P. Federic[137], P. Federicova[135], O.L. Fedin[39,a], M. Feickert[175], L. Feligioni[105], D.E. Fellers[127], C. Feng[64b], Z. Feng[118], M.J. Fenton[163], L. Ferencz[50], R.A.M. Ferguson[94], P. Fernandez Martinez[69], M.J.V. Fernoux[105], J. Ferrando[94], A. Ferrari[166], P. Ferrari[118,117], R. Ferrari[75a], D. Ferrere[58], C. Ferretti[109], M.P. Fewell[1], D. Fiacco[77a,77b], F. Fiedler[103], P. Fiedler[136], S. Filimonov[39], A. Filipčič[96], E.K. Filmer[160a], F. Filthaut[117], M.C.N. Fiolhais[134a,134c,c], L. Fiorini[168], W.C. Fisher[110], T. Fitschen[104], P.M. Fitzhugh[139], I. Fleck[146], P. Fleischmann[109], T. Flick[176], M. Flores[34d,ab], L.R. Flores Castillo[66a], L. Flores Sanz De Acedo[37], F.M. Follega[80a,80b], N. Fomin[33], J.H. Foo[159], A. Formica[139], A.C. Forti[104], E. Fortin[37], A.W. Fortman[18a], M.G. Foti[18a], L. Fountas[9,j], D. Fournier[68], H. Fox[94], P. Francavilla[76a,76b], S. Francescato[63], S. Franchellucci[58], M. Franchini[24b,24a], S. Franchino[65a], D. Francis[37], L. Franco[117], V. Franco Lima[37], L. Franconi[50], M. Franklin[63], G. Frattari[27], Y.Y. Frid[156], J. Friend[61], N. Fritzsche[37], A. Froch[58], D. Froidevaux[37], J.A. Frost[130], Y. Fu[64a], S. Fuenzalida Garrido[141f], M. Fujimoto[105], K.Y. Fung[66a], E. Furtado De Simas Filho[85e], M. Furukawa[158], J. Fuster[168], A. Gaa[57], A. Gabrielli[24b,24a], A. Gabrielli[159], P. Gadow[37], G. Gagliardi[59b,59a], L.G. Gagnon[18a], S. Gaid[165], S. Galantzan[156], J. Gallagher[1], E.J. Gallas[130], A.L. Gallen[166], B.J. Gallop[138], K.K. Gan[123], S. Ganguly[158], Y. Gao[54], F.M. Garay Walls[141a,141b], B. Garcia[30], C. García[168], A. Garcia Alonso[118], A.G. Garcia Caffaro[177], J.E. García Navarro[168], M. Garcia-Sciveres[18a], G.L. Gardner[132], R.W. Gardner[41], N. Garelli[162], R.B. Garg[148], J.M. Gargan[54], C.A. Garner[159], C.M. Garvey[34a],

JHEP12(2024)126

V.K. Gassmann[162], G. Gaudio[75a], V. Gautam[13], P. Gauzzi[77a,77b], J. Gavranovic[96], I.L. Gavrilenko[39], A. Gavrilyuk[39], C. Gay[169], G. Gaycken[127], E.N. Gazis[10], A.A. Geanta[28b], A. Gekow[123], C. Gemme[59b], M.H. Genest[62], A.D. Gentry[116], S. George[98], W.F. George[21], T. Geralis[48], A.A. Gerwin[124], P. Gessinger-Befurt[37], M.E. Geyik[176], M. Ghani[172], K. Ghorbanian[97], A. Ghosal[146], A. Ghosh[163], A. Ghosh[7], B. Giacobbe[24b], S. Giagu[77a,77b], T. Giani[118], A. Giannini[64a], S.M. Gibson[98], M. Gignac[140], D.T. Gil[88b], A.K. Gilbert[88a], B.J. Gilbert[43], D. Gillberg[35], G. Gilles[118], L. Ginabat[131], D.M. Gingrich[2,ae], M.P. Giordani[71a,71c], P.F. Giraud[139], G. Giugliarelli[71a,71c], D. Giugni[73a], F. Giuli[78a,78b], I. Gkialas[9,j], L.K. Gladilin[39], C. Glasman[102], G.R. Gledhill[127], G. Glemža[50], M. Glisic[127], I. Gnesi[45b], Y. Go[30], M. Goblirsch-Kolb[37], B. Gocke[51], D. Godin[111], B. Gokturk[22a], S. Goldfarb[108], T. Golling[58], M.G.D. Gololo[34g], D. Golubkov[39], J.P. Gombas[110], A. Gomes[134a,134b], G. Gomes Da Silva[146], A.J. Gomez Delegido[168], R. Gonçalo[134a], L. Gonella[21], A. Gongadze[154c], F. Gonnella[21], J.L. Gonski[148], R.Y. González Andana[54], S. González de la Hoz[168], R. Gonzalez Lopez[95], C. Gonzalez Renteria[18a], M.V. Gonzalez Rodrigues[50], R. Gonzalez Suarez[166], S. Gonzalez-Sevilla[58], L. Goossens[37], B. Gorini[37], E. Gorini[72a,72b], A. Gorišek[96], T.C. Gosart[132], A.T. Goshaw[53], M.I. Gostkin[40], S. Goswami[125], C.A. Gottardo[37], S.A. Gotz[112], M. Gouighri[36b], V. Goumarre[50], A.G. Goussiou[143], N. Govender[34c], R.P. Grabarczyk[130], I. Grabowska-Bold[88a], K. Graham[35], E. Gramstad[129], S. Grancagnolo[72a,72b], C.M. Grant[1,139], P.M. Gravila[28f], F.G. Gravili[72a,72b], H.M. Gray[18a], M. Greco[72a,72b], M.J. Green[1], C. Grefe[25], A.S. Grefsrud[17], I.M. Gregor[50], K.T. Greif[163], P. Grenier[148], S.G. Grewe[113], A.A. Grillo[140], K. Grimm[32], S. Grinstein[13,v], J.-F. Grivaz[68], E. Gross[174], J. Grosse-Knetter[57], L. Guan[109], J.G.R. Guerrero Rojas[168], G. Guerrieri[37], R. Gugel[103], J.A.M. Guhit[109], A. Guida[19], E. Guilloton[172], S. Guindon[37], F. Guo[14,115c], J. Guo[64c], L. Guo[50], L. Guo[14,t], Y. Guo[109], A. Gupta[51], R. Gupta[133], S. Gurbuz[25], S.S. Gurdasani[56], G. Gustavino[77a,77b], P. Gutierrez[124], L.F. Gutierrez Zagazeta[132], M. Gutsche[52], C. Gutschow[99], C. Gwenlan[130], C.B. Gwilliam[95], E.S. Haaland[129], A. Haas[121], M. Habedank[61], C. Haber[18a], H.K. Hadavand[8], A. Hadef[52], A.I. Hagan[94], J.J. Hahn[146], E.H. Haines[99], M. Haleem[171], J. Haley[125], G.D. Hallewell[105], L. Halser[20], K. Hamano[170], M. Hamer[25], E.J. Hampshire[98], J. Han[64b], L. Han[115a], L. Han[64a], S. Han[18a], Y.F. Han[159], K. Hanagaki[86], M. Hance[140], D.A. Hangal[43], H. Hanif[147], M.D. Hank[132], J.B. Hansen[44], P.H. Hansen[44], D. Harada[58], T. Harenberg[176], S. Harkusha[178], M.L. Harris[106], Y.T. Harris[25], J. Harrison[13], N.M. Harrison[123], P.F. Harrison[172], N.M. Hartman[113], N.M. Hartmann[112], R.Z. Hasan[98,138], Y. Hasegawa[145], F. Haslbeck[130], S. Hassan[17], R. Hauser[110], C.M. Hawkes[21], R.J. Hawkings[37], Y. Hayashi[158], D. Hayden[110], C. Hayes[109], R.L. Hayes[118], C.P. Hays[130], J.M. Hays[97], H.S. Hayward[95], F. He[64a], M. He[14,115c], Y. He[50], Y. He[99], N.B. Heatley[97], V. Hedberg[101], A.L. Heggelund[129], C. Heidegger[56], K.K. Heidegger[56], J. Heilman[35], S. Heim[50], T. Heim[18a], J.G. Heinlein[132], J.J. Heinrich[127], L. Heinrich[113,ac], J. Hejbal[135], A. Held[175], S. Hellesund[17], C.M. Helling[169], S. Hellman[49a,49b], R.C.W. Henderson[94], L. Henkelmann[33], A.M. Henriques Correia[37], H. Herde[101], Y. Hernández Jiménez[150], L.M. Herrmann[25], T. Herrmann[52], G. Herten[56], R. Hertenberger[112], L. Hervas[37], M.E. Hesping[103], N.P. Hessey[160a], J. Hessler[113], M. Hidaoui[36b], N. Hidic[137], E. Hill[159],

S.J. Hillier[21], J.R. Hinds[110], F. Hinterkeuser[25], M. Hirose[128], S. Hirose[161], D. Hirschbuehl[176], T.G. Hitchings[104], B. Hiti[96], J. Hobbs[150], R. Hobincu[28e], N. Hod[174], M.C. Hodgkinson[144], B.H. Hodkinson[130], A. Hoecker[37], D.D. Hofer[109], J. Hofer[168], T. Holm[25], M. Holzbock[37], L.B.A.H. Hommels[33], B.P. Honan[104], J.J. Hong[70], J. Hong[64c], T.M. Hong[133], B.H. Hooberman[167], W.H. Hopkins[6], M.C. Hoppesch[167], Y. Horii[114], M.E. Horstmann[113], S. Hou[153], M.R. Housenga[167], A.S. Howard[96], J. Howarth[61], J. Hoya[6], M. Hrabovsky[126], A. Hrynevich[50], T. Hryn'ova[4], P.J. Hsu[67], S.-C. Hsu[143], T. Hsu[68], M. Hu[18a], Q. Hu[64a], S. Huang[33], X. Huang[14,115c], Y. Huang[144], Y. Huang[103], Y. Huang[14], Z. Huang[104], Z. Hubacek[136], M. Huebner[25], F. Huegging[25], T.B. Huffman[130], M. Hufnagel Maranha De Faria[85a], C.A. Hugli[50], M. Huhtinen[37], S.K. Huiberts[17], R. Hulsken[107], N. Huseynov[12,g], J. Huston[110], J. Huth[63], R. Hyneman[7], G. Iacobucci[58], G. Iakovidis[30], L. Iconomidou-Fayard[68], J.P. Iddon[37], P. Iengo[74a,74b], R. Iguchi[158], Y. Iiyama[158], T. Iizawa[130], Y. Ikegami[86], D. Iliadis[157], N. Ilic[159], H. Imam[85c], G. Inacio Goncalves[85d], T. Ingebretsen Carlson[49a,49b], J.M. Inglis[97], G. Introzzi[75a,75b], M. Iodice[79a], V. Ippolito[77a,77b], R.K. Irwin[95], M. Ishino[158], W. Islam[175], C. Issever[19], S. Istin[22a,ai], H. Ito[173], R. Iuppa[80a,80b], A. Ivina[174], J.M. Izen[47], V. Izzo[74a], P. Jacka[135], P. Jackson[1], C.S. Jagfeld[112], G. Jain[160a], P. Jain[50], K. Jakobs[56], T. Jakoubek[174], J. Jamieson[61], W. Jang[158], M. Javurkova[106], P. Jawahar[104], L. Jeanty[127], J. Jejelava[154a], P. Jenni[56,f], C.E. Jessiman[35], C. Jia[64b], H. Jia[169], J. Jia[150], X. Jia[14,115c], Z. Jia[115a], C. Jiang[54], S. Jiggins[50], J. Jimenez Pena[13], S. Jin[115a], A. Jinaru[28b], O. Jinnouchi[142], P. Johansson[144], K.A. Johns[7], J.W. Johnson[140], F.A. Jolly[50], D.M. Jones[151], E. Jones[50], K.S. Jones[8], P. Jones[33], R.W.L. Jones[94], T.J. Jones[95], H.L. Joos[57,37], R. Joshi[123], J. Jovicevic[16], X. Ju[18a], J.J. Junggeburth[37], T. Junkermann[65a], A. Juste Rozas[13,v], M.K. Juzek[89], S. Kabana[141e], A. Kaczmarska[89], M. Kado[113], H. Kagan[123], M. Kagan[148], A. Kahn[132], C. Kahra[103], T. Kaji[158], E. Kajomovitz[155], N. Kakati[174], I. Kalaitzidou[56], C.W. Kalderon[30], N.J. Kang[140], D. Kar[34g], K. Karava[130], M.J. Kareem[160b], E. Karentzos[25], O. Karkout[118], S.N. Karpov[40], Z.M. Karpova[40], V. Kartvelishvili[94], A.N. Karyukhin[39], E. Kasimi[157], J. Katzy[50], S. Kaur[35], K. Kawade[145], M.P. Kawale[124], C. Kawamoto[90], T. Kawamoto[64a], E.F. Kay[37], F.I. Kaya[162], S. Kazakos[110], V.F. Kazanin[39], Y. Ke[150], J.M. Keaveney[34a], R. Keeler[170], G.V. Kehris[63], J.S. Keller[35], J.J. Kempster[151], O. Kepka[135], J. Kerr[160b], B.P. Kerridge[138], S. Kersten[176], B.P. Kerševan[96], L. Keszeghova[29a], S. Ketabchi Haghighat[159], R.A. Khan[133], A. Khanov[125], A.G. Kharlamov[39], T. Kharlamova[39], E.E. Khoda[143], M. Kholodenko[134a], T.J. Khoo[19], G. Khoriauli[171], J. Khubua[154b,*], Y.A.R. Khwaira[131], B. Kibirige[34g], D. Kim[6], D.W. Kim[49a,49b], Y.K. Kim[41], N. Kimura[99], M.K. Kingston[57], A. Kirchhoff[57], C. Kirfel[25], F. Kirfel[25], J. Kirk[138], A.E. Kiryunin[113], S. Kita[161], C. Kitsaki[10], O. Kivernyk[25], M. Klassen[162], C. Klein[35], L. Klein[171], M.H. Klein[46], S.B. Klein[58], U. Klein[95], A. Klimentov[30], T. Klioutchnikova[37], P. Kluit[118], S. Kluth[113], E. Kneringer[81], T.M. Knight[159], A. Knue[51], D. Kobylianskii[174], S.F. Koch[130], M. Kocian[148], P. Kodyš[137], D.M. Koeck[127], P.T. Koenig[25], T. Koffas[35], O. Kolay[52], I. Koletsou[4], T. Komarek[89], K. Köneke[57], A.X.Y. Kong[1], T. Kono[122], N. Konstantinidis[99], P. Kontaxakis[58], B. Konya[101], R. Kopeliansky[43], S. Koperny[88a],

JHEP12(2024)126

K. Korcyl[89], K. Kordas[157,e], A. Korn[99], S. Korn[57], I. Korolkov[13], N. Korotkova[39], B. Kortman[118], O. Kortner[113], S. Kortner[113], W.H. Kostecka[119], V.V. Kostyukhin[146], A. Kotsokechagia[37], A. Kotwal[53], A. Koulouris[37], A. Kourkoumeli-Charalampidi[75a,75b], C. Kourkoumelis[9], E. Kourlitis[113,ac], O. Kovanda[127], R. Kowalewski[170], W. Kozanecki[127], A.S. Kozhin[39], V.A. Kramarenko[39], G. Kramberger[96], P. Kramer[25], M.W. Krasny[131], A. Krasznahorkay[37], A.C. Kraus[119], J.W. Kraus[176], J.A. Kremer[50], T. Kresse[52], L. Kretschmann[176], J. Kretzschmar[95], K. Kreul[19], P. Krieger[159], K. Krizka[21], K. Kroeninger[51], H. Kroha[113], J. Kroll[135], J. Kroll[132], K.S. Krowpman[110], U. Kruchonak[40], H. Krüger[25], N. Krumnack[83], M.C. Kruse[53], O. Kuchinskaia[39], S. Kuday[3a], S. Kuehn[37], R. Kuesters[56], T. Kuhl[50], V. Kukhtin[40], Y. Kulchitsky[40], S. Kuleshov[141d,141b], M. Kumar[34g], N. Kumari[50], P. Kumari[160b], A. Kupco[135], T. Kupfer[51], A. Kupich[39], O. Kuprash[56], H. Kurashige[87], L.L. Kurchaninov[160a], O. Kurdysh[68], Y.A. Kurochkin[38], A. Kurova[39], M. Kuze[142], A.K. Kvam[106], J. Kvita[126], T. Kwan[107], N.G. Kyriacou[109], L.A.O. Laatu[105], C. Lacasta[168], F. Lacava[77a,77b], H. Lacker[19], D. Lacour[131], N.N. Lad[99], E. Ladygin[40], A. Lafarge[42], B. Laforge[131], T. Lagouri[177], F.Z. Lahbabi[36a], S. Lai[57], J.E. Lambert[170], S. Lammers[70], W. Lampl[7], C. Lampoudis[157,e], G. Lamprinoudis[103], A.N. Lancaster[119], E. Lançon[30], U. Landgraf[56], M.P.J. Landon[97], V.S. Lang[56], O.K.B. Langrekken[129], A.J. Lankford[163], F. Lanni[37], K. Lantzsch[25], A. Lanza[75a], M. Lanzac Berrocal[168], J.F. Laporte[139], T. Lari[73a], F. Lasagni Manghi[24b], M. Lassnig[37], V. Latonova[135], S.D. Lawlor[144], Z. Lawrence[104], R. Lazaridou[172], M. Lazzaroni[73a,73b], H.D.M. Le[110], E.M. Le Boulicaut[177], L.T. Le Pottier[18a], B. Leban[24b,24a], A. Lebedev[83], M. LeBlanc[104], F. Ledroit-Guillon[62], S.C. Lee[153], S. Lee[49a,49b], T.F. Lee[95], L.L. Leeuw[34c], M. Lefebvre[170], C. Leggett[18a], G. Lehmann Miotto[37], M. Leigh[58], W.A. Leight[106], W. Leinonen[117], A. Leisos[157,s], M.A.L. Leite[85c], C.E. Leitgeb[19], R. Leitner[137], K.J.C. Leney[46], T. Lenz[25], S. Leone[76a], C. Leonidopoulos[54], A. Leopold[149], R. Les[110], C.G. Lester[33], M. Levchenko[39], J. Levêque[4], L.J. Levinson[174], G. Levrini[24b,24a], M.P. Lewicki[89], C. Lewis[143], D.J. Lewis[4], L. Lewitt[144], A. Li[30], B. Li[64b], C. Li[64a], C-Q. Li[113], H. Li[64a], H. Li[64b], H. Li[115a], H. Li[15], H. Li[64b], J. Li[64c], K. Li[14], L. Li[64c], M. Li[14,115c], R. Li[177], S. Li[14,115c], S. Li[64d,64c,d], T. Li[5], X. Li[107], Z. Li[158], Z. Li[14,115c], Z. Li[64a], S. Liang[14,115c], Z. Liang[14], M. Liberatore[139], B. Liberti[78a], K. Lie[66c], J. Lieber Marin[85e], H. Lien[70], H. Lin[109], K. Lin[110], L. Linden[112], R.E. Lindley[7], J.H. Lindon[2], J. Ling[63], E. Lipeles[132], A. Lipniacka[17], A. Lister[169], J.D. Little[70], B. Liu[14], B.X. Liu[115b], D. Liu[64d,64c], E.H.L. Liu[21], J.B. Liu[64a], J.K.K. Liu[33], K. Liu[64d], K. Liu[64d,64c], M. Liu[64a], M.Y. Liu[64a], P. Liu[14], Q. Liu[64d,143,64c], X. Liu[64a], X. Liu[64b], Y. Liu[115b,115c], Y.L. Liu[64b], Y.W. Liu[64a], S.L. Lloyd[97], E.M. Lobodzinska[50], P. Loch[7], E. Lodhi[159], T. Lohse[19], K. Lohwasser[144], E. Loiacono[50], J.D. Lomas[21], J.D. Long[43], I. Longarini[163], R. Longo[167], I. Lopez Paz[69], A. Lopez Solis[50], N.A. Lopez-canelas[7], N. Lorenzo Martinez[4], A.M. Lory[112], M. Losada[120a], G. Löschcke Centeno[151], O. Loseva[39], X. Lou[49a,49b], X. Lou[14,115c], A. Lounis[68], P.A. Love[94], G. Lu[14,115c], M. Lu[68], S. Lu[132], Y.J. Lu[153], H.J. Lubatti[143], C. Luci[77a,77b], F.L. Lucio Alves[115a], F. Luehring[70], O. Lukianchuk[68], B.S. Lunday[132], O. Lundberg[149], B. Lund-Jensen[149,*], N.A. Luongo[6], M.S. Lutz[37], A.B. Lux[26], D. Lynn[30], R. Lysak[135], E. Lytken[101], V. Lyubushkin[40],

JHEP12(2024)126

T. Lyubushkina[40], M.M. Lyukova[150], M.Firdaus M. Soberi[54], H. Ma[30], K. Ma[64a], L.L. Ma[64b], W. Ma[64a], Y. Ma[125], J.C. MacDonald[103], P.C. Machado De Abreu Farias[85e], R. Madar[42], T. Madula[99], J. Maeda[87], T. Maeno[30], P.T. Mafa[34c], H. Maguire[144], V. Maiboroda[139], A. Maio[134a,134b,134d], K. Maj[88a], O. Majersky[50], S. Majewski[127], N. Makovec[68], V. Maksimovic[16], B. Malaescu[131], Pa. Malecki[89], V.P. Maleev[39], F. Malek[62,n], M. Mali[96], D. Malito[98], U. Mallik[82,*], S. Maltezos[10], S. Malyukov[40], J. Mamuzic[13], G. Mancini[55], M.N. Mancini[27], G. Manco[75a,75b], J.P. Mandalia[97], S.S. Mandarry[151], I. Mandić[96], L. Manhaes de Andrade Filho[85a], I.M. Maniatis[174], J. Manjarres Ramos[92], D.C. Mankad[174], A. Mann[112], S. Manzoni[37], L. Mao[64c], X. Mapekula[34c], A. Marantis[157,s], G. Marchiori[5], M. Marcisovsky[135], C. Marcon[73a], M. Marinescu[21], S. Marium[50], M. Marjanovic[124], A. Markhoos[56], M. Markovitch[68], M.K. Maroun[106], E.J. Marshall[94], Z. Marshall[18a], S. Marti-Garcia[168], J. Martin[99], T.A. Martin[138], V.J. Martin[54], B. Martin dit Latour[17], L. Martinelli[77a,77b], M. Martinez[13,v], P. Martinez Agullo[168], V.I. Martinez Outschoorn[106], P. Martinez Suarez[13], S. Martin-Haugh[138], G. Martinovicova[137], V.S. Martoiu[28b], A.C. Martyniuk[99], A. Marzin[37], D. Mascione[80a,80b], L. Masetti[103], J. Masik[104], A.L. Maslennikov[39], S.L. Mason[43], P. Massarotti[74a,74b], P. Mastrandrea[76a,76b], A. Mastroberardino[45b,45a], T. Masubuchi[128], T.T. Mathew[127], T. Mathisen[166], J. Matousek[137], D.M. Mattern[51], J. Maurer[28b], T. Maurin[61], A.J. Maury[68], B. Maček[96], D.A. Maximov[39], A.E. May[104], R. Mazini[34g], I. Maznas[119], M. Mazza[110], S.M. Mazza[140], E. Mazzeo[73a,73b], J.P. Mc Gowan[170], S.P. Mc Kee[109], C.A. Mc Lean[6], C.C. McCracken[169], E.F. McDonald[108], A.E. McDougall[118], L.F. Mcelhinney[94], J.A. Mcfayden[151], R.P. McGovern[132], R.P. Mckenzie[34g], T.C. Mclachlan[50], D.J. Mclaughlin[99], S.J. McMahon[138], C.M. Mcpartland[95], R.A. McPherson[170,z], S. Mehlhase[112], A. Mehta[95], D. Melini[168], B.R. Mellado Garcia[34g], A.H. Melo[57], F. Meloni[50], A.M. Mendes Jacques Da Costa[104], H.Y. Meng[159], L. Meng[94], S. Menke[113], M. Mentink[37], E. Meoni[45b,45a], G. Mercado[119], S. Merianos[157], C. Merlassino[71a,71c], L. Merola[74a,74b], C. Meroni[73a,73b], J. Metcalfe[6], A.S. Mete[6], E. Meuser[103], C. Meyer[70], J-P. Meyer[139], R.P. Middleton[138], L. Mijović[54], G. Mikenberg[174], M. Mikestikova[135], M. Mikuž[96], H. Mildner[103], A. Milic[37], D.W. Miller[41], E.H. Miller[148], L.S. Miller[35], A. Milov[174], D.A. Milstead[49a,49b], T. Min[115a], A.A. Minaenko[39], I.A. Minashvili[154b], A.I. Mincer[121], B. Mindur[88a], M. Mineev[40], Y. Mino[90], L.M. Mir[13], M. Miralles Lopez[61], M. Mironova[18a], M.C. Missio[117], A. Mitra[172], V.A. Mitsou[168], Y. Mitsumori[114], O. Miu[159], P.S. Miyagawa[97], T. Mkrtchyan[65a], M. Mlinarevic[99], T. Mlinarevic[99], M. Mlynarikova[37], S. Mobius[20], P. Mogg[112], M.H. Mohamed Farook[116], A.F. Mohammed[14,115c], S. Mohapatra[43], G. Mokgatitswane[34g], L. Moleri[174], B. Mondal[146], S. Mondal[136], K. Mönig[50], E. Monnier[105], L. Monsonis Romero[168], J. Montejo Berlingen[13], A. Montella[49a,49b], M. Montella[123], F. Montereali[79a,79b], F. Monticelli[93], S. Monzani[71a,71c], A. Morancho Tarda[44], N. Morange[68], A.L. Moreira De Carvalho[50], M. Moreno Llácer[168], C. Moreno Martinez[58], J.M. Moreno Perez[23b], P. Morettini[59b], S. Morgenstern[37], M. Morii[63], M. Morinaga[158], M. Moritsu[91], F. Morodei[77a,77b], P. Moschovakos[37], B. Moser[130], M. Mosidze[154b], T. Moskalets[46], P. Moskvitina[117], J. Moss[32,k], P. Moszkowicz[88a], A. Moussa[36d], Y. Moyal[174], E.J.W. Moyse[106], O. Mtintsilana[34g], S. Muanza[105],

JHEP12(2024)126

J. Mueller[133], D. Muenstermann[94], R. Müller[37], G.A. Mullier[166], A.J. Mullin[33], J.J. Mullin[132], A.E. Mulski[63], D.P. Mungo[159], D. Munoz Perez[168], F.J. Munoz Sanchez[104], M. Murin[104], W.J. Murray[172,138], M. Muškinja[96], C. Mwewa[30], A.G. Myagkov[39,a], A.J. Myers[8], G. Myers[109], M. Myska[136], B.P. Nachman[18a], K. Nagai[130], K. Nagano[86], R. Nagasaka[158], J.L. Nagle[30,ag], E. Nagy[105], A.M. Nairz[37], Y. Nakahama[86], K. Nakamura[86], K. Nakkalil[5], H. Nanjo[128], E.A. Narayanan[46], Y. Narukawa[158], I. Naryshkin[39], L. Nasella[73a,73b], S. Nasri[120b], C. Nass[25], G. Navarro[23a], J. Navarro-Gonzalez[168], A. Nayaz[19], P.Y. Nechaeva[39], S. Nechaeva[24b,24a], F. Nechansky[135], L. Nedic[130], T.J. Neep[21], A. Negri[75a,75b], M. Negrini[24b], C. Nellist[118], C. Nelson[107], K. Nelson[109], S. Nemecek[135], M. Nessi[37,h], M.S. Neubauer[167], F. Neuhaus[103], J. Neundorf[50], J. Newell[95], P.R. Newman[21], C.W. Ng[133], Y.W.Y. Ng[50], B. Ngair[120a], H.D.N. Nguyen[111], R.B. Nickerson[130], R. Nicolaidou[139], J. Nielsen[140], M. Niemeyer[57], J. Niermann[37], N. Nikiforou[37], V. Nikolaenko[39,a], I. Nikolic-Audit[131], K. Nikolopoulos[21], P. Nilsson[30], I. Ninca[50], G. Ninio[156], A. Nisati[77a], N. Nishu[2], R. Nisius[113], N. Nitika[71a,71c], J-E. Nitschke[52], E.K. Nkadimeng[34g], T. Nobe[158], T. Nommensen[152], M.B. Norfolk[144], B.J. Norman[35], M. Noury[36a], J. Novak[96], T. Novak[96], L. Novotny[136], R. Novotny[116], L. Nozka[126], K. Ntekas[163], N.M.J. Nunes De Moura Junior[85b], J. Ocariz[131], A. Ochi[87], I. Ochoa[134a], S. Oerdek[50,w], J.T. Offermann[41], A. Ogrodnik[137], A. Oh[104], C.C. Ohm[149], H. Oide[86], R. Oishi[158], M.L. Ojeda[37], Y. Okumura[158], L.F. Oleiro Seabra[134a], I. Oleksiyuk[58], S.A. Olivares Pino[141d], G. Oliveira Correa[13], D. Oliveira Damazio[30], J.L. Oliver[163], Ö.O. Öncel[56], A.P. O'Neill[20], A. Onofre[134a,134e], P.U.E. Onyisi[11], M.J. Oreglia[41], D. Orestano[79a,79b], N. Orlando[13], R.S. Orr[159], L.M. Osojnak[132], Y. Osumi[114], G. Otero y Garzon[31], H. Otono[91], P.S. Ott[65a], G.J. Ottino[18a], M. Ouchrif[36d], F. Ould-Saada[129], T. Ovsiannikova[143], M. Owen[61], R.E. Owen[138], V.E. Ozcan[22a], F. Ozturk[89], N. Ozturk[8], S. Ozturk[84], H.A. Pacey[130], A. Pacheco Pages[13], C. Padilla Aranda[13], G. Padovano[77a,77b], S. Pagan Griso[18a], G. Palacino[70], A. Palazzo[72a,72b], J. Pampel[25], J. Pan[177], T. Pan[66a], D.K. Panchal[11], C.E. Pandini[118], J.G. Panduro Vazquez[138], H.D. Pandya[1], H. Pang[15], P. Pani[50], G. Panizzo[71a,71c], L. Panwar[131], L. Paolozzi[58], S. Parajuli[167], A. Paramonov[6], C. Paraskevopoulos[55], D. Paredes Hernandez[66b], A. Pareti[75a,75b], K.R. Park[43], T.H. Park[159], M.A. Parker[33], F. Parodi[59b,59a], V.A. Parrish[54], J.A. Parsons[43], U. Parzefall[56], B. Pascual Dias[111], L. Pascual Dominguez[102], E. Pasqualucci[77a], S. Passaggio[59b], F. Pastore[98], P. Patel[89], U.M. Patel[53], J.R. Pater[104], T. Pauly[37], F. Pauwels[137], C.I. Pazos[162], M. Pedersen[129], R. Pedro[134a], S.V. Peleganchuk[39], O. Penc[37], E.A. Pender[54], S. Peng[15], G.D. Penn[177], K.E. Penski[112], M. Penzin[39], B.S. Peralva[85d], A.P. Pereira Peixoto[143], L. Pereira Sanchez[148], D.V. Perepelitsa[30,ag], G. Perera[106], E. Perez Codina[160a], M. Perganti[10], H. Pernegger[37], S. Perrella[77a,77b], O. Perrin[42], K. Peters[50], R.F.Y. Peters[104], B.A. Petersen[37], T.C. Petersen[44], E. Petit[105], V. Petousis[136], C. Petridou[157,e], T. Petru[137], A. Petrukhin[146], M. Pettee[18a], A. Petukhov[84], K. Petukhova[37], R. Pezoa[141f], L. Pezzotti[37], G. Pezzullo[177], A.J. Pfleger[37], T.M. Pham[175], T. Pham[108], P.W. Phillips[138], G. Piacquadio[150], E. Pianori[18a], F. Piazza[127], R. Piegaia[31], D. Pietreanu[28b], A.D. Pilkington[104], M. Pinamonti[71a,71c], J.L. Pinfold[2], B.C. Pinheiro Pereira[134a], J. Pinol Bel[13],

JHEP12(2024)126

A.E. Pinto Pinoargote[139,139], L. Pintucci[71a,71c], K.M. Piper[151], A. Pirttikoski[58], D.A. Pizzi[35], L. Pizzimento[66b], A. Pizzini[118], M.-A. Pleier[30], V. Pleskot[137], E. Plotnikova[40], G. Poddar[97], R. Poettgen[101], L. Poggioli[131], S. Polacek[137], G. Polesello[75a], A. Poley[147,160a], A. Polini[24b], C.S. Pollard[172], Z.B. Pollock[123], E. Pompa Pacchi[124], N.I. Pond[99], D. Ponomarenko[70], L. Pontecorvo[37], S. Popa[28a], G.A. Popeneciu[28d], A. Poreba[37], D.M. Portillo Quintero[160a], S. Pospisil[136], M.A. Postill[144], P. Postolache[28c], K. Potamianos[172], P.A. Potepa[88a], I.N. Potrap[40], C.J. Potter[33], H. Potti[152], J. Poveda[168], M.E. Pozo Astigarraga[37], A. Prades Ibanez[78a,78b], J. Pretel[170], D. Price[104], M. Primavera[72a], L. Primomo[71a,71c], M.A. Principe Martin[102], R. Privara[126], T. Procter[61], M.L. Proffitt[143], N. Proklova[132], K. Prokofiev[66c], G. Proto[113], J. Proudfoot[6], M. Przybycien[88a], W.W. Przygoda[88b], A. Psallidas[48], J.E. Puddefoot[144], D. Pudzha[56], D. Pyatiizbyantseva[39], J. Qian[109], R. Qian[110], D. Qichen[104], Y. Qin[13], T. Qiu[54], A. Quadt[57], M. Queitsch-Maitland[104], G. Quetant[58], R.P. Quinn[169], G. Rabanal Bolanos[63], D. Rafanoharana[56], F. Raffaeli[78a,78b], F. Ragusa[73a,73b], J.L. Rainbolt[41], J.A. Raine[58], S. Rajagopalan[30], E. Ramakoti[39], L. Rambelli[59b,59a], I.A. Ramirez-Berend[35], K. Ran[50,115c], D.S. Rankin[132], N.P. Rapheeha[34g], H. Rasheed[28b], V. Raskina[131], D.F. Rassloff[65a], A. Rastogi[18a], S. Rave[103], S. Ravera[59b,59a], B. Ravina[57], I. Ravinovich[174], M. Raymond[37], A.L. Read[129], N.P. Readioff[144], D.M. Rebuzzi[75a,75b], G. Redlinger[30], A.S. Reed[113], K. Reeves[27], J.A. Reidelsturz[176], D. Reikher[127], A. Rej[51], C. Rembser[37], M. Renda[28b], F. Renner[50], A.G. Rennie[163], A.L. Rescia[50], S. Resconi[73a], M. Ressegotti[59b,59a], S. Rettie[37], J.G. Reyes Rivera[110], E. Reynolds[18a], O.L. Rezanova[39], P. Reznicek[137], H. Riani[36d], N. Ribaric[53], E. Ricci[80a,80b], R. Richter[113], S. Richter[49a,49b], E. Richter-Was[88b], M. Ridel[131], S. Ridouani[36d], P. Rieck[121], P. Riedler[37], E.M. Riefel[49a,49b], J.O. Rieger[118], M. Rijssenbeek[150], M. Rimoldi[37], L. Rinaldi[24b,24a], P. Rincke[57,166], T.T. Rinn[30], M.P. Rinnagel[112], G. Ripellino[166], I. Riu[13], J.C. Rivera Vergara[170], F. Rizatdinova[125], E. Rizvi[97], B.R. Roberts[18a], S.S. Roberts[140], S.H. Robertson[107,z], D. Robinson[33], M. Robles Manzano[103], A. Robson[61], A. Rocchi[78a,78b], C. Roda[76a,76b], S. Rodriguez Bosca[37], Y. Rodriguez Garcia[23a], A.M. Rodríguez Vera[119], S. Roe[37], J.T. Roemer[37], O. Røhne[129], R.A. Rojas[106], C.P.A. Roland[131], J. Roloff[30], A. Romaniouk[81], E. Romano[75a,75b], M. Romano[24b], A.C. Romero Hernandez[167], N. Rompotis[95], L. Roos[131], S. Rosati[77a], B.J. Rosser[41], E. Rossi[130], E. Rossi[74a,74b], L.P. Rossi[63], L. Rossini[56], R. Rosten[123], M. Rotaru[28b], B. Rottler[56], C. Rougier[92], D. Rousseau[68], D. Rousso[50], A. Roy[167], S. Roy-Garand[159], A. Rozanov[105], Z.M.A. Rozario[61], Y. Rozen[155], A. Rubio Jimenez[168], V.H. Ruelas Rivera[19], T.A. Ruggeri[1], A. Ruggiero[130], A. Ruiz-Martinez[168], A. Rummler[37], Z. Rurikova[56], N.A. Rusakovich[40], H.L. Russell[170], G. Russo[77a,77b], J.P. Rutherfoord[7], S. Rutherford Colmenares[33], M. Rybar[137], E.B. Rye[129], A. Ryzhov[46], J.A. Sabater Iglesias[58], H.F-W. Sadrozinski[140], F. Safai Tehrani[77a], B. Safarzadeh Samani[138], S. Saha[1], M. Sahinsoy[84], A. Saibel[168], M. Saimpert[139], M. Saito[158], T. Saito[158], A. Sala[73a,73b], D. Salamani[37], A. Salnikov[148], J. Salt[168], A. Salvador Salas[156], D. Salvatore[45b,45a], F. Salvatore[151], A. Salzburger[37], D. Sammel[56], E. Sampson[94], D. Sampsonidis[157,e], D. Sampsonidou[127], J. Sánchez[168], V. Sanchez Sebastian[168], H. Sandaker[129], C.O. Sander[50], J.A. Sandesara[106], M. Sandhoff[176], C. Sandoval[23b], L. Sanfilippo[65a], D.P.C. Sankey[138], T. Sano[90],

JHEP12(2024)126

A. Sansoni[55], L. Santi[37,77b], C. Santoni[42], H. Santos[134a,134b], A. Santra[174], E. Sanzani[24b,24a], K.A. Saoucha[165], J.G. Saraiva[134a,134d], J. Sardain[7], O. Sasaki[86], K. Sato[161], C. Sauer[37], E. Sauvan[4], P. Savard[159,ae], R. Sawada[158], C. Sawyer[138], L. Sawyer[100], C. Sbarra[24b], A. Sbrizzi[24b,24a], T. Scanlon[99], J. Schaarschmidt[143], U. Schäfer[103], A.C. Schaffer[68,46], D. Schaile[112], R.D. Schamberger[150], C. Scharf[19], M.M. Schefer[20], V.A. Schegelsky[39], D. Scheirich[137], M. Schernau[141e], C. Scheulen[58], C. Schiavi[59b,59a], M. Schioppa[45b,45a], B. Schlag[148], S. Schlenker[37], J. Schmeing[176], C.R. Schmidt[52], M.A. Schmidt[176], K. Schmieden[103], C. Schmitt[103], N. Schmitt[103], S. Schmitt[50], L. Schoeffel[139], A. Schoening[65b], P.G. Scholer[35], E. Schopf[130], M. Schott[25], J. Schovancova[37], S. Schramm[58], T. Schroer[58], H-C. Schultz-Coulon[65a], M. Schumacher[56], B.A. Schumm[140], Ph. Schune[139], A.J. Schuy[143], H.R. Schwartz[140], A. Schwartzman[148], T.A. Schwarz[109], Ph. Schwemling[139], R. Schwienhorst[110], F.G. Sciacca[20], A. Sciandra[30], G. Sciolla[27], F. Scuri[76a], C.D. Sebastiani[95], K. Sedlaczek[119], S.C. Seidel[116], A. Seiden[140], B.D. Seidlitz[43], C. Seitz[50], J.M. Seixas[85b], G. Sekhniaidze[74a], L. Selem[62], N. Semprini-Cesari[24b,24a], A. Semushin[178,39], D. Sengupta[58], V. Senthilkumar[168], L. Serin[68], M. Sessa[78a,78b], H. Severini[124], F. Sforza[59b,59a], A. Sfyrla[58], Q. Sha[14], E. Shabalina[57], A.H. Shah[33], R. Shaheen[149], J.D. Shahinian[132], D. Shaked Renous[174], L.Y. Shan[14], M. Shapiro[18a], A. Sharma[37], A.S. Sharma[169], P. Sharma[30], P.B. Shatalov[39], K. Shaw[151], S.M. Shaw[104], Q. Shen[64c], D.J. Sheppard[147], P. Sherwood[99], L. Shi[99], X. Shi[14], S. Shimizu[86], C.O. Shimmin[177], I.P.J. Shipsey[130,*], S. Shirabe[91], M. Shiyakova[40,x], M.J. Shochet[41], D.R. Shope[129], B. Shrestha[124], S. Shrestha[123,ah], I. Shreyber[39], M.J. Shroff[170], P. Sicho[135], A.M. Sickles[167], E. Sideras Haddad[34g,164], A.C. Sidley[118], A. Sidoti[24b], F. Siegert[52], Dj. Sijacki[16], F. Sili[93], J.M. Silva[54], I. Silva Ferreira[85b], M.V. Silva Oliveira[30], S.B. Silverstein[49a], S. Simion[68], R. Simoniello[37], E.L. Simpson[104], H. Simpson[151], L.R. Simpson[109], S. Simsek[84], S. Sindhu[57], P. Sinervo[159], S. Singh[30], S. Sinha[50], S. Sinha[104], M. Sioli[24b,24a], I. Siral[37], E. Sitnikova[50], J. Sjölin[49a,49b], A. Skaf[57], E. Skorda[21], P. Skubic[124], M. Slawinska[89], I. Slazyk[17], V. Smakhtin[174], B.H. Smart[138], S.Yu. Smirnov[39], Y. Smirnov[39], L.N. Smirnova[39,a], O. Smirnova[101], A.C. Smith[43], D.R. Smith[163], E.A. Smith[41], J.L. Smith[104], R. Smith[148], H. Smitmanns[103], M. Smizanska[94], K. Smolek[136], A.A. Snesarev[39], H.L. Snoek[118], S. Snyder[30], R. Sobie[170,z], A. Soffer[156], C.A. Solans Sanchez[37], E.Yu. Soldatov[39], U. Soldevila[168], A.A. Solodkov[39], S. Solomon[27], A. Soloshenko[40], K. Solovieva[56], O.V. Solovyanov[42], P. Sommer[52], A. Sonay[13], W.Y. Song[160b], A. Sopczak[136], A.L. Sopio[54], F. Sopkova[29b], J.D. Sorenson[116], I.R. Sotarriva Alvarez[142], V. Sothilingam[65a], O.J. Soto Sandoval[141c,141b], S. Sottocornola[70], R. Soualah[165], Z. Soumaimi[36e], D. South[50], N. Soybelman[174], S. Spagnolo[72a,72b], M. Spalla[113], D. Sperlich[56], G. Spigo[37], B. Spisso[74a,74b], D.P. Spiteri[61], M. Spousta[137], E.J. Staats[35], R. Stamen[65a], A. Stampekis[21], E. Stanecka[89], W. Stanek-Maslouska[50], M.V. Stange[52], B. Stanislaus[18a], M.M. Stanitzki[50], B. Stapf[50], E.A. Starchenko[39], G.H. Stark[140], J. Stark[92], P. Staroba[135], P. Starovoitov[65a], S. Stärz[107], R. Staszewski[89], G. Stavropoulos[48], A. Stefl[37], P. Steinberg[30], B. Stelzer[147,160a], H.J. Stelzer[133], O. Stelzer-Chilton[160a], H. Stenzel[60], T.J. Stevenson[151], G.A. Stewart[37], J.R. Stewart[125], M.C. Stockton[37], G. Stoicea[28b], M. Stolarski[134a], S. Stonjek[113], A. Straessner[52],

JHEP12(2024)126

J. Strandberg[149], S. Strandberg[49a,49b], M. Stratmann[176], M. Strauss[124], T. Strebler[105], P. Strizenec[29b], R. Ströhmer[171], D.M. Strom[127], R. Stroynowski[46], A. Strubig[49a,49b], S.A. Stucci[30], B. Stugu[17], J. Stupak[124], N.A. Styles[50], D. Su[148], S. Su[64a], W. Su[64d], X. Su[64a], D. Suchy[29a], K. Sugizaki[158], V.V. Sulin[39], M.J. Sullivan[95], D.M.S. Sultan[130], L. Sultanaliyeva[39], S. Sultansoy[3b], T. Sumida[90], S. Sun[175], W. Sun[14], O. Sunneborn Gudnadottir[166], N. Sur[105], M.R. Sutton[151], H. Suzuki[161], M. Svatos[135], M. Swiatlowski[160a], T. Swirski[171], I. Sykora[29a], M. Sykora[137], T. Sykora[137], D. Ta[103], K. Tackmann[50,w], A. Taffard[163], R. Tafirout[160a], J.S. Tafoya Vargas[68], Y. Takubo[86], M. Talby[105], A.A. Talyshev[39], K.C. Tam[66b], N.M. Tamir[156], A. Tanaka[158], J. Tanaka[158], R. Tanaka[68], M. Tanasini[150], Z. Tao[169], S. Tapia Araya[141f], S. Tapprogge[103], A. Tarek Abouelfadl Mohamed[110], S. Tarem[155], K. Tariq[14], G. Tarna[28b], G.F. Tartarelli[73a], M.J. Tartarin[92], P. Tas[137], M. Tasevsky[135], E. Tassi[45b,45a], A.C. Tate[167], G. Tateno[158], Y. Tayalati[36e,y], G.N. Taylor[108], W. Taylor[160b], P. Teixeira-Dias[98], J.J. Teoh[159], K. Terashi[158], J. Terron[102], S. Terzo[13], M. Testa[55], R.J. Teuscher[159,z], A. Thaler[81], O. Theiner[58], T. Theveneaux-Pelzer[105], O. Thielmann[176], D.W. Thomas[98], J.P. Thomas[21], E.A. Thompson[18a], P.D. Thompson[21], E. Thomson[132], R.E. Thornberry[46], C. Tian[64a], Y. Tian[58], V. Tikhomirov[39,a], Yu.A. Tikhonov[39], S. Timoshenko[39], D. Timoshyn[137], E.X.L. Ting[1], P. Tipton[177], A. Tishelman-Charny[30], S.H. Tlou[34g], K. Todome[142], S. Todorova-Nova[137], S. Todt[52], L. Toffolin[71a,71c], M. Togawa[86], J. Tojo[91], S. Tokár[29a], K. Tokushuku[86], O. Toldaiev[70], G. Tolkachev[105], M. Tomoto[86,114], L. Tompkins[148,m], E. Torrence[127], H. Torres[92], E. Torró Pastor[168], M. Toscani[31], C. Tosciri[41], M. Tost[11], D.R. Tovey[144], I.S. Trandafir[28b], T. Trefzger[171], A. Tricoli[30], I.M. Trigger[160a], S. Trincaz-Duvoid[131], D.A. Trischuk[27], B. Trocmé[62], A. Tropina[40], L. Truong[34c], M. Trzebinski[89], A. Trzupek[89], F. Tsai[150], M. Tsai[109], A. Tsiamis[157], P.V. Tsiareshka[40], S. Tsigaridas[160a], A. Tsirigotis[157,s], V. Tsiskaridze[159], E.G. Tskhadadze[154a], M. Tsopoulou[157], Y. Tsujikawa[90], I.I. Tsukerman[39], V. Tsulaia[18a], S. Tsuno[86], K. Tsuri[122], D. Tsybychev[150], Y. Tu[66b], A. Tudorache[28b], V. Tudorache[28b], A.N. Tuna[63], S. Turchikhin[59b,59a], I. Turk Cakir[3a], R. Turra[73a], T. Turtuvshin[40], P.M. Tuts[43], S. Tzamarias[157,e], E. Tzovara[103], F. Ukegawa[161], P.A. Ulloa Poblete[141c,141b], E.N. Umaka[30], G. Unal[37], A. Undrus[30], G. Unel[163], J. Urban[29b], P. Urrejola[141a], G. Usai[8], R. Ushioda[142], M. Usman[111], F. Ustuner[54], Z. Uysal[84], V. Vacek[136], B. Vachon[107], T. Vafeiadis[37], A. Vaitkus[99], C. Valderanis[112], E. Valdes Santurio[49a,49b], M. Valente[160a], S. Valentinetti[24b,24a], A. Valero[168], E. Valiente Moreno[168], A. Vallier[92], J.A. Valls Ferrer[168], D.R. Van Arneman[118], T.R. Van Daalen[143], A. Van Der Graaf[51], P. Van Gemmeren[6], M. Van Rijnbach[37], S. Van Stroud[99], I. Van Vulpen[118], P. Vana[137], M. Vanadia[78a,78b], U.M. Vande Voorde[149], W. Vandelli[37], E.R. Vandewall[125], D. Vannicola[156], L. Vannoli[55], R. Vari[77a], E.W. Varnes[7], C. Varni[18b], D. Varouchas[68], L. Varriale[168], K.E. Varvell[152], M.E. Vasile[28b], L. Vaslin[86], A. Vasyukov[40], L.M. Vaughan[125], R. Vavricka[103], T. Vazquez Schroeder[37], J. Veatch[32], V. Vecchio[104], M.J. Veen[106], I. Veliscek[30], L.M. Veloce[159], F. Veloso[134a,134c], S. Veneziano[77a], A. Ventura[72a,72b], S. Ventura Gonzalez[139], A. Verbytskyi[113], M. Verducci[76a,76b], C. Vergis[97], M. Verissimo De Araujo[85b], W. Verkerke[118], J.C. Vermeulen[118], C. Vernieri[148], M. Vessella[163], M.C. Vetterli[147,ae], A. Vgenopoulos[103], N. Viaux Maira[141f],

T. Vickey[144], O.E. Vickey Boeriu[144], G.H.A. Viehhauser[130], L. Vigani[65b], M. Vigl[113], M. Villa[24b,24a], M. Villaplana Perez[168], E.M. Villhauer[54], E. Vilucchi[55], M.G. Vincter[35], A. Visibile[118], C. Vittori[37], I. Vivarelli[24b,24a], E. Voevodina[113], F. Vogel[112], J.C. Voigt[52], P. Vokac[136], Yu. Volkotrub[88b], E. Von Toerne[25], B. Vormwald[37], V. Vorobel[137], K. Vorobev[39], M. Vos[168], K. Voss[146], M. Vozak[118], L. Vozdecky[124], N. Vranjes[16], M. Vranjes Milosavljevic[16], M. Vreeswijk[118], N.K. Vu[64d,64c], R. Vuillermet[37], O. Vujinovic[103], I. Vukotic[41], I.K. Vyas[35], S. Wada[161], C. Wagner[148], J.M. Wagner[18a], W. Wagner[176], S. Wahdan[176], H. Wahlberg[93], C.H. Waits[124], J. Walder[138], R. Walker[112], W. Walkowiak[146], A. Wall[132], E.J. Wallin[101], T. Wamorkar[6], A.Z. Wang[140], C. Wang[103], C. Wang[11], H. Wang[18a], J. Wang[66c], P. Wang[104], P. Wang[99], R. Wang[63], R. Wang[6], S.M. Wang[153], S. Wang[14], T. Wang[64a], W.T. Wang[82], W. Wang[14], X. Wang[167], X. Wang[64c], Y. Wang[64d], Y. Wang[115a], Y. Wang[64a], Z. Wang[109], Z. Wang[64d,53,64c], Z. Wang[109], A. Warburton[107], R.J. Ward[21], N. Warrack[61], S. Waterhouse[98], A.T. Watson[21], H. Watson[54], M.F. Watson[21], E. Watton[61,138], G. Watts[143], B.M. Waugh[99], J.M. Webb[56], C. Weber[30], H.A. Weber[19], M.S. Weber[20], S.M. Weber[65a], C. Wei[64a], Y. Wei[56], A.R. Weidberg[130], E.J. Weik[121], J. Weingarten[51], C. Weiser[56], C.J. Wells[50], T. Wenaus[30], B. Wendland[51], T. Wengler[37], N.S. Wenke[113], N. Wermes[25], M. Wessels[65a], A.M. Wharton[94], A.S. White[63], A. White[8], M.J. White[1], D. Whiteson[163], L. Wickremasinghe[128], W. Wiedenmann[175], M. Wielers[138], C. Wiglesworth[44], D.J. Wilbern[124], H.G. Wilkens[37], J.J.H. Wilkinson[33], D.M. Williams[43], H.H. Williams[132], S. Williams[33], S. Willocq[106], B.J. Wilson[104], D.J. Wilson[104], P.J. Windischhofer[41], F.I. Winkel[31], F. Winklmeier[127], B.T. Winter[56], J.K. Winter[104], M. Wittgen[148], M. Wobisch[100], T. Wojtkowski[62], Z. Wolffs[118], J. Wollrath[37], M.W. Wolter[89], H. Wolters[134a,134c], M.C. Wong[140], E.L. Woodward[43], S.D. Worm[50], B.K. Wosiek[89], K.W. Woźniak[89], S. Wozniewski[57], K. Wraight[61], C. Wu[21], M. Wu[115b], M. Wu[117], S.L. Wu[175], X. Wu[58], X. Wu[64a], Y. Wu[64a], Z. Wu[4], J. Wuerzinger[113,ac], T.R. Wyatt[104], B.M. Wynne[54], S. Xella[44], L. Xia[115a], M. Xia[15], M. Xie[64a], A. Xiong[127], J. Xiong[18a], D. Xu[14], H. Xu[64a], L. Xu[64a], R. Xu[132], T. Xu[109], Y. Xu[143], Z. Xu[54], Z. Xu[115a], B. Yabsley[152], S. Yacoob[34a], Y. Yamaguchi[86], E. Yamashita[158], H. Yamauchi[161], T. Yamazaki[18a], Y. Yamazaki[87], S. Yan[61], Z. Yan[106], H.J. Yang[64c,64d], H.T. Yang[64a], S. Yang[64a], T. Yang[66c], X. Yang[37], X. Yang[14], Y. Yang[46], Y. Yang[64a], W-M. Yao[18a], H. Ye[57], J. Ye[14], S. Ye[30], X. Ye[64a], Y. Yeh[99], I. Yeletskikh[40], B. Yeo[18b], M.R. Yexley[99], T.P. Yildirim[130], P. Yin[43], K. Yorita[173], S. Younas[28b], C.J.S. Young[37], C. Young[148], C. Yu[14,115c], Y. Yu[64a], J. Yuan[14,115c], M. Yuan[109], R. Yuan[64d,64c], L. Yue[99], M. Zaazoua[64a], B. Zabinski[89], I. Zahir[36a], E. Zaid[54], Z.K. Zak[89], T. Zakareishvili[168], S. Zambito[58], J.A. Zamora Saa[141d,141b], J. Zang[158], D. Zanzi[56], R. Zanzottera[73a,73b], O. Zaplatilek[136], C. Zeitnitz[176], H. Zeng[14], J.C. Zeng[167], D.T. Zenger Jr[27], O. Zenin[39], T. Ženiš[29a], S. Zenz[97], S. Zerradi[36a], D. Zerwas[68], M. Zhai[14,115c], D.F. Zhang[144], J. Zhang[64b], J. Zhang[6], K. Zhang[14,115c], L. Zhang[64a], L. Zhang[115a], P. Zhang[14,115c], R. Zhang[175], S. Zhang[109], S. Zhang[92], T. Zhang[158], X. Zhang[64c], Y. Zhang[143], Y. Zhang[99], Y. Zhang[115a], Z. Zhang[18a], Z. Zhang[64b], Z. Zhang[68], H. Zhao[143], T. Zhao[64b], Y. Zhao[140], Z. Zhao[64a], Z. Zhao[64a], A. Zhemchugov[40], J. Zheng[115a], K. Zheng[167], X. Zheng[64a], Z. Zheng[148], D. Zhong[167],

JHEP12(2024)126

B. Zhou[109], H. Zhou[7], N. Zhou[64c], Y. Zhou[15], Y. Zhou[115a], Y. Zhou[7], C.G. Zhu[64b], J. Zhu[109], X. Zhu[64d], Y. Zhu[64c], Y. Zhu[64a], X. Zhuang[14], K. Zhukov[70], N.I. Zimine[40], J. Zinsser[65b], M. Ziolkowski[146], L. Živković[16], A. Zoccoli[24b,24a], K. Zoch[63], T.G. Zorbas[144], O. Zormpa[48], W. Zou[43], L. Zwalinski[37]

[1] *Department of Physics, University of Adelaide, Adelaide; Australia*
[2] *Department of Physics, University of Alberta, Edmonton AB; Canada*
[3] [(a)] *Department of Physics, Ankara University, Ankara;* [(b)] *Division of Physics, TOBB University of Economics and Technology, Ankara; Türkiye*
[4] *LAPP, Université Savoie Mont Blanc, CNRS/IN2P3, Annecy; France*
[5] *APC, Université Paris Cité, CNRS/IN2P3, Paris; France*
[6] *High Energy Physics Division, Argonne National Laboratory, Argonne IL; United States of America*
[7] *Department of Physics, University of Arizona, Tucson AZ; United States of America*
[8] *Department of Physics, University of Texas at Arlington, Arlington TX; United States of America*
[9] *Physics Department, National and Kapodistrian University of Athens, Athens; Greece*
[10] *Physics Department, National Technical University of Athens, Zografou; Greece*
[11] *Department of Physics, University of Texas at Austin, Austin TX; United States of America*
[12] *Institute of Physics, Azerbaijan Academy of Sciences, Baku; Azerbaijan*
[13] *Institut de Física d'Altes Energies (IFAE), Barcelona Institute of Science and Technology, Barcelona; Spain*
[14] *Institute of High Energy Physics, Chinese Academy of Sciences, Beijing; China*
[15] *Physics Department, Tsinghua University, Beijing; China*
[16] *Institute of Physics, University of Belgrade, Belgrade; Serbia*
[17] *Department for Physics and Technology, University of Bergen, Bergen; Norway*
[18] [(a)] *Physics Division, Lawrence Berkeley National Laboratory, Berkeley CA;* [(b)] *University of California, Berkeley CA; United States of America*
[19] *Institut für Physik, Humboldt Universität zu Berlin, Berlin; Germany*
[20] *Albert Einstein Center for Fundamental Physics and Laboratory for High Energy Physics, University of Bern, Bern; Switzerland*
[21] *School of Physics and Astronomy, University of Birmingham, Birmingham; United Kingdom*
[22] [(a)] *Department of Physics, Bogazici University, Istanbul;* [(b)] *Department of Physics Engineering, Gaziantep University, Gaziantep;* [(c)] *Department of Physics, Istanbul University, Istanbul; Türkiye*
[23] [(a)] *Facultad de Ciencias y Centro de Investigaciónes, Universidad Antonio Nariño, Bogotá;* [(b)] *Departamento de Física, Universidad Nacional de Colombia, Bogotá; Colombia*
[24] [(a)] *Dipartimento di Fisica e Astronomia A. Righi, Università di Bologna, Bologna;* [(b)] *INFN Sezione di Bologna; Italy*
[25] *Physikalisches Institut, Universität Bonn, Bonn; Germany*
[26] *Department of Physics, Boston University, Boston MA; United States of America*
[27] *Department of Physics, Brandeis University, Waltham MA; United States of America*
[28] [(a)] *Transilvania University of Brasov, Brasov;* [(b)] *Horia Hulubei National Institute of Physics and Nuclear Engineering, Bucharest;* [(c)] *Department of Physics, Alexandru Ioan Cuza University of Iasi, Iasi;* [(d)] *National Institute for Research and Development of Isotopic and Molecular Technologies, Physics Department, Cluj-Napoca;* [(e)] *National University of Science and Technology Politechnica, Bucharest;* [(f)] *West University in Timisoara, Timisoara;* [(g)] *Faculty of Physics, University of Bucharest, Bucharest; Romania*
[29] [(a)] *Faculty of Mathematics, Physics and Informatics, Comenius University, Bratislava;* [(b)] *Department of Subnuclear Physics, Institute of Experimental Physics of the Slovak Academy of Sciences, Kosice; Slovak Republic*
[30] *Physics Department, Brookhaven National Laboratory, Upton NY; United States of America*
[31] *Universidad de Buenos Aires, Facultad de Ciencias Exactas y Naturales, Departamento de Física, y CONICET, Instituto de Física de Buenos Aires (IFIBA), Buenos Aires; Argentina*
[32] *California State University, CA; United States of America*
[33] *Cavendish Laboratory, University of Cambridge, Cambridge; United Kingdom*
[34] [(a)] *Department of Physics, University of Cape Town, Cape Town;* [(b)] *iThemba Labs, Western*

JHEP12(2024)126

Cape;[(c)] *Department of Mechanical Engineering Science, University of Johannesburg, Johannesburg;*[(d)] *National Institute of Physics, University of the Philippines Diliman (Philippines);*[(e)] *University of South Africa, Department of Physics, Pretoria;*[(f)] *University of Zululand, KwaDlangezwa;*[(g)] *School of Physics, University of the Witwatersrand, Johannesburg; South Africa*

[35] *Department of Physics, Carleton University, Ottawa ON; Canada*

[36] [(a)] *Faculté des Sciences Ain Chock, Université Hassan II de Casablanca;*[(b)] *Faculté des Sciences, Université Ibn-Tofail, Kénitra;*[(c)] *Faculté des Sciences Semlalia, Université Cadi Ayyad, LPHEA-Marrakech;*[(d)] *LPMR, Faculté des Sciences, Université Mohamed Premier, Oujda;*[(e)] *Faculté des sciences, Université Mohammed V, Rabat;*[(f)] *Institute of Applied Physics, Mohammed VI Polytechnic University, Ben Guerir; Morocco*

[37] *CERN, Geneva; Switzerland*

[38] *Affiliated with an institute formerly covered by a cooperation agreement with CERN*

[39] *Affiliated with an institute covered by a cooperation agreement with CERN*

[40] *Affiliated with an international laboratory covered by a cooperation agreement with CERN*

[41] *Enrico Fermi Institute, University of Chicago, Chicago IL; United States of America*

[42] *LPC, Université Clermont Auvergne, CNRS/IN2P3, Clermont-Ferrand; France*

[43] *Nevis Laboratory, Columbia University, Irvington NY; United States of America*

[44] *Niels Bohr Institute, University of Copenhagen, Copenhagen; Denmark*

[45] [(a)] *Dipartimento di Fisica, Università della Calabria, Rende;*[(b)] *INFN Gruppo Collegato di Cosenza, Laboratori Nazionali di Frascati; Italy*

[46] *Physics Department, Southern Methodist University, Dallas TX; United States of America*

[47] *Physics Department, University of Texas at Dallas, Richardson TX; United States of America*

[48] *National Centre for Scientific Research "Demokritos", Agia Paraskevi; Greece*

[49] [(a)] *Department of Physics, Stockholm University;*[(b)] *Oskar Klein Centre, Stockholm; Sweden*

[50] *Deutsches Elektronen-Synchrotron DESY, Hamburg and Zeuthen; Germany*

[51] *Fakultät Physik, Technische Universität Dortmund, Dortmund; Germany*

[52] *Institut für Kern- und Teilchenphysik, Technische Universität Dresden, Dresden; Germany*

[53] *Department of Physics, Duke University, Durham NC; United States of America*

[54] *SUPA — School of Physics and Astronomy, University of Edinburgh, Edinburgh; United Kingdom*

[55] *INFN e Laboratori Nazionali di Frascati, Frascati; Italy*

[56] *Physikalisches Institut, Albert-Ludwigs-Universität Freiburg, Freiburg; Germany*

[57] *II. Physikalisches Institut, Georg-August-Universität Göttingen, Göttingen; Germany*

[58] *Département de Physique Nucléaire et Corpusculaire, Université de Genève, Genève; Switzerland*

[59] [(a)] *Dipartimento di Fisica, Università di Genova, Genova;*[(b)] *INFN Sezione di Genova; Italy*

[60] *II. Physikalisches Institut, Justus-Liebig-Universität Giessen, Giessen; Germany*

[61] *SUPA — School of Physics and Astronomy, University of Glasgow, Glasgow; United Kingdom*

[62] *LPSC, Université Grenoble Alpes, CNRS/IN2P3, Grenoble INP, Grenoble; France*

[63] *Laboratory for Particle Physics and Cosmology, Harvard University, Cambridge MA; United States of America*

[64] [(a)] *Department of Modern Physics and State Key Laboratory of Particle Detection and Electronics, University of Science and Technology of China, Hefei;*[(b)] *Institute of Frontier and Interdisciplinary Science and Key Laboratory of Particle Physics and Particle Irradiation (MOE), Shandong University, Qingdao;*[(c)] *School of Physics and Astronomy, Shanghai Jiao Tong University, Key Laboratory for Particle Astrophysics and Cosmology (MOE), SKLPPC, Shanghai;*[(d)] *Tsung-Dao Lee Institute, Shanghai;*[(e)] *School of Physics, Zhengzhou University; China*

[65] [(a)] *Kirchhoff-Institut für Physik, Ruprecht-Karls-Universität Heidelberg, Heidelberg;*[(b)] *Physikalisches Institut, Ruprecht-Karls-Universität Heidelberg, Heidelberg; Germany*

[66] [(a)] *Department of Physics, Chinese University of Hong Kong, Shatin, N.T., Hong Kong;*[(b)] *Department of Physics, University of Hong Kong, Hong Kong;*[(c)] *Department of Physics and Institute for Advanced Study, Hong Kong University of Science and Technology, Clear Water Bay, Kowloon, Hong Kong; China*

[67] *Department of Physics, National Tsing Hua University, Hsinchu; Taiwan*

[68] *IJCLab, Université Paris-Saclay, CNRS/IN2P3, 91405, Orsay; France*

[69] *Centro Nacional de Microelectrónica (IMB-CNM-CSIC), Barcelona; Spain*

[70] *Department of Physics, Indiana University, Bloomington IN; United States of America*

JHEP12(2024)126

[71] [(a)] INFN Gruppo Collegato di Udine, Sezione di Trieste, Udine; [(b)] ICTP, Trieste; [(c)] Dipartimento Politecnico di Ingegneria e Architettura, Università di Udine, Udine; Italy
[72] [(a)] INFN Sezione di Lecce; [(b)] Dipartimento di Matematica e Fisica, Università del Salento, Lecce; Italy
[73] [(a)] INFN Sezione di Milano; [(b)] Dipartimento di Fisica, Università di Milano, Milano; Italy
[74] [(a)] INFN Sezione di Napoli; [(b)] Dipartimento di Fisica, Università di Napoli, Napoli; Italy
[75] [(a)] INFN Sezione di Pavia; [(b)] Dipartimento di Fisica, Università di Pavia, Pavia; Italy
[76] [(a)] INFN Sezione di Pisa; [(b)] Dipartimento di Fisica E. Fermi, Università di Pisa, Pisa; Italy
[77] [(a)] INFN Sezione di Roma; [(b)] Dipartimento di Fisica, Sapienza Università di Roma, Roma; Italy
[78] [(a)] INFN Sezione di Roma Tor Vergata; [(b)] Dipartimento di Fisica, Università di Roma Tor Vergata, Roma; Italy
[79] [(a)] INFN Sezione di Roma Tre; [(b)] Dipartimento di Matematica e Fisica, Università Roma Tre, Roma; Italy
[80] [(a)] INFN-TIFPA; [(b)] Università degli Studi di Trento, Trento; Italy
[81] Universität Innsbruck, Department of Astro and Particle Physics, Innsbruck; Austria
[82] University of Iowa, Iowa City IA; United States of America
[83] Department of Physics and Astronomy, Iowa State University, Ames IA; United States of America
[84] Istinye University, Sariyer, Istanbul; Türkiye
[85] [(a)] Departamento de Engenharia Elétrica, Universidade Federal de Juiz de Fora (UFJF), Juiz de Fora; [(b)] Universidade Federal do Rio De Janeiro COPPE/EE/IF, Rio de Janeiro; [(c)] Instituto de Física, Universidade de São Paulo, São Paulo; [(d)] Rio de Janeiro State University, Rio de Janeiro; [(e)] Federal University of Bahia, Bahia; Brazil
[86] KEK, High Energy Accelerator Research Organization, Tsukuba; Japan
[87] Graduate School of Science, Kobe University, Kobe; Japan
[88] [(a)] AGH University of Krakow, Faculty of Physics and Applied Computer Science, Krakow; [(b)] Marian Smoluchowski Institute of Physics, Jagiellonian University, Krakow; Poland
[89] Institute of Nuclear Physics Polish Academy of Sciences, Krakow; Poland
[90] Faculty of Science, Kyoto University, Kyoto; Japan
[91] Research Center for Advanced Particle Physics and Department of Physics, Kyushu University, Fukuoka; Japan
[92] L2IT, Université de Toulouse, CNRS/IN2P3, UPS, Toulouse; France
[93] Instituto de Física La Plata, Universidad Nacional de La Plata and CONICET, La Plata; Argentina
[94] Physics Department, Lancaster University, Lancaster; United Kingdom
[95] Oliver Lodge Laboratory, University of Liverpool, Liverpool; United Kingdom
[96] Department of Experimental Particle Physics, Jožef Stefan Institute and Department of Physics, University of Ljubljana, Ljubljana; Slovenia
[97] School of Physics and Astronomy, Queen Mary University of London, London; United Kingdom
[98] Department of Physics, Royal Holloway University of London, Egham; United Kingdom
[99] Department of Physics and Astronomy, University College London, London; United Kingdom
[100] Louisiana Tech University, Ruston LA; United States of America
[101] Fysiska institutionen, Lunds universitet, Lund; Sweden
[102] Departamento de Física Teorica C-15 and CIAFF, Universidad Autónoma de Madrid, Madrid; Spain
[103] Institut für Physik, Universität Mainz, Mainz; Germany
[104] School of Physics and Astronomy, University of Manchester, Manchester; United Kingdom
[105] CPPM, Aix-Marseille Université, CNRS/IN2P3, Marseille; France
[106] Department of Physics, University of Massachusetts, Amherst MA; United States of America
[107] Department of Physics, McGill University, Montreal QC; Canada
[108] School of Physics, University of Melbourne, Victoria; Australia
[109] Department of Physics, University of Michigan, Ann Arbor MI; United States of America
[110] Department of Physics and Astronomy, Michigan State University, East Lansing MI; United States of America
[111] Group of Particle Physics, University of Montreal, Montreal QC; Canada
[112] Fakultät für Physik, Ludwig-Maximilians-Universität München, München; Germany
[113] Max-Planck-Institut für Physik (Werner-Heisenberg-Institut), München; Germany
[114] Graduate School of Science and Kobayashi-Maskawa Institute, Nagoya University, Nagoya; Japan

JHEP12(2024)126

[115] [(a)] Department of Physics, Nanjing University, Nanjing;[(b)] School of Science, Shenzhen Campus of Sun Yat-sen University;[(c)] University of Chinese Academy of Science (UCAS), Beijing; China
[116] Department of Physics and Astronomy, University of New Mexico, Albuquerque NM; United States of America
[117] Institute for Mathematics, Astrophysics and Particle Physics, Radboud University/Nikhef, Nijmegen; Netherlands
[118] Nikhef National Institute for Subatomic Physics and University of Amsterdam, Amsterdam; Netherlands
[119] Department of Physics, Northern Illinois University, DeKalb IL; United States of America
[120] [(a)] New York University Abu Dhabi, Abu Dhabi;[(b)] United Arab Emirates University, Al Ain; United Arab Emirates
[121] Department of Physics, New York University, New York NY; United States of America
[122] Ochanomizu University, Otsuka, Bunkyo-ku, Tokyo; Japan
[123] Ohio State University, Columbus OH; United States of America
[124] Homer L. Dodge Department of Physics and Astronomy, University of Oklahoma, Norman OK; United States of America
[125] Department of Physics, Oklahoma State University, Stillwater OK; United States of America
[126] Palacký University, Joint Laboratory of Optics, Olomouc; Czech Republic
[127] Institute for Fundamental Science, University of Oregon, Eugene, OR; United States of America
[128] Graduate School of Science, Osaka University, Osaka; Japan
[129] Department of Physics, University of Oslo, Oslo; Norway
[130] Department of Physics, Oxford University, Oxford; United Kingdom
[131] LPNHE, Sorbonne Université, Université Paris Cité, CNRS/IN2P3, Paris; France
[132] Department of Physics, University of Pennsylvania, Philadelphia PA; United States of America
[133] Department of Physics and Astronomy, University of Pittsburgh, Pittsburgh PA; United States of America
[134] [(a)] Laboratório de Instrumentação e Física Experimental de Partículas — LIP, Lisboa;[(b)] Departamento de Física, Faculdade de Ciências, Universidade de Lisboa, Lisboa;[(c)] Departamento de Física, Universidade de Coimbra, Coimbra;[(d)] Centro de Física Nuclear da Universidade de Lisboa, Lisboa;[(e)] Departamento de Física, Universidade do Minho, Braga;[(f)] Departamento de Física Teórica y del Cosmos, Universidad de Granada, Granada (Spain);[(g)] Departamento de Física, Instituto Superior Técnico, Universidade de Lisboa, Lisboa; Portugal
[135] Institute of Physics of the Czech Academy of Sciences, Prague; Czech Republic
[136] Czech Technical University in Prague, Prague; Czech Republic
[137] Charles University, Faculty of Mathematics and Physics, Prague; Czech Republic
[138] Particle Physics Department, Rutherford Appleton Laboratory, Didcot; United Kingdom
[139] IRFU, CEA, Université Paris-Saclay, Gif-sur-Yvette; France
[140] Santa Cruz Institute for Particle Physics, University of California Santa Cruz, Santa Cruz CA; United States of America
[141] [(a)] Departamento de Física, Pontificia Universidad Católica de Chile, Santiago;[(b)] Millennium Institute for Subatomic physics at high energy frontier (SAPHIR), Santiago;[(c)] Instituto de Investigación Multidisciplinario en Ciencia y Tecnología, y Departamento de Física, Universidad de La Serena;[(d)] Universidad Andres Bello, Department of Physics, Santiago;[(e)] Instituto de Alta Investigación, Universidad de Tarapacá, Arica;[(f)] Departamento de Física, Universidad Técnica Federico Santa María, Valparaíso; Chile
[142] Department of Physics, Institute of Science, Tokyo; Japan
[143] Department of Physics, University of Washington, Seattle WA; United States of America
[144] Department of Physics and Astronomy, University of Sheffield, Sheffield; United Kingdom
[145] Department of Physics, Shinshu University, Nagano; Japan
[146] Department Physik, Universität Siegen, Siegen; Germany
[147] Department of Physics, Simon Fraser University, Burnaby BC; Canada
[148] SLAC National Accelerator Laboratory, Stanford CA; United States of America
[149] Department of Physics, Royal Institute of Technology, Stockholm; Sweden
[150] Departments of Physics and Astronomy, Stony Brook University, Stony Brook NY; United States of America

JHEP12(2024)126

[151] Department of Physics and Astronomy, University of Sussex, Brighton; United Kingdom
[152] School of Physics, University of Sydney, Sydney; Australia
[153] Institute of Physics, Academia Sinica, Taipei; Taiwan
[154] [(a)] E. Andronikashvili Institute of Physics, Iv. Javakhishvili Tbilisi State University, Tbilisi;[(b)] High Energy Physics Institute, Tbilisi State University, Tbilisi;[(c)] University of Georgia, Tbilisi; Georgia
[155] Department of Physics, Technion, Israel Institute of Technology, Haifa; Israel
[156] Raymond and Beverly Sackler School of Physics and Astronomy, Tel Aviv University, Tel Aviv; Israel
[157] Department of Physics, Aristotle University of Thessaloniki, Thessaloniki; Greece
[158] International Center for Elementary Particle Physics and Department of Physics, University of Tokyo, Tokyo; Japan
[159] Department of Physics, University of Toronto, Toronto ON; Canada
[160] [(a)] TRIUMF, Vancouver BC;[(b)] Department of Physics and Astronomy, York University, Toronto ON; Canada
[161] Division of Physics and Tomonaga Center for the History of the Universe, Faculty of Pure and Applied Sciences, University of Tsukuba, Tsukuba; Japan
[162] Department of Physics and Astronomy, Tufts University, Medford MA; United States of America
[163] Department of Physics and Astronomy, University of California Irvine, Irvine CA; United States of America
[164] University of West Attica, Athens; Greece
[165] University of Sharjah, Sharjah; United Arab Emirates
[166] Department of Physics and Astronomy, University of Uppsala, Uppsala; Sweden
[167] Department of Physics, University of Illinois, Urbana IL; United States of America
[168] Instituto de Física Corpuscular (IFIC), Centro Mixto Universidad de Valencia — CSIC, Valencia; Spain
[169] Department of Physics, University of British Columbia, Vancouver BC; Canada
[170] Department of Physics and Astronomy, University of Victoria, Victoria BC; Canada
[171] Fakultät für Physik und Astronomie, Julius-Maximilians-Universität Würzburg, Würzburg; Germany
[172] Department of Physics, University of Warwick, Coventry; United Kingdom
[173] Waseda University, Tokyo; Japan
[174] Department of Particle Physics and Astrophysics, Weizmann Institute of Science, Rehovot; Israel
[175] Department of Physics, University of Wisconsin, Madison WI; United States of America
[176] Fakultät für Mathematik und Naturwissenschaften, Fachgruppe Physik, Bergische Universität Wuppertal, Wuppertal; Germany
[177] Department of Physics, Yale University, New Haven CT; United States of America
[178] Yerevan Physics Institute, Yerevan; Armenia

[a] Also Affiliated with an institute covered by a cooperation agreement with CERN
[b] Also at An-Najah National University, Nablus; Palestine
[c] Also at Borough of Manhattan Community College, City University of New York, New York NY; United States of America
[d] Also at Center for High Energy Physics, Peking University; China
[e] Also at Center for Interdisciplinary Research and Innovation (CIRI-AUTH), Thessaloniki; Greece
[f] Also at CERN, Geneva; Switzerland
[g] Also at CMD-AC UNEC Research Center, Azerbaijan State University of Economics (UNEC); Azerbaijan
[h] Also at Département de Physique Nucléaire et Corpusculaire, Université de Genève, Genève; Switzerland
[i] Also at Departament de Fisica de la Universitat Autonoma de Barcelona, Barcelona; Spain
[j] Also at Department of Financial and Management Engineering, University of the Aegean, Chios; Greece
[k] Also at Department of Physics, California State University, Sacramento; United States of America
[l] Also at Department of Physics, King's College London, London; United Kingdom
[m] Also at Department of Physics, Stanford University, Stanford CA; United States of America
[n] Also at Department of Physics, Stellenbosch University; South Africa
[o] Also at Department of Physics, University of Fribourg, Fribourg; Switzerland
[p] Also at Department of Physics, University of Thessaly; Greece
[q] Also at Department of Physics, Westmont College, Santa Barbara; United States of America
[r] Also at Faculty of Physics, Sofia University, 'St. Kliment Ohridski', Sofia; Bulgaria

JHEP12(2024)126

[s] Also at Hellenic Open University, Patras; Greece
[t] Also at Henan University; China
[u] Also at Imam Mohammad Ibn Saud Islamic University; Saudi Arabia
[v] Also at Institucio Catalana de Recerca i Estudis Avancats, ICREA, Barcelona; Spain
[w] Also at Institut für Experimentalphysik, Universität Hamburg, Hamburg; Germany
[x] Also at Institute for Nuclear Research and Nuclear Energy (INRNE) of the Bulgarian Academy of Sciences, Sofia; Bulgaria
[y] Also at Institute of Applied Physics, Mohammed VI Polytechnic University, Ben Guerir; Morocco
[z] Also at Institute of Particle Physics (IPP); Canada
[aa] Also at Institute of Physics, Azerbaijan Academy of Sciences, Baku; Azerbaijan
[ab] Also at National Institute of Physics, University of the Philippines Diliman (Philippines); Philippines
[ac] Also at Technical University of Munich, Munich; Germany
[ad] Also at The Collaborative Innovation Center of Quantum Matter (CICQM), Beijing; China
[ae] Also at TRIUMF, Vancouver BC; Canada
[af] Also at Università di Napoli Parthenope, Napoli; Italy
[ag] Also at University of Colorado Boulder, Department of Physics, Colorado; United States of America
[ah] Also at Washington College, Chestertown, MD; United States of America
[ai] Also at Yeditepe University, Physics Department, Istanbul; Türkiye
[*] Deceased

JHEP12(2024)126